A Comparative Study Between CFRP and Steel Shear Reinforcement Bar in Self Compacting Reinforced Concrete Beams

Mohsen Kobraei

FACULTY OF ENGINEERING
UNIVERSITY OF MALAYA
KUALA LUMPUR

2012

A Comparative Study Between CFRP and Steel

Shear Reinforcement Bar in Self Compacting

Reinforced Concrete Beams

Mohsen Kobraei

DISSERTATION SUBMITTED IN PARTIAL FULFILLMENT OF THE
REQUIREMENTS FOR THE DEGREE OF
MASTER OF ENGINEERING SCIENCE

FACULTY OF ENGINEERING
UNIVERSITY OF MALAYA
KUALA LUMPUR

2012

Dedicated to my lovely parents

UNIVERSITI MALAYA

<u>ORGINAL LITERARY WORK DECLATION</u>

NAME OF CANDIDATE: MOHSEN KOBRAEI

REGISTRATION/MATRIC NO.: KGA 080084

NAME OF DEGREE: MASTER'S DEGREE

TITLE OF PROJECT PAPER/RESEARCH REPORT/DISSERTATION/THESIS ("THIS WORK"):

A COMPARATIVE STUDY BETWEEN CFRP AND STEEL AS SHEAR REINFORCEMENT BAR IN SELF COMPACTING REINFORCED CONCRETE BEAMS

FIELD OF STUDY: CIVIL ENGINEERING – STRUCTURAL ENGINEERING

I do solemnly and sincerely declare that:

(1) I am the sole author/writer of this Work;
(2) This Work is original;
(3) Any use of any work in which copyright exists was done by way of fair dealing and for permitted purposes and any excerpt or extract from, or reference to or reproduction of any copyright work has been disclosed expressly and sufficiently and the title of the Work and its authorship have been acknowledged in this Work;
(4) I do not have any actual knowledge nor do I ought reasonably to know that the making of this work constitutes an infringement of any copyright work;
(5) I hereby assign all and every right in the copyright to this Work to the University of Malaya ('UM"), who henceforth shall be owner of the copyright in this Work and that any reproduction or use in any form or by any means whatsoever is prohibited without the written consent of UM having been first had and obtained;
(6) I am fully aware that if in the course of making this Work I have infringed any copyright whether intentionally or otherwise, I may be subject to legal action or any other action as may be determined by UM,

CANDIDATE'S SIGNATURE: DATE:

Subscribed and solemnly declared before,

WHITENESS'S SIGNATURE: DATE:

NAME: DESIGNATION:

ABSTRACT

Fibre Reinforced Polymer (FRP) as an alternative to steel Reinforced Concrete (RC) beams has become increasingly popular. The main advantages of FRP include high strength to weight ratio and its corrosion resistance. Such benefits in the field of civil engineering are hard to ignore. In this work, the effect of using Carbon Fibre Reinforced Polymer (CFRP) bars as shear reinforcement in RC beams has been studied. All beams were cast using High Strength Self-Compacting Concrete (HSCC). Self-Compacting Concrete (SCC) offers many advantages such as having a low noise-level when used in plants and construction sites; eliminating problems associated with vibrations; requiring less labour; improving quality and durability; and faster construction of structures.

The shear behaviours and modes of failure for seven full scale laboratory specimens have been analysed. These specimens were shear reinforced using CFRP and steel stirrups. The shear capacity and behaviour of RC beams using CFRP stirrups were compared with the shear those of RC beams using steel stirrups. Further, this work has examined the effect of reducing CFRP shear reinforcement spacings with the shear behaviour of reinforced concrete beams.

Furthermore, in this research the ultimate moment capacity, load-deflection relationship, the crack initiation load, and the crack width of the beams were studied. Among other the results of this study show that using internally straight CFRP shear reinforcement is an excellent alternative to using the normal steel stirrups in RC beams. The use of propose shear reinforcements will help to avoid brittle rupture and causes beams to exhibit more deflections. In addition, this study showed that the RC beam with CFRP stirrups, and the RC beams with straight steel bar as shear reinforcement, showed

similar behaviour. The beams with CFRP stirrups bar had smaller cracks spacing and they are more resistant to propagation of shear cracks.

ABSTRAK

Polimer Bertetulang Gentian *(FRP)* sebagai alternatif kepada keluli di dalam rasuk konkrit bertetulang menjadi semakin popular. Kelebihan FRP termasuk kekuatan tinggi kepada nisbah berat diri dan ketahanan karat, dan kelebihannya tidak boleh diabaikan dalam kejuruteraan awam. Kesan penggunaan Karbon Polimer Bertetulang Gentian *(CFRP)* sebagai tetulang ricih menggantikan keluli, di dalam rasuk konkrit bertetulang telah dikaji di dalam penyelidikan ini. Semua rasuk dituang menggunakan Konkrit pemadatan sendiri *(SCC)* sebagai kategori baru Konkrit Kekuatan Tinggi *(HSCC).* SCC menawarkan banyak kelebihan seperti tahap yang rendah di loji serta tapak pembinaan; penghapusan masalah-masalah yang berkaitan dengan getaran; pengurangan buruh yang terlibat; pembinaan yang lebih cepat, kualiti yang lebih baik serta peningkatan ketahanan struktur yang dituang menggunakan konkrit jenis ini.

Kajian telah dilakukan terhadap kelakuan ricih dan mod kegagalan bagi tujuh spesimen makmal skala penuh dengan pengukuhan pada kawasan ricih menggunakan CFRP serta stirrups keluli biasa, analisis perbandingan dibuat ke atas kapasiti ricih dan kelakuan rasuk konkrit bertetulang yang menggunakan CFRP stirrups dan keluli biasa. Kajian ini juga meneliti kesan pengurangan jurang antara jarak CFRP tetulang ricih terhadap tingkah laku ricih rasuk konkrit bertetulang.

Di samping itu, kajian ini telah mengkaji keupayaan momen muktamad rasuk bertetulang dengan konkrit pemadatan sendiri, kawalan beban-pesongan, beban pada retak pertama dan lebar retak. Keputusan kajian ini menunjukkan bahawa pengunaan CFRP lurus di dalam rasuk sebgai tetulang ricih adalah alternatif yang sangat baik untuk stirrups biasa dalam rasuk konkrit bertetulang. Selain itu, penggunaan tetulang ricih akan membantu untuk mengelakkan keretakan rapuh serta membawa nilai

pesongan yang lebih tinggi. Di samping itu, rasuk konkrit bertetulang dengan CFRP sebagai bar tetulang ricih dibandingkan dengan rasuk RC dengan stirrups normal dan bar keluli lurus sebagai tetulang ricih, menunjukkan tingkah laku yang serupa. Selain itu, dengan penurunan jarak CFRP bar tetulang ricih, peningkatana keretakan namun dengan pengurangan lebar telah diperhatikan.

ACKNOWLEDGMENT

I am deeply indebted to my supervisor, Prof. Ir. Dr. Mohd Zamin Jumaat for his constants encouragement and guidance throughout this research.

The writing of this research has been the most challenging undertaking of my life to date. I could not have completed this work without the support and help of many people.

I would also like to convey thanks to the University of Malaya for providing the financial means and laboratory facilities.

I would like to deliver my thankfulness to Prof. Dr. Hamid Reza Kobraei for his guidelines and supports.

Last but not least, heartfelt thanks extended to my beloved family for their love, support and encouragement.

TABLE OF CONTENTS

LIST OF TABLES

LIST OF FIGURES

LIST OF NOTATIONS

$a =$ depth of equivalent rectangular stress block

$b =$ width of rectangular cross section

$d =$ distance from extreme compression fibre to centroid of tension reinforcement

$A_f =$ area of FRP reinforcement

$A_s =$ area of tension steel reinforcement

$E_f =$ design or guaranteed modulus of elasticity of FRP defined as mean modulus of sample of test specimens

$f_c' =$ specified compressive strength of concrete,

$f_{cu} =$ characteristic cube strength of *concrete*

$f_f =$ stress in FRP reinforcement in tension

$f_{fu}^* =$ guaranteed tensile strength of FRP bar,

$f_{fu} =$ design tensile strength of FRP, considering reductions for service environment

$C_E =$ environmental reduction factor for various fibre type and exposure conditions, for CFRP and used condition was 1.0

$f_y =$ specified yield stress of nonprestressed steel reinforcement

$M_n =$ nominal moment capacity

$M_u =$ factored moment at section

$V_c =$ nominal shear strength provided by concrete

$V_u =$ factored shear force at section

$\rho =$ steel reinforcement ratio

$\rho_f =$ FRP reinforcement ratio

$\rho_{fb} =$ FRP reinforcement ratio producing balanced strain conditions

$\rho_b =$ steel reinforcement ratio producing balanced strain conditions

ρ_{min} = minimum reinforcement ratio for steel

α = shear span, distance from support to the first concentrated load

β_1 = factor taken as 0.85 for concrete strength f_c' up to and including 28 MPa. For strength above 28 MPa, this factor is reduced continuously at a rate of 0.05 per each 7 MPa of strength in excess of 28 MPa, but is not taken less than 0.65.

1.0 INTRODUCTION

1.1 Introduction

For years, civil engineers have searched for alternatives to steels and other metal alloys to combat the high costs of repair and maintenance of structural failure caused by corrosion and fatigue. For example, cost estimates for maintenance of highway bridge decks composed of steel-reinforced concrete are up to $90 billion per year. Composite materials, formed by the combination of two or more distinct materials in a microscopic scale, have become more popular in the engineering fields since 1940s. Fibre Reinforced Polymer (FRP) is a relatively new category of composite material manufactured from fibres and resins. In civil engineering, a FRP composite is considered to be an efficient and economical material for developing new structures as well as for the repair and replacement of deteriorating structures. The mechanical properties of FRPs make them ideal for widespread applications in construction worldwide.

Corrosion of steel reinforcement is a major cause of deterioration in reinforced concrete structures. This deterioration is especially more acute for structures exposed to harsh environmental conditions such as bridges, concrete pavements, parking garages, sea walls, wharfs, floating pier and tanks. The concrete structures reinforced with FRP composite can alleviate problems commonly caused by corrosion of steel reinforcement and can increase the anticipated service time of such structures. The climatic conditions may be a factor in accelerating the corrosion process. During the winter season, a large amount of salts is used for ice removal and road treatment in many places. These conditions normally accelerate the need of costly repairs and may even lead to catastrophic failure. Utilizing FRP materials as an alternative reinforcement in

reinforced concrete structures is becoming a more acceptable practice specifically in structures subject to severe environmental conditions. Thus, using FRP reinforcement has the potential to eliminate the corrosion and its associated deterioration.

Stirrups for shear reinforcement normally enclose the longitudinal reinforcement and are thus the closest reinforcement to the outer concrete surface. Consequently, they are more susceptible to severe environmental conditions and may be subjected to related deterioration that results in reductions of the service life of the structure. Thus, employing the non-corrodible FRP as a substitute for the conventional stirrups ones provides more protection for structural members subjected to severe environmental exposure. However, from the design point of view, the direct replacement of steel with FRP bars is not possible due to various differences in their mechanical properties. There are significant differences in tensile strength and the modulus of elasticity between FRP bas and stirrup rebar. Steel has higher tensile strength and lower elastic modulus than FRP. Other differences include the bond characteristics, and the absence of yielding plateau in the stress-strain relationships of FRP materials. Extensive research programs have been conducted to examine the flexural behaviour of concrete members reinforced with FRP reinforcement. However, the use of FRP as shear reinforcement (stirrups) for concrete members has not been adequately explored. However, more work is needed in this area to yield satisfactory guidelines and to provide a rational model to predict the shear strength of FRP reinforced concrete structures. The shear failure of reinforced concrete beams is frequently sudden and brittle in nature. Thus the design must ensure that the shear strength equals or exceeds the flexural strength of FRP uniformly along the structure. Therefore one has to first consider the flexural design to determine the cross-section and the flexural reinforcement. Thus, concrete beams are generally reinforced with shear reinforcement to ensure that, upon overloading, the flexural

failure occurs rather than shear failure. The shear strength of the reinforced concrete structures are usually consists of two components: concrete contribution, *Vc,* and shear reinforcement contribution, *Vs.* The design shear strength is considered based on the summation of both contributions along with the appropriate factors of safety.

The qualitative and quantitative analysis for designing a structural model requires understanding of the properties of the materials. The qualitative knowledge of the material properties is essential for choosing which physical and mechanical properties of the composite material are important for structural analysis and design and why they are important. The quantitative properties of material are also needed to analyse and predict the behaviour and the capacity of structural member. This information can be determined through experimental studies. Finally the result from analytical models must be compared with actual structures in full-scale. Careful modelling of the structures can reduce the number of required experimental tests. As expected, conducting tests is time-consuming, and expensive. Moreover, the laboratory specimen often does not simulate the exact conditions of actual structures.

In recent years a number of researchers studied the behaviour of beams with FRP rods as reinforcement in bending. For instance, Nawy et al., (1971) have examined the behaviour of glass fibre reinforced concrete beams. They examined the cracking, deflection, reinforcement stress, and the ultimate load of beams reinforced with different reinforcement ratios of glass fibre reinforced polymer (GFRP) bars. Nakano et al., (1993) conducted research using continuous Aramid fibre bars, continuous carbon fibre bars and deformed steel bars. Michaluck et al., (1998) explored the flexural behaviour of one-way slabs reinforced by FRP reinforcements.

Essentially, the properties of FRP composites can be determined in two ways, the theoretical calculation and the experimental measurements. Since an FRP composite is an inhomogeneous material, it can be considered theoretically. Experimentally specimen maybe prepared at different levels and scales. Theoretical methods are not currently available to correctly predict the characteristics of FRP rebar such as bond properties and long term durability. Consequently, specimen experimentation is commonly used. In engineering applications, characteristic properties and specifications of material are usually made available by the manufacture. Carbon fibre reinforced polymer (CFRP) is most commonly used material among the few types of FRPs such as GFRP, CFRP, and aramid fibre reinforced polymer (AFRP). Due to cost consideration, CFRP is not used as conventional reinforcing bars. Typically CFRP is used as a pre-stressing tendon or Near Surface Mounted (NSM) strengthening. NSM is one of the most recent and promising strengthening techniques for reinforced concrete (RC) structures. NSM is based on the application of circular (Lorenzis and Nanni, 2002) or rectangular cross section bars (Blaschko and Zilch, 1999) of FRP materials installed into pre-cut slits that are formed on the surface of concrete elements to be strengthened.

1.2 Importance of Study

Fibres provide resistance and function as an essential component in fibre-reinforced composites. Consequently, fibres used for manufacturing composites must have favourable physical characteristic such as strength, stiffness, durability, sufficient elongation at failure, and preferably low cost. The performance of fibres is affected by their length, cross-sectional shape, and chemical composition. Fibres are available in different cross-sectional shapes and sizes. The most commonly used fibres for producing FRPs are made of glass, aramid, and carbon.

Similar to steel reinforcement, FRP bars are produced in different diameters, depending on the manufacturing process. The surface of the rods can be spiral, straight, sanded-straight, sanded-braided, and deformed. The mechanical properties of some commercially available FRP reinforcing bars are given in Table 2.1 and 2.2. Figure 2.1 depicts the typical stress-tensile strain relationship of steel with commercially available carbon, aramid, and glass FRP bars.

To manufacture a beam with respects to a usual method, normal stirrups in shear area should be used. Of course to build a beam with standard method, more time is needed to bend bars and to make stirrups. Nevertheless, more beams for the same period could be made by using straight CFRP bar as a shear reinforcement. The major problem however, is the corrosion of steel reinforcement which results in deterioration of reinforced concrete. In huge structures, there is an additional problem in reinforcement placing. In this case the effect is more significant at junction support of beams to columns. Hence it should be thought about reducing reinforcement bars without decreasing the beam strength. According to studies published in this area, using externally straight FRP shear reinforcement bars increase the shear capacity of the beam. Therefore, this study will examine internally straight CFRP bars to reinforcing shear zone as shear reinforcement. This research has never been done before and presents a new idea and method in building RC beams.

1.3 Objectives

The application of FRP as reinforcement for concrete structures is rapidly increasing and it is now being intensively researched as a primary means of reinforcement for concrete. These efforts reflect the urgent need for completely understanding the behaviour of FRP reinforced concrete elements. However, limited research work has

been carried out to examine the shear behaviour of the self-compacting reinforced concrete beams.

The significant objectives of this practice are as follows:

(a)   To investigate the effect of shear reinforcement bar on the shear capacity in reinforced concrete beams. Here the focus has been on high strength self-compacting concrete category.

(b)   To study the effect of normal steel stirrups and straight steel bars as shear reinforcement on shear and flexural behaviour of reinforced concrete beams.

(c)   To explore the effect of CFRP straight bars as shear reinforcement on shear and flexural behaviour of reinforced concrete beams.

(d)   To study the influence of CFRP shear reinforcement spacing in high strength self-compacting reinforced concrete beams.

(e)   To develop a computer programme to analyse the shear capacity of FRP reinforced concrete beams.

1.4 Methodology

Basically, this study is carried out through three vital phases, which are listed below:

(a) Literature review

To comprehensively study previous researches, especially on the usage of FRP-bars in concrete beams and their relation to shear behaviour of concrete beams and how to mix a SCC concrete prior to experimental work.

(b) Experimental programme and Computer programming

To conduct the initial mix design and develop the final mix design. By optimizing past mix designs, a high strength SCC is manufactured. After finalising the mix design, the next step is to build and test the considered beams.

These beams include one reference beam and other manufactured beams by CFRP-bars. During experimental works, a computer programme base on FORTRAN language has been developed for analysis of concrete beams .

(c) Comparison of experimental and Calculated results

To compare experimental data with the calculated results, which come from ACI regulation. The outline of this work is shown in the following flowchart, Figure 1.2.

1.5 Scope of Study

This research is based on the comparative study of shear behaviour in seven full scale laboratory concrete beams which are reinforced on shear zone by straight CFRP and steel combination, and by normal steel stirrups. These beams were cast by self-compacting concrete with a target compressive strength of 95 MPa cured for 28 days. Moreover, the spacing of shear reinforcement fibres were examined. A computer programme to analyse FRP RC beams behaviour, especially on shear essential was carried out.

1.6 Thesis Outline

LITERATURE REVIEW: This work present more details on the mechanical and material properties of FRP bars, and examines their effects on shear behaviour in concrete beams. In the final sections of this work, a recent method for shear strengthening and a new category of high performance concrete has been described.

COMPUTER PROGRAMMING: The presented software designs and analyses the FRP reinforced concrete beams and it is based on ACI 440 written in FORTRAN programming language.

EXPERIMENTAL PROGRAMME: This (section) explains how to build concrete beams and presents the procedures for set-up and testing.

RESULTS AND DISCUSSIONS: This (part) focuses on results taken from experimental tests and also examines the comparison of the results of concrete beams with a reference beams.

CONCLUSIONS: This (section) summarizes the main conclusions and the overall findings of this thesis project with recommendations for further works.
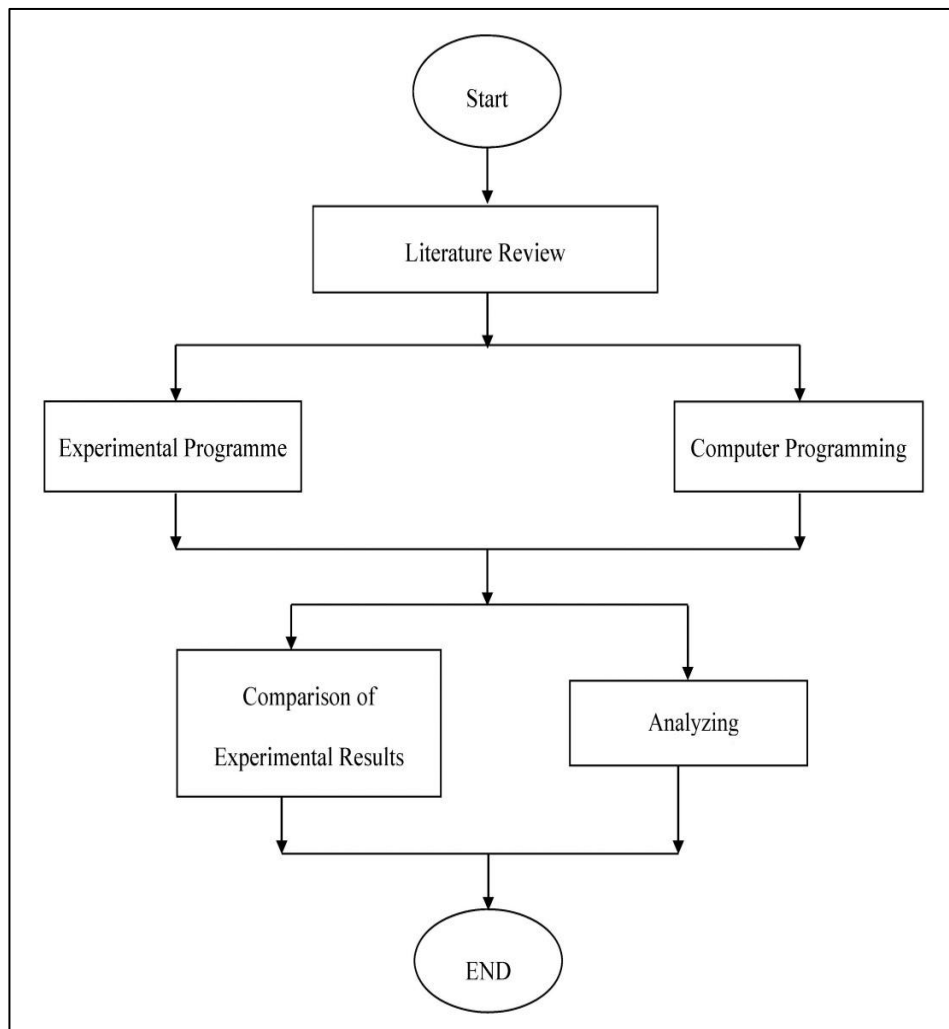
Figure 1.1. Flowchart of methodology analysing

2.1   Introduction

This section presents the properties and characteristics of FRP materials. The shear behaviour, design procedure, and the application of FRP as shear reinforcement in concrete beams are explained. This section with the near surface mounted (NSM) method and finally focus on self-compacting concrete and its properties are concluded.

2.2   FRP-bars Materials

The mechanical properties of FRP bars are significantly different than steel bars. The properties of FRP composites depend mainly both on the properties of matrix and fibre, as well as on their volume fractions. Generally, FRP bars have lower weight, lower ¥ young's modulus but higher strength than steel. The most commonly available fibre types are the carbon (CFRP), the glass (GFRP) and the aramid (AFRP) fibres.

Table 2.1 list some of the advantages and disadvantages of FRP reinforcement reported by ACI 440.1R-06.

The determination of both the geometrical and mechanical properties of FRP bars requires the use of specific procedures (ASTM D 618, ACI 440.3R-04).

FRP bars have densities ranging from one fifth to one fourth of the steel density. The reduction in weight substantially eases the handling of FRP bars on the project site (ACI Committee 440, 2001).

The tensile properties of FRP are what make them an attractive alternative to steel reinforcement. When loaded in tension, FRP bars do not exhibit any plastic behaviour (yielding) before rupture. Therefore, FRP reinforcement is not recommended for

moment frames or zones where moment redistribution is required. Table 2.2 shows the most common tensile properties of reinforcing bars, in compliance with the values reported by ACI 440.1R-06. Figure 2.1.a, depicts the typical stress-strain behaviour of FRP bars compared to that of steel bars. Using FRP bars in constructions has some advantages such as having a light weight as shown in Figure 2.1.b.

The CNR-DT (2003-2006), suggests that all types of FRP bars can be used, provided that the characteristic strength is not lower than 400 MPa. In addition, the average value of the young's modulus of elasticity in the longitudinal direction should not be less than 100 GPa for CFRP bars, 35 GPa for GFRP bars, and 65 GPa for AFRP bars. The compressive modulus of elasticity of FRP reinforcing bars appears to be smaller than its tensile modulus of elasticity. In fact, most of FRP RC design guidelines recommend against relying only on the strength and stiffness contributions provided by the compressed FRP bars.

FRP reinforcing bars are susceptible to static fatigue phenomenon ("creep rupture"), which is a progressive reduction of strength under long term loads. In general, carbon fibres are the least susceptible to creep rupture, whereas aramid fibres are moderately susceptible, and the glass fibres are the most susceptible (ACI Committee 440, 2006). The static fatigue in FRP materials is highly influenced by environmental factors, such as temperature and moisture.

The bond between the FRP bar and the surrounding concrete is ensured by propagation of stresses whose values depend on the bar geometry, chemical and physical characteristics of its surface as well as on the concrete's compressive strength. The latter parameter is less important for FRP bars than for steel bars.

Table 2.1 Advantages and Disadvantages of FRP Reinforcement(ACI Committee 440, 2006)

Advantages of FRP Reinforcement	Disadvantages of FRP Reinforcement
High longitudinal tensile strength	No yielding before brittle rapture
Corrosion resistance	Low transverse strength
Nonmagnetic	Low modulus of elasticity
High fatigue endurance	Susceptibility of damage to polymeric resins and fibres under ultraviolet radiation exposure
Lightweight (about 1/5 to1/4 the density of steel)	High coefficient of thermal expansion perpendicular to the fibres, relative to concrete
Low thermal and electric conductivity	May be susceptible to fire depending on matrix type and concrete cover thickness

Table 2.2 Typical Tensile Properties of Reinforcing FRP Bars (ACI Committee 440, 2006)

	Steel	GFRP	CFRP	AFRP
Nominal yield stress, MPa	276 to 517	N/A	N/A	N/A
Tensile strength, MPa	483 to 690	483 to 1600	600 to 3690	1720 to 2540
Elastic modulus, GPa	200	35 to 51	120 to 580	41 to 125
Yield strain, %	0.14 to 0.25	N/A	N/A	N/A
Rupture strain, %	6.0 to 12.0	1.2 to 3.1	0.5 to 1.7	1.9 to 4.4
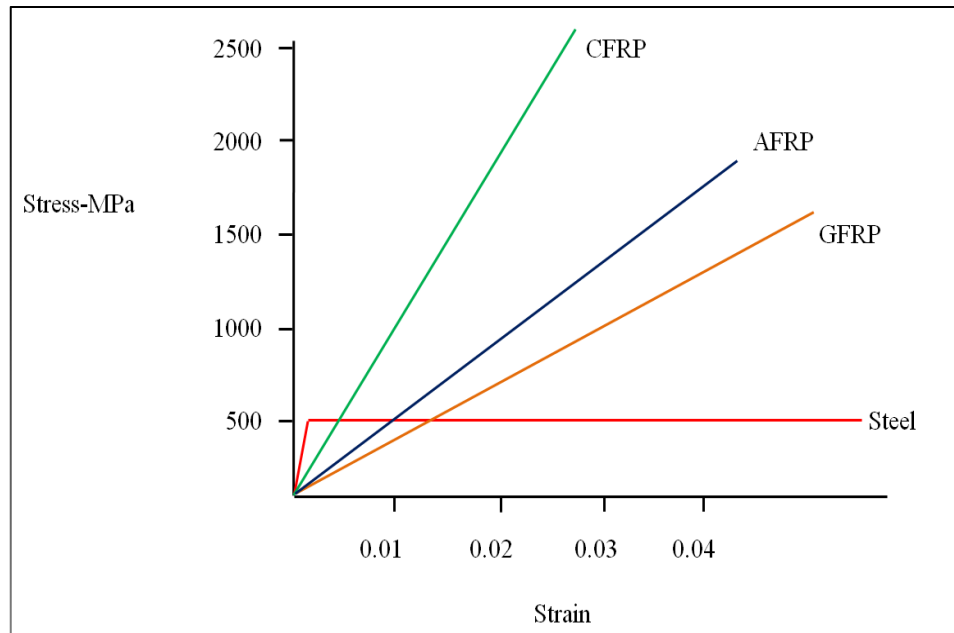
Figure 2.1.a. Stress – Strain Curves of Typical of Reinforcing Bars (ACI Committee 440, 2001)

Figure 2.1.b. Application of FRP in construction industry

2.3 Shear Behaviour in Concrete Beams

The following section investigates shear behaviour such as mechanism of shear, mode of failure and type of cracks and shear in reinforced concrete beams with/without shear reinforcement bars.

2.3.1 Shear in Reinforced Concrete Beams without Shear Reinforcement

The shear behaviour of reinforced concrete beams without shear reinforcement has been comprehensively studied. However, a good understanding of shear behaviour of such beams is still limited. This is referred to the complexity and sensitivity of the affecting parameters that govern the shear strength of concrete beams without shear reinforcement.

2.3.1.1 Mechanisms of shear resisting

The ASCE-ACI Committee 445 (1999) identified four components for shear transfer in cracked concrete beams. These five components are:

(a) Shear resistance provided by the un-cracked concrete above the neutral axis;

(b) The interface shear transfer along the two faces of the cracks after the appearance of shear cracks, which is sometimes noted as "aggregate interlock;"

(c) Dowel action of the longitudinal reinforcement;

(d) Arch action, which is significant in deep member with a shear span-to-depth ratio, *a/d,* less than 2.5.

Generally the above-mentioned four components are referred to as concrete contribution to the shear strength, V_c. The shear resistance components for a slender beam without shear reinforcement are shown in Figure 2.2.
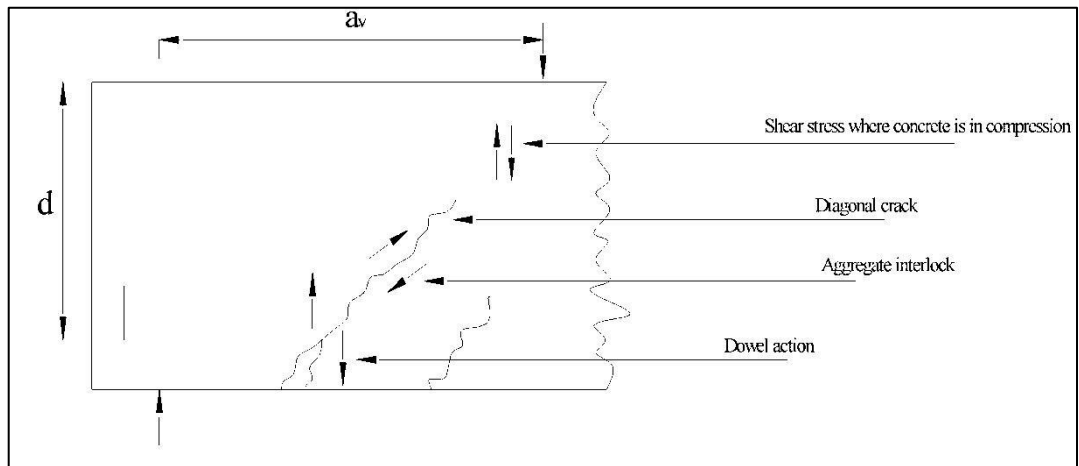
Figure 2.2 Shear resistance components in a cracked concrete beam without shear reinforcement (Ginley and Choo 1990).

2.3.1.2 Type of cracking and modes of shear failure

When the principal tensile stress at any location exceeds the cracking strength of the concrete crack forms. Cracks usually form perpendicular to the directions of the principal stress. For members with unaxial stress the principal tress will be parallel to the longitudinal direction of the member resulting in parallel cracks perpendicular to the member's axis. For members subjected to biaxial stresses, as the case of flexural and shear stresses, the principal tensile stress will be inclined at an angle with the member's axis. Therefore, the shear cracks are usually inclined to the member's axis.

Two different modes of shear cracks are specified by Winter and Nilson (1979): (i) web-shear cracks and (iv) flexure-shear cracks. When the flexural stresses are small at the particular location, the diagonal tension stresses are inclined at about 45° and are numerically equal to the shear stresses with a maximum at the neutral axis. As a result, diagonal web-shear cracks start mostly near the neutral axis and then propagate in both directions as shown in Figure 2.3.a.

Larg V and Small M
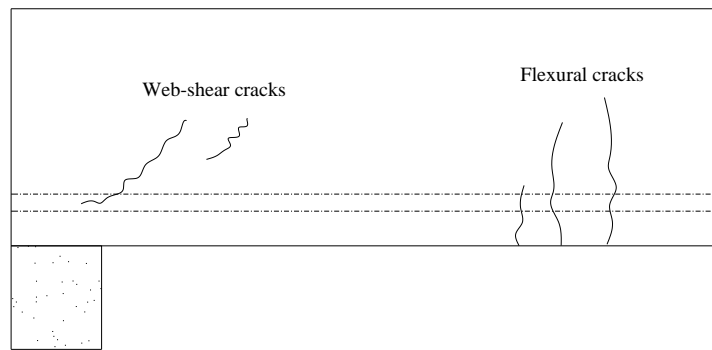
(a) Web-shear cracking

Larg V and Larg M
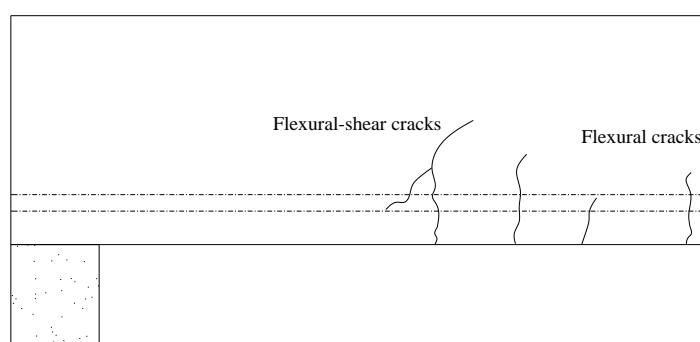
(b) Flexural-shear cracking

Figure 2.3 Diagonal tension cracking in concrete beam (Winter and Nilson 1979).

The situation will be different when both shear forces and bending moments have large values. The flexural cracks will appear and their widths are controlled by the presence of longitudinal reinforcement. However, when the diagonal tension stress at the upper end of one or more of these cracks exceeds the tensile strength of the concrete, the crack bends in-diagonal direction and continues to grow in length and width as shown in Figure 2.3.b. These cracks are known as flexure-shear cracks and more are common than web-shear cracks.

The behaviour of beams failing in shear varies widely depending on the relative contributions of beam action and arch action and the amount of shear reinforcement (MacGregor 1997). The moments and shears at inclined cracking and failure of a rectangular beam without shear reinforcement are shown in Figure 2.4. The shaded areas in the figure show the reduction in strength due to shear. Thus, the shear reinforcement is provided to achieve the full flexural capacity.

According to MacGregor (1997) classification, shown in Figure 2.4, the shear span can be classified based on shear span-to-depth ratio, a/d, into four types:
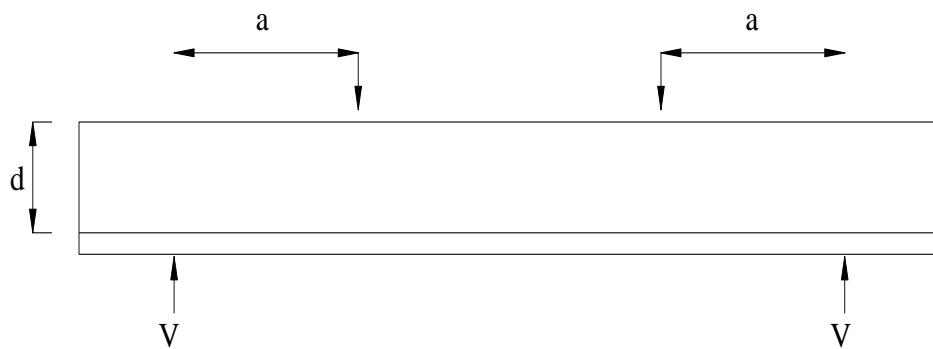
(a) Beam
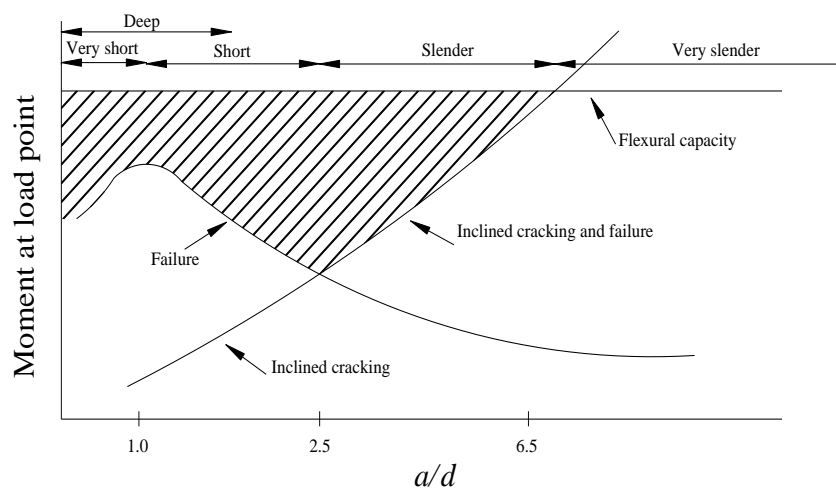
(b) Moment at cracking and failure (MacGregor 1997).

16
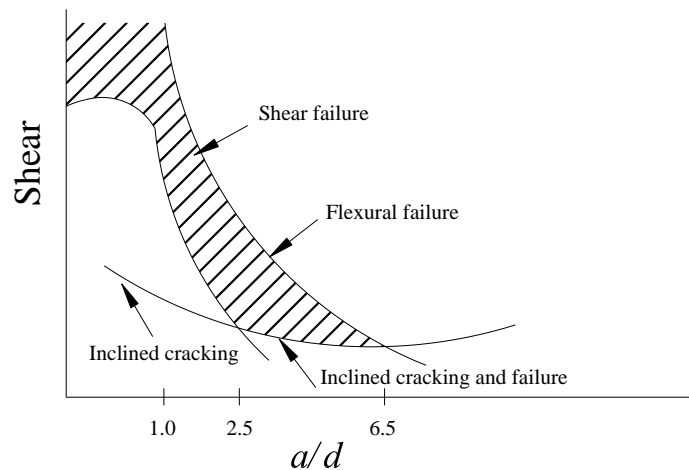
(c) Shear at cracking and failure

Figure 2.4 Effect of shear span to depth ratio $\left(\frac{a}{d}\right)$ on shear strength of beams without shear reinforcement (MacGregor 1997).

(a) Very short: with shear span to depth ratio, aid, equals 0 to 1.0. These beams develop inclined cracks joining the load and the support. The cracks, in turn, destroy the horizontal shear flow from the longitudinal steel to the compression zone and the behaviour changes from beam action to arch action. The failure of such beams, which is commonly referred to as deep beams, is shown in Figure 2.5.

Type of failure:

1. Anchorage failure
2. Bearing failure
3. Flexural failure
4, 5. Crushing of compression strut
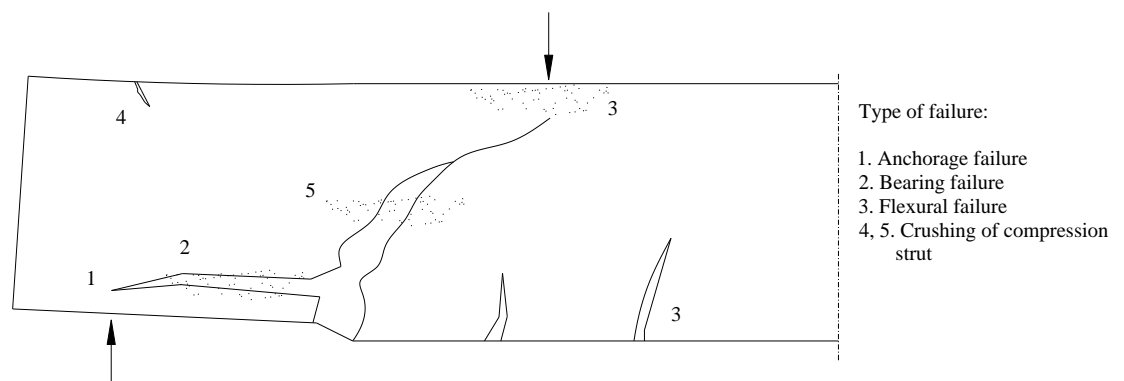
Figure 2.5 Type of failure of deep beam (ASCE-ACI 1973).

(b) Short: with aid ranges from 1 to 2.5. These beams develop inclined cracks and after redistribution of internal forces are able to carry additional load, in part by arch action. The final failure of such beams will result from a bond failure, a splitting failure or a dowel failure along the tension reinforcement as shown in Figure 2.6(a) or by crushing of the compression zone over the shear crack as shown in Figure 2.6(b).

Loss of bond due to splitting crack
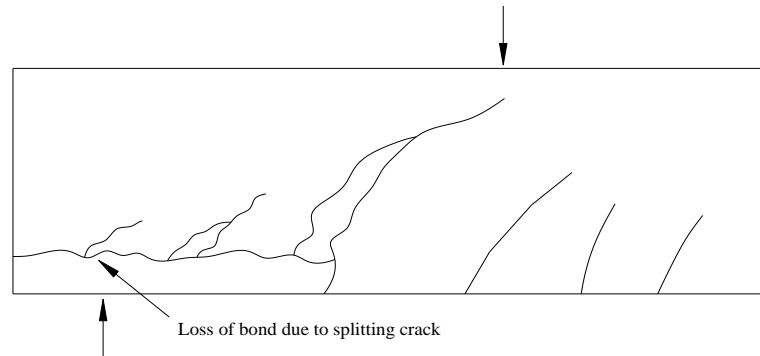
(a) Shear-tension failure

Craushing
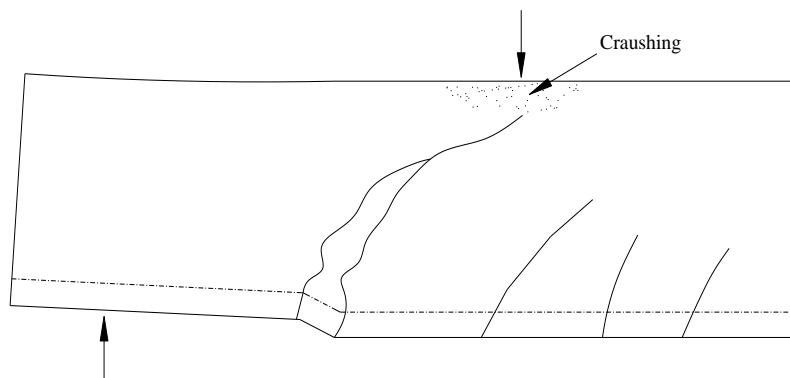
(b) Shear-compression failure

Figure 2.6 Modes of failure of short shear spans with $\left(\frac{a}{d}\right)$ ranging 1.5 to 2.5 (ASCE-ACI 1973).

(c) Slender: with aid ranges from 2.5 to about 6. In these beams the inclined cracks disturb the equilibrium to such an extent that the beam fails at inclined cracking as shown in Figure 2.7.

Loss of bond due to splitting crack
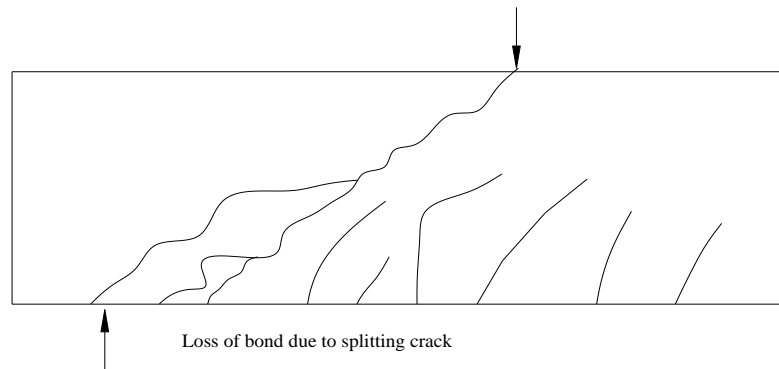
Figure 2.7 Typical Shear failure of slender beam.

(d) Very slender: with aid greater than about 6. These beams will fail in flexure prior to the formation of inclined cracks.

2.3.1.3 Factors affecting shear strength

For beams without shear reinforcement, the shear resisting capacity includes the five resisting mechanisms listed earlier. The shear resisting capacity (shear strength) is influenced by the following variables as introduced by the ASCE-ACI (1999):

(a) The concrete tensile strength;

(b) The longitudinal reinforcement ratio;

(c) Shear span-to-depth ratio;

(d) Axial forces; and

(e) Depth of concrete members (size effect).

2.3.2 Shear in Reinforced Concrete Beams with Shear Reinforcement

The shear failure of the concrete beams is brittle and catastrophic in nature. This failure occurs without sufficient advance warning. Thus, the purpose of using shear

reinforcement is to ensure that the full flexural capacity of the concrete member can be developed.

2.3.2.1   Internal forces in a concrete beam with shear reinforcement

The main purpose for providing shear reinforcement to a reinforced concrete element is to achieve its flexural capacity, minimize the shear deformation, and keep the element away from the brittle shear failure. The internal forces in a typical concrete beam reinforced with steel stirrups and intersecting a diagonal shear crack are shown in Figure 2.7(a). The shear is transferred across line A-B-C and consequently accumulate the following contributions:

(a)   The shear in the compression zone, V_{cz};

(b)   The vertical component of the shear transferred across the crack by interlock of the aggregate particles on the two faces of the diagonal crack, V_{ay};

(c)   The dowel action of the longitudinal reinforcement, V_d, and

(d)   The shear transferred by tension in the stirrups, V_s.

The loading history of such a beam is shown qualitatively in Figure 2.8(b).

As shown in Figure 2.8(b) the summation of the internal shear resistance components must equal the applied shear force which is represented by the uppermost line. Prior to flexural cracking, all shear is carried by the un-cracked concrete. Between flexural and inclined cracking, the external shear is resisted by V_{cz}, V_{ay}, and V_d (the concrete components).

As soon as the inclined cracks appear, the stirrups resist a portion of the applied shear and noted as stirrup contribution, V_s. Eventually, the stirrups crossing the crack yield, and V_s remains constant for higher applied shears. Once the stirrup yields, the inclined crack opens more rapidly. As the inclined crack widens, the aggregate interlocking component, V_{ay}, decrease further, forcing V_d and V_{cz} (dowel action and un-cracked concrete contributions) to increase at accelerated rate until either splitting (dowel)

failure occurs or the compression zone fails due to combined shear and compressive stresses.
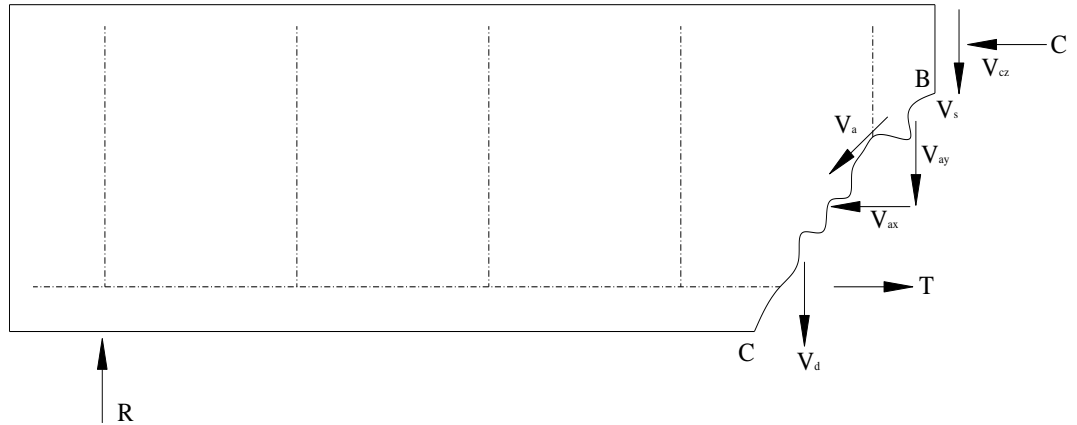
(a) Shear resisting mechanism.
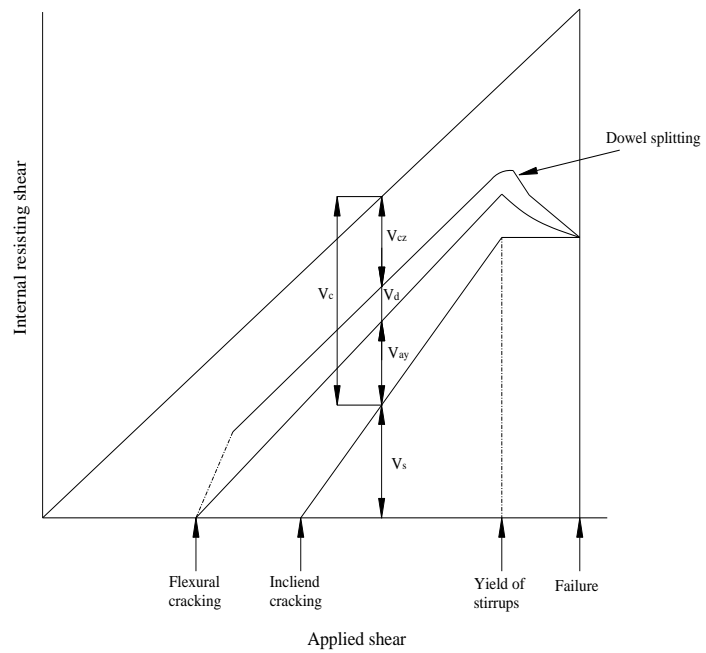
(b) Distribution of initial shear.

Figure 2.8 Internal forces in a cracks concrete beam with stirrups (ASCE-ACI 1973).

Each of three aforementioned shear resisting components of this process except V_s has a brittle load-deflection response. As a result it is difficult to quantify the contribution of V_{cz}, V_{ay} and V_d at ultimate. In design, these are lumped together as V_c referred to as "the

shear carried by concrete". Thus the nominal shear strength, V_n, is assumed to be as follows:

$$V_n = V_c + V_s \qquad (2.1)$$

Traditionally in North American design practice, V_c, is taken equal to the shear force at the initiation of inclined shear cracking, V_{cr}, which approximately equals the ultimate shear strength of slender concrete beams without stirrups.

2.3.2.2   Role of shear reinforcement in concrete beams

Prior to diagonal cracking, the strain in the stirrups is equal to the corresponding strain in surrounding concrete. The stresses in the stirrups prior to diagonal cracking will not exceed 20to 40 MPa (MacGregor 1997). Winter and Nilson (1979) reported that there is no noticeable effect for the shear reinforcement prior to the formation of diagonal cracks and the shear reinforcement could be free of stress until the diagonal cracking. Thus, the stirrups do not prevent the appearance of the diagonal cracks; they come into play only after the cracks have formed. The stirrups enhance to the shear performance of a beam, in addition to their contribution to the shear strength, V_s, by the following means:

(a) Improve the contribution of the dowel action. The stirrups effectively support the longitudinal reinforcement that crossing the flexural shear cracks close to the stirrup.

(b) Control the widths of the diagonal shear cracks and, in turn, maintain the contribution provided by the aggregate interlock.

(c) Confine the cross section when closely spaced stirrups are used. This increases the compressive strength of the concrete and enhances the zones affected by the arch action.

(d) Enhance the bond and prevent the breakdown when splitting cracks develop in anchorage zone due to dowel forces.

It can be summarized that the shear reinforcement in concrete beams maintain the overall integrity of the concrete contribution, V_c, allowing the development of additional shear forces, V_s, which increases the shear capacity and prevents the premature shear failure.

2.3.2.3 Modes of shear failure

There are various modes of failure that can be observed in concrete beams reinforced with shear reinforcement. These modes of failure can be summarized as:

(a) Failure of shear reinforcement (stirrups). When the steel stirrups reaches their yield stress, the shear crack widths get wider resulting in breakdown of the aggregate interlocking. Consequently, the beam fails in shear due to crushing or shearing of the compression zone above the neutral axis.

(b) Failure due to crushing of the beam web. This failure mode usually happens either when the beam has a thin web that may crush due to inclined compressive strength or when the beam is provided with very high shear reinforcement ratio.

(c) Failure of the stirrups anchorage. The functionality of the stirrups depends on their mechanical anchorage. Losing the anchorage before stirrup yielding will cause a sudden failure of the beam without achieving the stirrup capacity.

(d) Failure of the flexural reinforcement. The shear cracking yields more tensile stresses in the flexural reinforcement which may lead to yielding of the longitudinal reinforcement or anchorage failure.

(e) Failure to meet the serviceability requirements. However, there is no specific shear crack width specified in the design codes, but the larger shear crack widths at service load may not be accepted.

2.3.3   Shear Strength Analysis of Reinforced Concrete Beams

The manner in which the shear failures occur varies widely depending on the dimensions, geometry, loading and properties of the members. For this reason, there is no unique way to design for shear (MacGregor 1997). Moreover, for complex phenomena influenced by many variables understanding the meaning of particular experiments and the range of applicability of the results is extremely difficult unless the research is guided by an adequate theory which can identify the important parameters (Collins et al. 2007). Several attempts have been made to rationalize the shear design procedures for reinforced and pre-stressed concrete members decades ago. Some of these procedures were reviewed in the ASCE-ACI Committee 426(1973) report. Recently, the ASCE-ACI Committee 445 (1999) has published an up dated report reviewing some of the shear models developed for concrete members. This section provides summary of the shear models for reinforced concrete beams. Some of these models are based on the equilibrium conditions and some others depend on the compression field approach as follows:

(a) Models based on equilibrium approach:
   a. The 45° Truss Model.
   b. Variable-Angle Truss Model.
   c. The Modified Truss Model.

(b) Methods based on compression field approach:
   a. Compression Field Theory (CFT).
   b. Modified Compression Field Theory (MCFT).
   c. Rotating-Angle Softened Truss Model (RA-STM).
   d. Fixed-Angle Softened Truss Model (FA-STM).
   e. Disturbed Stress Field Model (DSFM).

(c) Shear Friction Model (SFM).

(d) Strain Based Shear Strength Model

2.4 Design Procedures

Although there are significant efforts to rationalize shear behaviour in concrete beams, many current code requirements are based on empirical for estimating the shear strength of concrete beams. The following subsections present the different design approaches used in national and international codes of practice. Other codes of practice are similar to or slightly different from the aforementioned approaches.

2.4.1 American Concrete Institute, ACI 318

The ACI code adopts the 45-degree truss model with an additional term for the concrete contribution, as follows:

$$V_d = \emptyset\, V_n \tag{2.2}$$

$$V_n = V_c + V_n \tag{2.3}$$

$$V_c = \left(\sqrt{f_c'} + 120\, \rho_{si}\, \frac{V_u d}{M_u} \right) \frac{b_w\, d}{7} \quad \leq \quad 0.3\, \sqrt{f_c'}\, b_w\, d \tag{2.4}$$

Where $\emptyset$ is the strength reduction factor for shear ($\emptyset = 0.85$) and V_u and M_u are the applied shear force and moment at the critical section.

The $\frac{V_u d}{M_u}$ term is generally small. Therefore ACI 318 allows the use of the following simplified equation:

$$V_c = 0.17\, \sqrt{f_c'}\, b_w\, d \tag{2.5}$$

Equation (2.4) and (2.5) for V_c are applied for $\frac{V_u d}{M_u}$ values higher than 1.0. However, the ACI code uses a multiplier to V_c for deep flexural beams, as given by:

$$V_c = \left(3.5 - 2.5 \frac{M_u}{V_u d}\right) 0.17 \sqrt{f_c'} \; b_w \; d \qquad (2.6)$$

For the stirrup contribution to shear, the conservative 45-degree truss model is used as follows:

$$V_s = \frac{A_{sv} \, f_{xsy} \, d}{S} \qquad (2.7)$$

The stirrup contribution, V_s given by equation (2.7), is determined based on the 45-degree truss model assuming that all the stirrups crossing the shear crack have reached yield and hence equation (2.7) governs the shear-yield (shear-tension) mode of failure.

To avoid shear failure initiated by crushing of the concrete before utilization of the full capacity of the shear reinforcement, the ACI 318 limits V_s to $\frac{2}{3} \sqrt{f_c'} \, b_w \, d$; hence, the upper bound condition of ACI equation (2.3) for shear-compression failure may be rewritten as follows:

$$V_n = V_c + \left\{\frac{2}{3} \sqrt{f_c'} \, b_w \, d \right\} \qquad (2.8)$$

The ACI 318 code requires a minimum amount of shear reinforcement for non-pre-stressed members reinforced with steel, as given by the following equation:

$$\rho_{sw \, min} = \frac{A_{sv \, min}}{b_w \, S} = \frac{0.345}{f_{syv}} \qquad (2.9)$$

2.4.2 Canadian Standards Association, CSA-M23.3-94

The Canadian code CSA-M23.3-94 permits two alternative methods of shear design of reinforced concrete beams, namely, the simplified methods and the general method. The simplified method is based on the traditional "concrete plus steel contributions" approach whereas the general method is derived from the modified compression field theory.

2.4.2.1 Simplified Method

The simplified method is based on the 45-degreetruss model with an effective depth of d. The shear resistance V_d can be determined by the following equation:

$$V_d = V_{cd} + V_{sd} \tag{2.10}$$

The concrete contribution is given by:

$$V_{cd} = 0.25 \, \lambda \, \phi_c \, \sqrt{f_c'} \, b_w \, d \qquad\qquad d \leq 300 \; mm \tag{2.11}$$

$$V_{cd} = \frac{260}{\frac{1000}{d}} \lambda \, \phi_c \, \sqrt{f_c'} \, b_w \, d \; \geq 0.1 \, \lambda \, \phi \, \sqrt{f_c'} \, b_w \, d \qquad d > 300 \; mm \tag{2.12}$$

Where λ equals 1.0 for normal density concrete and ϕ_c is the material safety factor for concrete ($\phi_c = 0.60$).

The steel contribution is given by:

$$V_{sd} = \frac{\phi_c \, A_{sv} \, f_{syv} \, d}{S} \qquad \leq \qquad 0.8 \, \lambda \, \phi_c \, \sqrt{f_c'} \, b_w \, d \tag{2.13}$$

Where ϕ_c is the material safety factor for steel ($\phi_c = 0.85$).

The 1994 CSA23.3 code requires a minimum amount of shear reinforcement for non-pre-stressed members reinforced with steel, as given by the following equation:

$$\rho_{SV\ min} = \frac{A_{SV}\ min}{b_w\ S} = 0.06\ \frac{\sqrt{f_c'}}{f_{syv}} \tag{2.14}$$

2.4.2.2 General Method

The general method is based on the MCFT, however, it is formulated in the form of a concrete contribution plus steel contribution approach. Designing or analysing using the general method requires the determination of the effective shear depth jd , which is assumed in the Canadian Standard as being not less than 0.9d.

The nominal shear strength of a beam can be determined by the following equation:

$$V_d = \frac{V_{cd}}{V_{sd}} \quad \le \quad 0.25\ f_c'\ b_w\ jd \tag{2.15}$$

$$V_{cd} = 1.3\ \lambda\ \phi_c\ \beta\ \sqrt{f_c'}\ b_w\ jd \tag{2.16}$$
$$V_{sd} = \frac{\phi_c\ A_{sv}\ f_{syv}}{S}\ jd\ cot\theta \tag{2.17}$$

Where β and θ are determined from Figure 2.9 for sections with shear reinforcement, $v_f = \frac{V_u}{b_w}\ jd$ and ε_x is the longitudinal strain of flexural tension chord of the member, which can be estimated as:

$$\varepsilon_x = \frac{\frac{M_u}{jd} + 0.5\ V_u \cot\theta}{E_s\ A_{sl}} \tag{2.18}$$

Where M_u is the moment at the critical section, A_{sl} is the cross-sectional area of longitudinal steel in the flexural tension side of a beam and E_s is the elastic modulus of longitudinal steel in the flexural tension side of beam.
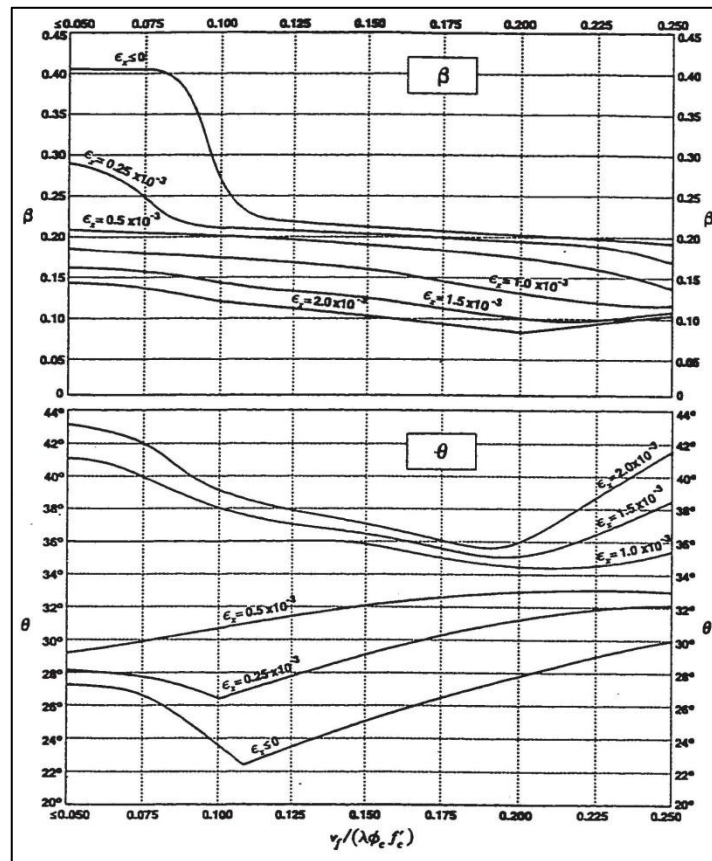
Figure 2.9 Values of β and θ for sections with shear reinforcement (CSA23.3-1994

general method)

The determination of ε_x is dependent on the location of the critical section that dictates

the values of M_u and V_u. Visualizing the beam as a variable-angle truss, the yielding of

shear reinforcement occurs over a length of $jd\ cot\theta$ (Collins et al. 1996). It is

reasonable to consider the section in the middle of this length as being critical.

Therefore, the critical section may be taken at a distance of $0.5jd\ cot\theta$ is taken as

approximately equal to jd. The θ values given by Figure 2.9 have been chosen to insure

that the stirrup strain ε_{sv} is at least 0.002 and to insure that, for highly stressed

members, the principal compressive stress in the concrete does not exceed the crushing

strength (Collins et al. 1996).
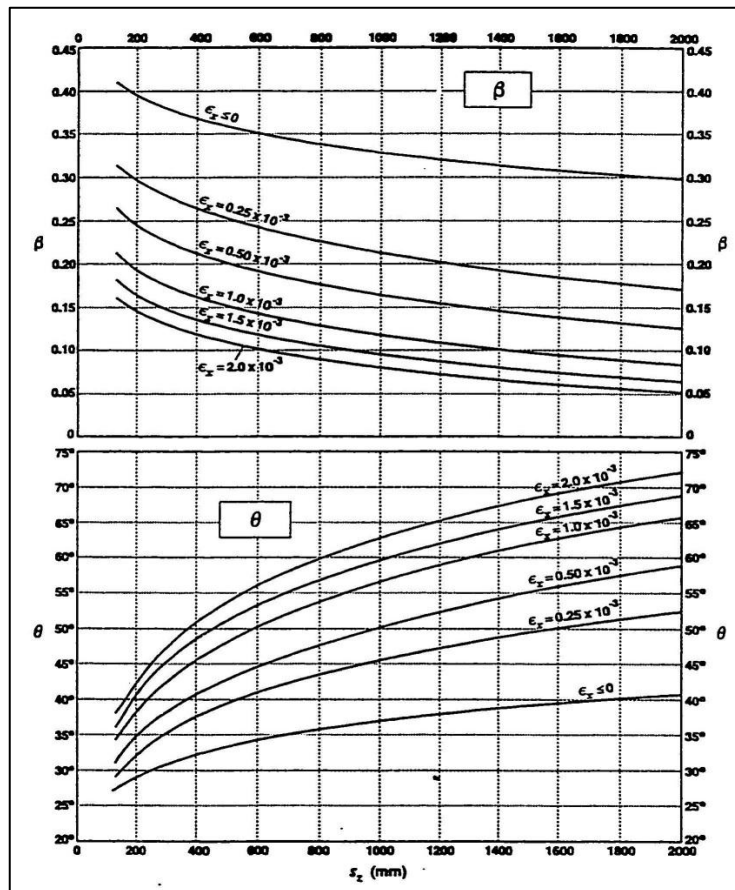
Figure 2.10 Values of β and θ for sections without shear reinforcement (CSA23.3-1994

general method)

β and θ are determined from Figure 2.10 for sections without shear reinforcement, where S_z is the spacing of the cracks perpendicular to longitudinal reinforcement. This spacing is a function of the maximum distance between longitudinal bars or longitudinal bars and the flexural compression zone. For beams with less than the minimum shear reinforcement and no intermediate layers of longitudinal crack control reinforcement, the crack spacing parameter S_z may be taken as *jd* (or 0.9*d*).

There is no direct solution to find the shear strength of a beam using the general method. First, the applied shear load V_u has to be assumed and the design shear strength V_d can be determined by equations (2.15), (2.16) and (2.17). This process is iterated until V_u equals V_d.

30

2.4.3 Eurocode, EC2 Part 1

The Euro-code (EC2 1992) is partly based on the theory of plasticity by Nielsen (1984).

Two methods of design are given:

(a) The Standard Method, which combines a concrete contribution and stirrup contribution based on the 45-degree truss model.

(b) The Variable Strut Inclination Method.

Shear design is based on three values of shear resistance, stated as V_{rd1}, V_{rd2} and V_{rd3}. V_{rd1} refers to the shear capacity of a concrete member without shear reinforcement, determined from an empirical formula:

$$V_{rd1} = [\tau_{rd} k_d \beta \ (1.2 + 40 \ \rho_{sl})] b_w \ d \tag{2.19}$$

Where τ_{rd} is the basic design shear strength ($\tau_{rd} = 0.254 \ f_{ctk \ 0.05}/\gamma_c$), $f_{ctk \ 0.05}$ is the lower 5% fractile characteristics tensile strength ($f_{ctk \ 0.05} = 0.7 \ f_{ctm}$), f_{ctm} is the mean value of the tensile concrete strength ($f_{ctm} = 0.30 \ (f_c')^{2/3}$, γ_c is the material safety factor for concrete ($\gamma_c = 1.50$), k_d is the size effect factor ($k_d = 1.6 - 0.001 \ d \ \geq$ 1.0), ρ_{si} is the ratio of the longitudinal steel reinforcement ($\rho_{si} \leq 0.02$) and $\beta = 2.5 \frac{d}{a} (1.0 \ \leq \beta \leq 5.0)$.

The resistance V_{rd2} is the shear capacity of a beam when web crushing occurs according to the plasticity theory (Nielsen 1984). The maximum V_{rd2} value that can be attained is limited by the effective stress in the compression strut such that:

$$V_{rd2}(\max \ ) = 0.5 \ v \ f_{cd} \ b_w(0.9d) \tag{2.20}$$

$$v = 0.7 - \frac{f_c'}{200} \geq 0.50 \tag{2.21}$$

Where $f_{cd} = f_c'/\gamma_c$ and $\gamma_c = 1.50$.

The minimum shear reinforcement, $f_{SW\ min}$, is specified by the Eurocod2 (1992) in a table format, as a function of the concrete strength, f_c', and yield strength of the stirrups, f_{syv}. The difference between the Standard Method and the Variable Strut Inclination Method is in the determination of the resistance V_{rd3}. The alternative method of calculating V_{rd3} are discussed below.

2.4.3.1 Standard Method

The Standard Method is similar to the prevision of the ACI 318 with the total resistance given as follows:

$$V_{rd3} = V_{cd} + V_{sd} \tag{2.22}$$

$$V_{cd} = V_{rd1} \tag{2.23}$$

$$V_{sd} = \frac{A_{sv}\left(\frac{f_{syv}}{\gamma_s}\right)}{S}\ 0.9d \tag{2.24}$$

Where V_{cd} is the design concrete contribution in shear, V_{rd1} is given by equation (2.19), $V_{rd3}(\text{max})$ is given by equations (2.20) and (2.21) and γ_s is the material safety factor for steel ($\gamma_s = 1.15$).

2.4.3.2 Variable Strut Inclination Method

The variable strut inclination method is based on a truss with an angle θ chosen within the ranges of:

   (a) $0.4 < \cot\theta < 2.5$ for beams with constant longitudinal reinforcement

(b) $0.5 < \cot \theta < 2.0$ for beams with curtailed longitudinal reinforcement

The shear resistance based on the crushing of the compressive strut is:

$$V_{rd2} = \frac{b_w\ (0.9d) v\ (f_c'\ /\ \gamma_c)}{(\cot \theta + \tan \theta)} \tag{2.25}$$

The shear resistance based on a truss model with stirrups yielding is:

$$V_{rd3} = \frac{A_{sv}\ (f_{syv}\ /\ \gamma_c)}{S}\ 0.9d \cot \theta \tag{2.26}$$

A limitation based on the plasticity theory is placed on the effectiveness of the shear reinforcement such that:

$$\frac{A_{sv}\ (f_{syv}\ /\ \gamma_c)}{b_w\ S} \leq 0.5 v\ (f_c'\ /\ \gamma_c) \tag{2.27}$$

2.4.4   British Standard BS8110

Similar to ACI cod, the BS8110 code adopts the 45-degree truss model with an additional term for the concrete contribution. The following equations are used for shear design of beams reinforced with steel:

$$V_d = V_{cd} + V_{sd} \qquad \leq \quad 0.80\ \sqrt{f_{cu}}\ b_w\ d \quad \leq 5.0\ b_w\ d \tag{2.28}$$

$$V_{cd} = 0.925\ (100\ \rho_l)^{1/3}\ (f_{cu}\ /\ 40)^{1/3}\ (400\ /\ d)^{1/3}\ b_w\ d\ /\gamma_c \tag{2.29}$$

$$V_{sd} = \frac{A_{sv}\ f_{syv}\ d}{\gamma_s\ S} \tag{2.30}$$

Where f_{cu} is the concrete cube strength ($f_{cu} = 1.25\, f_c'$). γ_c is the material safety factor for concrete ($\gamma_c = 1.25$), Gama s is the material safety factor for concrete ($\gamma_s = 1.1.5$) and $(f_{cu}/40)^{1/3}$ should not exceed 1.0.

The 1985 BS8110 code requires a minimum amount of shear reinforcement for non-pre-stressed members reinforced with steel, as given by the following equation:

$$f_{SV\ min} = \frac{A_{SV\ min}}{b_w\ S} = \frac{0.4}{f_{syv}\ \gamma_s} \tag{2.31}$$

2.5 FRP as Shear Reinforcement for Flexural Members

The use of FRP as shear reinforcement for concrete beams has been reported by various researchers in many countries. The majority of the work done has been devoted to evaluation of the shear strengthening of existing concrete members using FRP laminates as external shear reinforcement. However, the use of FRP as initial shear reinforcement in the form of stirrups has not been fully investigated. The following sections review the available results of research work conducted to evaluate the behaviour of FRP as shear reinforcement for concrete members.

2.5.1 Open Stirrups

The shear behaviour of concrete beams reinforced with GFRP bars has been investigated by Vijay et al. (1996). The work addresses the shear behaviour of concrete beams reinforced with FRP bars and stirrups. The experimental programme examined the applicability of ACI equation, the failure modes and the ductility factors based on energy and deformability concepts. Six beams were tested using a two-point loading system. The parameters of this study were the concrete compressive strength and the

stirrup spacing. Dimensions, details and test results of beams tested by Vijay et al. (1996) are summarized in Table 2.3. The fatigue of this investigation can be summarized as follows:

(a) The ACI 318 shear equation is conservative and adequate for the design of FRP stirrups. The following equation was used to predict the concrete contribution in shearV_{cf}.

$$V_{cf} = 0.17\sqrt{f_c'}\, b_w\, d \tag{2.32}$$

(b) The permissible design stress values in FRP stirrups should be based on their bend capacity and the bond characteristics. In this study, the strength capacity of the stirrups was observed to be 248 Mpa, which corresponds to about 38 present of the strength parallel to the fibres.

A design procedure for concrete beams reinforced for shear and/or flexural with GFRP bars was proposed by Alsayad et al. (1996 and 1997). GFRP bars in the form of single loop stirrups with overlapping ends were used as shear reinforcement. Seven beams were designed to fail in shear and were tested under a two point loading system. The parameters considered were the material type of the longitudinal reinforcement and the material type of the shear reinforcement. Dimensions, and details and test results of beams tested by Alsayad et al. (1996 and 1997) are summarized in Table 2.4 and 2.5. The findings of this study can be summarized as follows:

(a) All beams failed in shear. For the beams with GFRP stirrups, shear failure was due to the slippage of the stirrups rather that rupture.

(b) The following modification to the ACI equation for shear was proposed:

$$k_1 \, V_c + \, k_2 \, V_s \tag{2.33}$$

$$V_c = \frac{1}{6} \, \sqrt{f_c'} \tag{2.34}$$

$$V_s = \frac{A_v \, f_v \, d}{S} \tag{2.35}$$

Where the values of k_1 and k_2 are:

1.0 and 1.0 for beams by steel for flexural and shear

0.5 and 0.5 for beams reinforced with GFRP for flexural and shear

1.0 and 0.5 for beams reinforced with steel for flexural and GFRP for shear

0.5 and 1.0 for beams reinforced with GFRO for flexural and steel for shear

(c) The proposed modification to the ACI equation was checked against the measured shear capacity and the results were found to be within the acceptable accuracy.

2.5.2 Closed-Loop Stirrups

The shear behaviour of concrete beams reinforced with FRP bars for flexural and shear was examined by Zhao et al. (1995). In particular, the contribution of FRP stirrups was studied in terms of the strain in the stirrups, shear crack opening and shear deformation. FRP stirrups were manufactured continuously in the form of closed loop. The shape and dimensions of beam specimens are shown in Figure 2.11. A notch was provided at the most probable location of diagonal crack initiation in one half span of the beam so as to induce a diagonal crack within the target region for measurements of crack opening and stirrup strain. Nineteen beams were tested with variation of the flexural reinforcement

ratio, the location and spacing of stirrups, the material type of the stirrups and the shear span-to-depth ratio, *a/d*. dimensions, details and test results of beams that failed in shear are summarized in Table 2.6. the finding of this study can be summarized as following:

(a) All beam specimens expect two failed in shear. The failure was classified as shear-compression failure since none of the stirrups ruptured expect in one beam.

(b) When the shear-compression failure was dominate, the higher stiffness of stirrup resulted in the higher shear capacity and smaller strain at ultimate.

(c) The concrete contribution, V_{cf} for beams reinforced with FRP as longitudinal reinforcement was evaluated by the conventional code equations taking into account the ratio of the stiffness of FRP to that of steel, E_f / E_s. The following expression was used in this study to predict the concrete contribution:

$$V_{cf} = 0.20 \ (1 + \beta_P + \beta_d) \left\{ 0.75 + \frac{1.4}{ad} \right\} f_c'^{\sqrt{3}} b_w \ d \tag{2.36}$$

$$\beta_P = (100 \ \rho_{fl}^*)^{\sqrt{2}} - 1 \leq 0.73 \tag{2.37}$$

$$\beta_d = \left(\frac{1000}{d} \right)^{\sqrt{4}} - 1 \tag{2.38}$$

$$\rho_{fl}^* = \rho_{fl} \left(\frac{E_{fl}}{E_s} \right) \tag{2.39}$$

Where E_{fl} is the elastic modulus of FRP longitudinal reinforcement and E_s is the elastic modulus of steel ($E_s = 200$ GPa).

(d) The ratio of flexural reinforcement had insignificant effect on the shear capacity.

(e) The strain distribution along a diagonal crack can be expressed by a cubic function as illustrated in Figure 2.12.

The size effect of the specimens for concrete beams reinforcement with FRP was investigated by Maruyama and Zhao (1996). The contribution of FRP stirrups was studied in terms of the strain stirrups, shear crack opening and shear deformation. CFRP grids were used for flexural reinforcement and GFRP bars of three different sizes were used for shear reinforcement in the form of closed-loop stirrups. The configuration of beam specimens was similar to that of those tested by Zhao et al (1995), as shown in Figure 2.11. The experimental programme consisted of testing of nine specimens of three different size of beams of rectangular cross-section, $150 \, x \, 300mm$, $300 \times 600mm$ and $450 \times 900mm$. The beam length was selected to provide a shear span-to-depth ratio of 2.5. In addition to the effective depth, the test parameters included the amount of shear reinforcement and influence of the botch (Figure 2.11) on the shear strength. The finding of this study can be summarized as follows:

(a) All beam specimens failed in shear. The failure was classified as one of the following modes of failure: (i) diagonal tension failure for beam without stirrups, (ii) shear-compression failure for beams with large amount of stirrups, (iii) rupture of stirrups and (iv) shear-compression with rupture of stirrups (balanced mode of failure).

(b) It was observed that the difference in reinforcing materials does not significantly influence the size effect as far as the concrete contribution for shear capacity, V_{cf} is concerned.

$$V_{cf} = 0.20 \, \beta_p \beta_d \left\{ 0.75 + 1.4 \left(\frac{a}{d} \right) \right\} f_c'^{1/3} \, b_w \, d \tag{2.40}$$

(c) Based on the test results of this study, the strain distribution along a diagonal crack was assumed to be proportional to η_i which is defined by the following function:

$$\eta_i = 1 - 3.3 \left(\frac{L_i}{L_o} - 0.7\right)^2 \tag{2.41}$$

Where η_i equal 1.0 at the point of intersection of the shear crack with the longitudinal reinforcement and zero at the tip of the shear crack, and $\frac{L_i}{L_o}$ ratio is defined in Figure 2.12.

(d) Taking into account the strain distribution of stirrups, the contribution of stirrups V_{sf} was determined using the following equation:

$$V_{sf} = A_{fv} \, E_{fv} \, \varepsilon_{fv} \, jd \, / \, S \tag{2.42}$$

Where ε_{fv} is the ultimate strain of FRP stirrups which was formulated as a function of a/d and amount of shear reinforcement, and ε_{fv} is the elastic modulus of shear reinforcement.

Figure 2.11 Details of specimens by Zhao et al (1995)

Figure 2.12 Model of stirrup strain distribution by Zhao et al (1995)

Seven concrete beams reinforced for flexural and shear with GFRP bars were tested by Duranovic et al. (1997) to examine the shear strength and the modes of failure. GFRP closed-loop stirrups of $10 \times 4mm$ rectangular cross-section were used as shear reinforcement. The bend capacity of the GFRP stirrups was varied from 390 to 410 MPa. Two beams reinforced with steel bars were tested as control specimens. The main variable of this study was the stirrup spacing. Dimensions, details and test results of beams failed in shear are summarized in Table 2.7. the finding of this investigation can be summarized as follows:

(a) Failure of the beams was due to either shear for beams without shear reinforcement, or flexural compression or shear-rupture for beams with shear reinforcement. Two beams reinforced with GFRP stirrups failed in shear by rupture of the stirrups. However, stresses measured by means of strain gauges on the GFRP stirrups never exceeded 270 Mpa.

(b) The shear strength of beams was predicted by using the modifications proposed by the Eurocrete Project (1996) to British code BS8110. The measured strain in the stirrups exceeded the design strain value of 0.0025 recommended by

Eurocrete Project (1996). Therefore, the predicted values were very conservative when compared to the measured values.

2.5.3 Preformed Spirals

The flexural and shear behaviour of reinforced and prestressed concrete beams using CFRP or AFRP bars were investigated by Yonekura et al. (1993). The objective of this study was to examine the flexural strength. Modes of failure and shear strength of reinforced and prestressed concrete beams using FRP as longitudinal and shear reinforcement. CFRP strands and AFRP bars were used as prestressing tendons and longitudinal reinforcement. Beams prestressed by conventional steel bars were tested as control specimens. AFRP spiral reinforcement was used as shear reinforcement. Twenty I-shaped beams were tested in the flexural phase of this study and 12 beams were tested in the shear phase. Details of the test specimens are shown in Figure 2.13. the parameters selected for the experimental programme were the type of prestressing tendons, the type of longitudinal reinforcement, quantities of prestressing tendons, the amount of initial prestressing force and the amount of shear reinforcement provided by varying the pitch of the FRP spiral. Dimensions, details and test results of reinforced concrete beams failed in shear are summarized in Table 2.8. The finding of the shear phase of this study investigation can be summarized as follows:

(a) The beams tested for shear failed either by shear-compression or by rupture of the spiral shear reinforcement.

(b) The shear strengths of prestressed concrete beams using FRP tendons and FRP spiral stirrups are smaller than those using steel tendons and steel stirrups when similar shear contribution was provided by the stirrups.

(c) The proposed equation predicted safely the shear strength of reinforced and prestressed beams tested for shear. The ratios of observed to calculated shear strength were greater than 1.0 for all beams; an average of 1.23 was obtained.

(d) The ultimate flexural and shear strengths of prestressed concrete beams using FRP bars were improved by increasing the prestress force.

The shear performance of specially designed concrete beams reinforced with FRP stirrups was studied by Nagasaka et al. (1993). The objective was to investigate the effect of pre-shaped FRP stirrups on the shear behaviour of concrete beams. Four types of bars, braided CFRP bars, braided AFRP bars, hybrid glass and carbon FRP bars and steel bars were used as shear reinforcement. These shear reinforcements were used in the form of rectangular spiral stirrups, expect for the hybrid bars that were in the form of rectangular closed-loop stirrups. The FRP stirrups were characterized by the ensile strength parallel to the fibres, f_{fuv}, and the bend capacity of the stirrup f_{bend}. Thirty-five beams of effective cross-sectional dimensions of were specially detailed and subjected to anti-symmetrical loading, as illustrated in Figure 2.14. the variables considered were the type and reinforcement ratio of stirrups, the concrete compressive strength and the clear span. Dimensions, details and test results of the beams tested by Nagasaka et al. (1993) are summarized in Table 2.9. the finding of this this investigation can be summarized as follows:

(a) Shear failure of the beams with FRP stirrups occurred due to rupture of the stirrups at the bend zone or due to crushing of a concrete strut formed between diagonal cracks.

(b) The shear strength of beams that failed due to rupture of the stirrups increased almost linearly with increasing ratio of shear reinforcement and decreased almost linearly with the clear span of the beam.

(c) The shear strength of beams that failed due to concrete crushing increased with increasing ratio of shear reinforcement, but the rate of increase had a tendency to reduce when the ratio was over 1%.

(d) The shear strength of beams increased roughly linearly with the square root of $\rho_{fv} E_{fv}$. This demonstrates that shear strength was affected by the axial rigidity of the shear reinforcement.

(e) The rupture and crushing modes were distinguished by the shear reinforcement factor $\rho_{fv} f_{bend} / f_c'$, and the critical value of the factor was found to be about 0.30. For beams with a small $\rho_{fv} f_{bend} / f_c'$ factor, a rupture mode of failure occurs, and for beams with high $\rho_{fv} f_{bend} / f_c'$ factor, crushing mode of failure occurs.
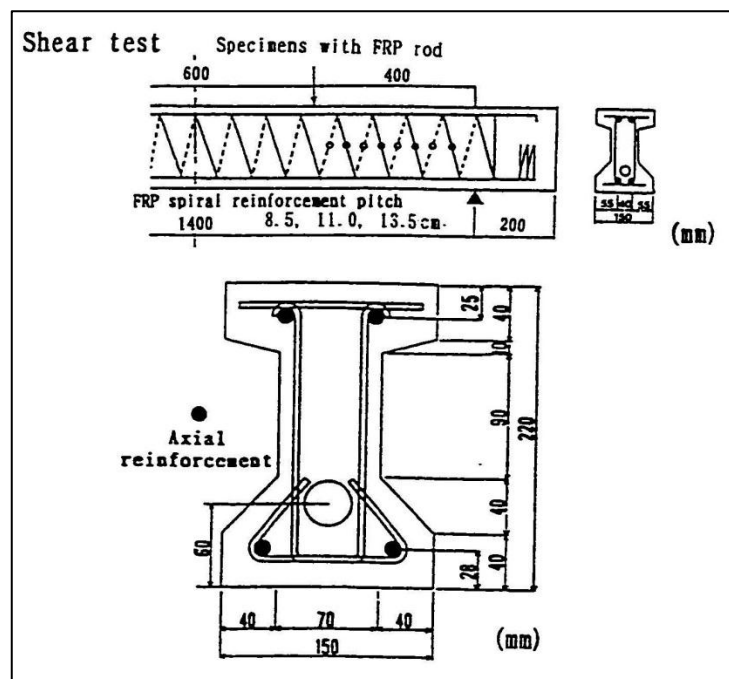
Figure 2.13 Detais of specimens by Yonekura et al. (1993)
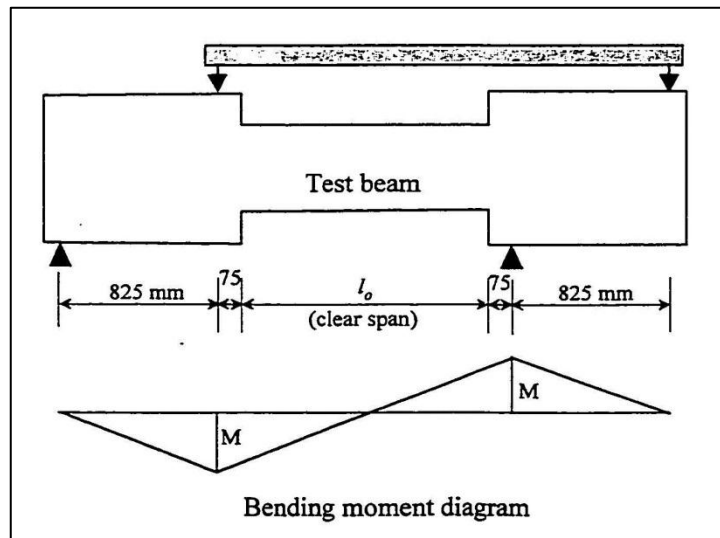
Figure 2.14 Outline of specimens and test setup by Nagasaka et al. (1993)

The shear capacity of concrete beams using FRP as flexural and shear reinforcement was investigated experimentally by Tattori and Wakui (1993). CFRP composite cables were used as longitudinal reinforcement. GFRP, AFRP, CFRP and Vinylon FRP bars were used as shear reinforcement in the form of spiral. Specially designed specimens were tested to evaluate the dowel capacity of CFRP flexural reinforcement. Shear tests of reinforced concrete beams were conducted on several beams with different types of shear reinforcement. The shear force contributed by the shear reinforcement was measured by means of strain gauges installed on the FRP spirals. Dimensions, details and test results of the beams tested by Tattori and Wakui (1993) are summarized in Table 2.10. the finding of this this investigation can be summarized as follows:

(a) The shear force carried by the compression zone and aggregate interlock was measured to be related to the tensile stiffness of the longitudinal reinforcement. Therefore, the shear capacity of concrete beams without shear reinforcement was proposed to be the larger V_{cf1} and V_{cf2}, given as follows:

$$V_{cf1} = 0.2\,(f_c')^{1/3}\,(\rho_{fl}^*)^{1/3}\left(\frac{1000}{d}\right)^{1/4}\left(0.75 + \frac{1.4}{a\,d}\right)b_w\,d \tag{2.43}$$

$$V_{cf2} = 0.244\,(f_c')^{2/3}\left(1 + \sqrt{\rho_{fl}^*}\right)\frac{\left\{1 + 3.33\left(\frac{r}{d}\right)\right\}}{\left\{a + \left(\frac{a}{d}\right)^2\right\}}\,b_w\,d \tag{2.44}$$

Where $\rho_{fl}^* = \rho_{fl}\,(E_{fl}/E_s)$ and r is the length of the loading plate in the direction of the beam span.

   (b) The dowel capacity of the test specimens using FRP reinforcement is about 70% of those using reinforcing steel with almost the same diameter. This ratio happened to correspond to the factor $(E_{fl}/E_s)^{1/3}$, which is included in equations (2.43) and (2.44).

   (c) The stirrup strain value at ultimate was observed to be more than 1%, but did not reach the guaranteed value of the rupture strain, corresponding to f_{fuv}.

   (d) Based on the measured shear force contributed by the FRP spirals, the contribution of concrete to the shear resisting force was observed to be equal to the shear cracking load of the beams.

   (e) The stirrups contribution to the shear capacity of concrete beams with FRP spirals was estimated using the following equation:

$$V_{sf} = \frac{A_{fv}\,E_{fv}\,jd}{S}\,\varepsilon_{fv} \tag{2.45}$$

Where jd is the shear depth of the beam ($jd = d/1.15$) and ε_{fv} is the stirrup strain at ultimate. Based on the experimental results, the value of ε_{fv} was recommended to be 0.01 as far as the mode of failure is shear-rupture. There was no correlation observed between ρ_{fl} obtained by shear tests and a/d, and f_c'.

2.5.4   On-site Fabricated Stirrups

A new process to fabricate CFRP stirrups with a curved shape has been reported by Okumura et al. (1993). 10mm CFRP rope shaped pre-pregnated bars were used as shear reinforcement in the form of spirals. The strength of the bend was evaluated experimentally to be more than 0.9 f_{fuv} for $rb/db = 3.0$ and equivalent to f_{fuv} for $\frac{rb}{db} > 6.0$. Three beams reinforced for shear with CFRP spirals were tested under a two-point loading system. The beams were reinforced for flexural with steel bars. A beam without shear reinforcement was also tested as a control of the beams was predicted using Niwa's equation (1986) as the sum of the concrete compression, V_c, and the shear reinforcement contribution, V_{sf}, based on the truss model:

$$V_n = 0.2\, \rho_{sl}^{1/3} \left(\frac{1000}{d}\right)^{1/4} f_c'^{1/3}\, b_w\, d + \frac{A_{fv}\, f_{fv}\, jd}{S} \qquad (2.46)$$

Where *jd* is the shear depth (*jd = d/1.15*), ρ_{sl} is the reinforcement ratio of the steel longitudinal reinforcement and f_{fv} is the stress in the FRP spiral at ultimate.

The finding of this research can be summarized as follows:

- (a) Failure of beams occurred by rupture of the CFRP spirals. The spiral stress at ultimate was 65% of the tensile strength parallel to the fibres.
- (b) The contribution of the shear reinforcement was found to be between 55 and 70 percent of the calculated V_s. The reason for this was attributed to:
  - (i)   The tensile strength of CFRP pre-pregnated bars was reduced due to the kink effect at the crack location.
  - (ii) The crack width was large and the concrete contribution to the shear strength was reduced.

2.5.5 Two Dimensional Grids

The concept of using FRP planer grids for shear reinforcement in concrete beams has been investigated by Erik and Bakht (1996). Five 4 meter long beams, having a $225 \, x \, x \, 500mm$ cross-section, were tested to failure. Two configuration of CFRP grid, shown in Figure 2.15 and designed as Type I and Type II, were used to provide shear reinforcement for the beams. A modulus of elasticity of 71 GPa and tensile strength of 1200 MPA were obtained in laboratory testing of the CFRP grids. The cross-sectional area of the bars comprising the grids was $9.3mm^2$. Multiple grids were stacked to provide the necessary cross-sectional are of the bars for the beams. Conventional reinforcement consisting of steel was used in one of the beams. The beams with CFRP grids were designed to provide the same tensile stiffness as the steel stirrups. One beam was constructed using steel stirrups, two identical beams were constructed using Type I grid and two identical beams were constructed using Type II grid. All tested beams failed in flexural by concrete crushing after yielding of flexural steel. The strains in the CFRP grids did not exceed the ultimate tensile strain, so that no failure of the shear reinforcement occurred. The cross-bars of the grids also provided sufficient anchorage for the grids, so that no pull-out occurred in these tests. Based on their study, Erik and Bakht (1996) recommended the use of FRP planer grids for shear reinforcement in concrete beams as they require less labour for preparation and installation.

It should be mentioned that the use of FRP grids as shear reinforcement does not provide confinement for the concrete in the compression and tension sides of the beam and might permit vertical delamination of the concrete in thin-webbed beams.
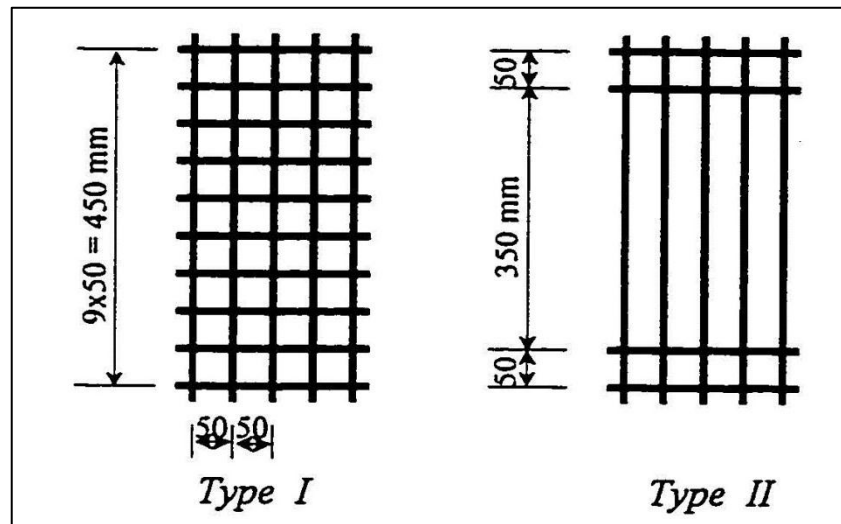
Figure 2.15 CFRP grids used by Erik and Bakht (1996)

2.5.6 FRP Diagonal Bars

The fundamental performance of reinforced concrete beams with diagonal FRP bars was investigated by Sonobe et al. (1995). Braided aramid FRP bars were used as longitudinal, diagonal reinforcement and stirrups for three specimens. The guaranteed tensile strength of the AFRP bars was 1320 MPa, and the elastic modulus was 59 GPa. Two specimens with steel reinforcement were also constructed. Details of a typical specimens and the test rig are shown in Figure 2.16. the parameters included the ratio of diagonal reinforcement to longitudinal reinforcement. The specimens were tested under ant symmetrical cycle load. Specimens with FRP diagonal reinforcement failed by rupture of stirrups and longitudinal reinforcement. The shear strength of the beams was calculated by the following equation:

$$V_n = V_{cf} + V_{sf} + A_{fvD} \, f_{fvD} \, sin\alpha_s \tag{2.47}$$

$$f_{fvD} = \frac{V_{cf} + V_{sf}}{A_{fl} \; + \; A_{fvD} \cos \alpha_s} \frac{L}{2 \, jd} \tag{2.48}$$

48

Where V_{cf} and V_{sf} are the shear resistance force carried by the concrete and the stirrups, respectively, which can be determined according to the modified Arakawa's equations, A_{fvD} is the area of diagonal reinforcement. α_s is the angle between diagonal reinforcement, L is the clear span length and jd is taken as $0.87d$.

The finding of this study can be summarized as follows:

(a) The shear strength of FRP reinforced specimens increases as the amount of diagonal reinforcement increases.

(b) The proposed method predicted well the shear strength of the specimens with FRP diagonal reinforcement.
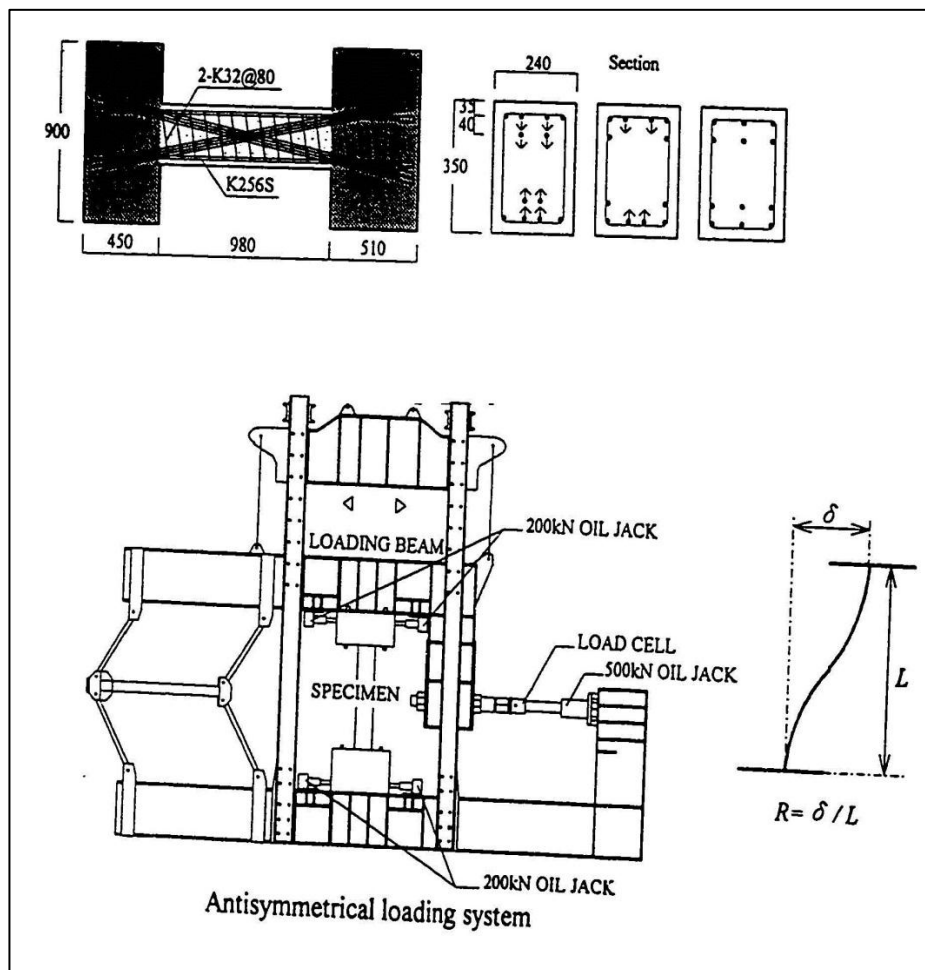
Figure 2.16 Details of specimens and test setup by Sonobe et al. (1995)

Table 2.3. Characteristics of beams tested by Vijay et al. (1996)

Beam No.	b_w mm	h mm	d mm	a/d	f'_c MPa	Reinforce-ment code	type	A_{fl} mm²	f_{ful} Mpa	E_{fl} Gpa	ρ_{fl} %	type	S mm	A_{fvl} mm²	f_{fuv} MPa	f_{bend} MPa	E_{fv} GPa	ρ_{fv} %	V_{test} kN	V_u MPa	Mode of failure
(1)	(2)	(3)	(4)	(5)	(6)	(7)	(8)	(9)	(10	(11)	(12)	(13)	(14)	(15)	(16)	(17)	(18)	(19)	(20)	(21)	(22)
1	150	300	264.5	1.89	44.8	F0	G	567	655	54	1.43	-							44.8	1.129	DT
2	150	300	264.5	1.89	44.8	FF	G	567	655	54	1.43	G	101.6	142	655	248	54	0.93	126.8	6.196	ST
3	150	300	264.5	1.89	44.8	FF	G	567	655	54	1.43	G	152.4	142	655	248	54	0.62	115	2.899	ST
4	150	300	264.5	1.89	31	F0	G	254	655	54	0.64	-							44.8	1.129	DT
5	150	300	264.5	1.89	31	FF	G	254	655	54	0.64	G	101.6	142	655	248	54	0.93	123.2	3.105	ST
6	150	300	264.5	1.89	31	FF	G	254	655	54	0.64	G	152.4	142	655	248	54	0.62	123.2	3.108	ST

Table 2.4. Characteristics of beams tested by Alsayed et al. (1996)

Beam No.	b_w mm	h mm	d mm	a/d	f'_c MPa	Reinforcement code	type	A_{fl} mm²	f_{ful} Mpa	E_{fl} Gpa	ρ_{fl} %	type	S mm	A_{fvl} mm²	f_{fuv} MPa	f_{bend} MPa	E_{fv} GPa	ρ_{fv} %	V_{test} kN	V_u MPa	Mode of failure
(1)	(2)	(3)	(4)	(5)	(6)	(7)	(8)	(9)	(10)	(11)	(12)	(13)	(14)	(15)	(16)	(17)	(18)	(19)	(20)	(21)	(22)
1	200	360	311	3.23	35.8	SS	S	603	553	200	0.97	S	150	56.6	286	N/A	200	0.19	88.9	1.430	ST
2	200	360	309.5	3.23	35.5	FF	G	851	700	36	1.37	G	150	63.3	565	N/A	42	0.21	68.5	1.107	ST
3	200	360	311	3.23	39.5	SS	S	603	553	200	0.97	S	150	56.6	286	N/A	200	0.19	100.4	1.614	ST
4	200	360	309.5	3.23	39.5	FF	G	851	700	36	1.37	G	150	63.3	565	N/A	42	0.21	57.8	0.936	ST

Table 2.5. Characteristics of beams tested by Vijay et al. (1996)

Beam No.	b_w mm	h mm	d mm	a/d	f'_c MPa	Reinforcement code	type	A_{fl} mm²	f_{ful} Mpa	E_{fl} Gpa	ρ_{fl} %	type	S mm	A_{fvl} mm²	f_{fuv} MPa	f_{bend} MPa	E_{fv} GPa	ρ_{fv} %	V_{test} kN	V_u MPa	Mode of failure
(1)	(2)	(3)	(4)	(5)	(6)	(7)	(8)	(9)	(10)	(11)	(12)	(13)	(14)	(15)	(16)	(17)	(18)	(19)	(20)	(21)	(22)
1	200	360	309	2.36	35.7	FF	G	804	764	43	1.30	G	80	63.3	565	N/A	42	0.40	108.9	1.762	ST
2	200	360	310	2.36	35.7	SF	S	616	553	200	0.99	G	80	63.3	565	N/A	42	0.40	144.4	2.330	ST
3	200	360	309	2.36	35.2	FS	G	804	764	43	1.30	S	80	56.6	286	N/A	200	0.35	103.5	1.675	ST

Table 2.6. Characteristics of beams tested by Zhao et al. (1995)

Beam No.	b_w mm	h mm	d mm	a/d	f'_c MPa	Reinforcement code	type	A_{fl} mm²	f_{ful} Mpa	E_{fl} Gpa	ρ_{fl} %	type	S mm	A_{fvl} mm²	f_{fuv} MPa	f_{bend} MPa	E_{fv} GPa	ρ_{fv} %	V_{test} kN	V_u MPa	Mode of failure
(1)	(2)	(3)	(4)	(5)	(6)	(7)	(8)	(9)	(10)	(11)	(12)	(13)	(14)	(15)	(16)	(17)	(18)	(19)	(20)	(21)	(22)
1	150	300	250	3	34.3	F0	C	568	1124	105	1.51	-							45	1.200	DT
2	150	300	250	3	34.3	F0	C	1136	1124	105	3.03	-							46	1.227	DT
3	150	300	250	3	34.3	FF	C	1136	1124	105	3.03	G	90	56.6	1100	N/A	39	0.42	113	3.013	SC
4	150	300	250	3	34.3	FF	C	1136	1124	105	3.03	C	90	56.6	1300	N/A	100	0.42	125.9	3.357	SC
5	150	300	250	3	34.3	F0	C	852	1124	105	2.27	-							40.5	1.080	DT
6	150	300	250	3	34.3	FF	C	852	1124	105	2.27	G	90	56.6	1100	N/A	39	0.42	116.2	3.099	SC
7	150	300	250	2	34.3	FF	C	568	1124	105	1.51	G	90	56.6	1100	N/A	39	0.42	123.3	3.288	SC
8	150	300	250	4	34.3	FF	C	568	1124	105	1.51	G	90	56.6	1100	N/A	39	0.42	73.3	1.955	SC

Table 2.7. Characteristics of beams tested by Duranovi et al. (1997)

Beam No.	b_w mm	h mm	d mm	a /d	f'_c MPa	Reinforcement code	type	A_{fl} mm²	f_{ful} Mpa	E_{fl} Gpa	ρ_{fl} %	type	S mm	A_{fvl} mm²	f_{fuv} MPa	f_{bend} MPa	E_{fv} GPa	ρ_{fv} %	V_{test} kN	V_u MPa	Mode of failure
(1)	(2)	(3)	(4)	(5)	(6)	(7)	(8)	(9)	(10)	(11)	(12)	(13)	(14)	(15)	(16)	(17)	(18)	(19)	(20)	(21)	(22)
1	150	250	210	3.65	38.1	F0	G	429	1000	45	1.36	-							52.9	1.679	DT
2	150	250	210	3.65	32.9	F0	G	429	1000	45	1.36	-							43.9	1.394	DT
3	150	250	210	3.65	39.8	FF	G	429	1000	45	1.36	G	80	153	1000	N/A	45	0.35	97.9	3.110	ST
4	150	250	210	3.65	39.8	FF	G	429	1000	45	1.36	G	80	153	1000	N/A	45	0.35	133.1	4.225	ST

Table 2.8. Characteristics of beams tested by Yonekura et al. (1993)

Beam No.	b_w mm	h mm	d mm	a/d	f_c' MPa	Reinforcement code	type	A_{fl} mm²	f_{ful} Mpa	E_{fl} Gpa	ρ_{fl} %	type	S mm	A_{fvl} mm²	f_{fuv} MPa	f_{bend} MPa	E_{fv} GPa	ρ_{fv} %	V_{test} kN	V_u MPa	Mode of failure
(1)	(2)	(3)	(4)	(5)	(6)	(7)	(8)	(9)	(10)	(11)	(12)	(13)	(14)	(15)	(16)	(17)	(18)	(19)	(20)	(21)	(22)
1	70	220	180	2.67	62	FS	C	228	2110	145	1.81	S	40	47.2					52.9	1.679	DT
2	70	220	180	2.67	59.8	FS	C	307	2110	145	2.44	S	40	47.2					43.9	1.394	DT

Table 2.9. Characteristics of beams tested by Nagasaka et al. (1993)

Beam No.	b_w mm	h mm	d mm	a/d	f'_c MPa	Reinforcement code	type	A_{fl} mm²	f_{ful} Mpa	E_{fl} Gpa	ρ_{fl} %	type	S mm	A_{fvl} mm²	f_{fuv} MPa	f_{bend} MPa	E_{fv} GPa	ρ_{fv} %	V_{test} kN	V_u MPa	Mode of failure
(1)	(2)	(3)	(4)	(5)	(6)	(7)	(8)	(9)	(10)	(11)	(12)	(13)	(14)	(15)	(16)	(17)	(18)	(19)	(20)	(21)	(22)
1	250	300	253	1.19	28.9	FF	A	1200	1295	56	1.90	C	80	100	1285	903	112	0.5	246.2	3.893	ST
2	250	300	253	1.19	34.0	FF	A	1200	1295	56	1.90	C	40	100	1285	903	112	1	310.9	4.917	ST
3	250	300	253	1.19	32.8	FF	A	1200	1295	56	1.90	C	27	100	1285	903	112	1.48	359.0	5.677	ST
4	250	300	253	1.78	28.9	FF	A	1200	1295	56	1.90	C	80	100	1285	903	112	0.5	204.0	3.226	ST
5	250	300	253	1.78	28.9	FF	A	1200	1295	56	1.90	C	40	100	1285	903	112	1	276.6	4.374	ST
6	250	300	253	2.37	28.9	FF	A	1200	1295	56	1.90	C	27	100	1285	903	112	1.48	282.5	4.467	SC
7	250	300	253	2.37	32.8	FF	A	1200	1295	56	1.90	C	80	100	1285	903	112	0.5	158.9	2.513	ST
8	250	300	253	1.78	32.8	FF	A	1200	1295	56	1.90	C	40	100	1285	903	112	1	229.5	3.629	ST
9	250	300	253	1.78	33.4	FF	A	1200	1295	56	1.90	A	80	100	1373	824	60	0.5	201.1	3.179	ST
10	250	300	253	1.78	34.7	FF	A	1200	1295	56	1.90	A	40	100	1373	824	60	1	271.7	4.296	SC
11	250	300	253	1.78	33.4	FF	A	1200	1295	56	1.90	H	80	100	716	481	44	0.5	169.7	2.683	ST
12	250	300	253	1.78	33.4	FF	A	1200	1295	56	1.90	H	40	100	716	481	44	1	243.2	3.846	ST
13	250	300	253	1.78	34.7	FF	A	1200	1295	56	1.90	G	80	100	1354	608	46	0.5	175.5	2.776	ST
14	250	300	253	1.78	36.0	FF	A	1200	1295	56	1.90	G	40	100	1354	608	46	1	228.5	3.614	ST
15	250	300	253	1.78	34.1	F0	A	1200	1295	56	1.90	-							112.8	1.784	DT

Table 2.9. Characteristics of beams tested by Nagasaka et al. (1993)

Beam No.	b_w mm	h mm	d mm	a/d	f'_c MPa	Reinforcement code	type	A_{fl} mm²	f_{ful} Mpa	E_{fl} Gpa	ρ_{fl} %	type	S mm	A_{fvl} mm²	f_{fuv} MPa	f_{bend} MPa	E_{fv} GPa	ρ_{fv} %	V_{test} kN	V_u MPa	Mode of failure
(1)	(2)	(3)	(4)	(5)	(6)	(7)	(8)	(9)	(10)	(11)	(12)	(13)	(14)	(15)	(16)	(17)	(18)	(19)	(20)	(21)	(22)
16	250	300	253	1.78	34.1	S0	S	1020	1295	206	1.61	-							105.9	1.675	DT
17	250	300	253	1.78	22.9	F0	A	1200	1295	56	1.90	-							83.4	1.318	DT
18	250	300	253	1.78	38.2	FS	A	1200	1295	56	1.90	S	40	80	1432	-	206	0.8	270.7	4.281	SC
19	250	300	253	1.78	23.5	FF	A	1200	1295	56	1.90	C	40	100	1285	903	112	1	207.0	3.273	SC
20	250	300	253	1.78	22.5	FF	A	1200	1295	56	1.90	C	27	100	1285	903	112	1.48	221.7	3.505	SC
21	250	300	253	2.37	24.3	FF	A	1200	1295	56	1.90	C	40	100	1285	903	112	1	182.4	2.885	SC
22	250	300	253	2.37	22.9	FF	A	1200	1295	56	1.90	C	27	100	1285	903	112	1.48	191.3	3.024	SC
23	250	300	253	1.78	22.5	FF	A	1200	1295	56	1.90	A	40	100	1373	824	60	1	190.3	3.009	SC
24	250	300	253	1.78	22.5	FF	A	1200	1295	56	1.90	A	27	100	1373	824	60	1.48	203.1	3.211	SC
25	250	300	253	1.78	23.5	FF	A	1200	1295	56	1.90	H	40	100	716	481	44	1	190.3	3.009	SC
26	250	300	253	1.78	23.5	FF	A	1200	1295	56	1.90	H	27	100	716	481	44	1.48	211.9	3.350	SC
27	250	300	253	1.78	26.0	SF	S	1197	844	184	1.89	H	40	100	716	481	44	1	208.0	3.288	SC
28	250	300	253	1.78	25.2	SS	S	1197	844	184	1.89	S	40	80	1432	-	206	0.8	262.9	4.157	SC
29	250	300	253	1.78	39.5	SS	S	1197	844	184	1.89	S	40	80	1432	-	206	0.8	354.1	5.599	SC

Table 2.10. Characteristics of beams tested by Tottori et al. (1993)

Beam No.	b_w mm	h mm	d mm	a/d	f'_c MPa	Reinforcement code	type	A_{fl} mm²	f_{ful} Mpa	E_{fl} Gpa	ρ_{fl} %	type	S mm	A_{fvl} mm²	f_{fuv} MPa	f_{bend} MPa	E_{fv} GPa	ρ_{fv} %	V_{test} kN	V_u MPa	Mode of failure
(1)	(2)	(3)	(4)	(5)	(6)	(7)	(8)	(9)	(10)	(11)	(12)	(13)	(14)	(15)	(16)	(17)	(18)	(19)	(20)	(21)	(22)
1	200	400	325	3.23	44.4	FF	C	456	2070	137	0.70	G	250	73.6	716	N/A	40	0.15	103.0	1.584	S
2	200	400	325	3.23	44.7	FF	C	456	2070	137	0.70	G	250	73.6	716	N/A	40	0.15	105.9	1.630	S
3	200	400	325	3.23	44.9	FF	C	456	2070	137	0.70	A	250	36	1511	N/A	69	0.07	84.9	1305	S
4	200	400	325	2.15	44.6	FF	C	456	2070	137	0.70	C	250	34	1413	N/A	110	0.07	161.9	2.490	S
5	200	400	325	3.23	44.8	FF	C	456	2070	137	0.70	C	250	34	1413	N/A	110	0.07	83.4	1.283	S
6	200	400	325	4.31	44.6	FF	C	456	2070	137	0.70	C	250	34	1413	N/A	110	0.07	73.6	1.132	S
7	200	400	325	3.23	45.0	FF	C	456	2070	137	0.70	C	250	20.2	2040	N/A	144	0.04	98.1	1.509	S
8	200	400	325	3.23	44.7	FF	C	456	2070	140	0.70	C	175	20.2	1746	N/A	137	0.06	107.9	1.660	S
9	200	400	325	3.23	44.7	FF	C	456	2070	140	0.70	C	100	20.2	1746	N/A	137	0.10	156.9	2.415	S
10	200	400	325	3.23	39.4	FF	C	456	2070	140	0.70	A	250	60	1089	N/A	58	0.12	103.0	1.585	S
11	200	400	325	3.23	39.4	FF	A	600	1297	58	0.92	A	250	45	1236	N/A	58	0.09	83.4	1.283	S
12	200	400	325	3.23	39.4	FF	A	600	1297	58	0.92	A	175	45	1236	N/A	58	0.13	98.1	1.509	S
13	200	400	325	3.23	39.4	FF	A	600	1297	58	0.92	A	100	45	1236	N/A	58	0.23	132.4	2.037	S

Table 2.10. Characteristics of beams tested by Tottori et al. (1993)

Beam No.	b_w mm	h mm	d mm	a/d	f'_c MPa	Reinforcement code	type	A_{fl} mm²	f_{ful} Mpa	E_{fl} Gpa	ρ_{fl} %	type	S mm	A_{fvl} mm²	f_{fuv} MPa	f_{bend} MPa	E_{fv} GPa	ρ_{fv} %	V_{test} kN	V_u MPa	Mode of failure
(1)	(2)	(3)	(4)	(5)	(6)	(7)	(8)	(9)	(10)	(11)	(12)	(13)	(14)	(15)	(16)	(17)	(18)	(19)	(20)	(21)	(22)
14	200	400	325	3.23	39.4	FF	A	600	1297	58	0.92	A	250	60	1089	N/A	58	0.12	107.4	1.653	S
15	200	400	325	3.23	39.4	FF	A	600	1297	58	0.92	A	250	60	1089	N/A	58	0.12	78.5	1.207	S
16	200	400	325	3.23	57.8	FF	A	600	1297	58	0.92	A	250	60	1089	N/A	58	0.12	107.4	1.653	S
17	200	400	325	3.23	39.4	FF	A	600	1297	58	0.92	C	250	20.2	1746	N/A	137	0.04	86.3	1.328	S
18	200	400	285	2.11	37.2	SF	S	2323	294	206	4.07	V	75	81.4	602	N/A	36	0.54	230.5	4.044	S
19	200	400	285	2.11	37.2	SF	S	2323	294	206	4.07	V	150	81.4	602	N/A	36	0.27	221.7	3.890	S
20	200	400	285	3.16	35.3	SF	S	2323	294	206	4.07	V	75	81.4	602	N/A	36	0.54	169.7	2.977	S
21	200	400	285	3.16	35.3	SF	S	2323	294	206	4.07	V	150	81.4	602	N/A	36	0.27	137.3	2.409	S
22	200	400	285	3.16	35.3	SF	S	2323	294	206	4.07	V	225	81.4	602	N/A	36	0.18	117.7	2.065	S
23	200	400	285	4.21	31.4	SF	S	2323	294	206	4.07	V	150	81.4	602	N/A	36	0.27	115.38	2.031	S
24	200	400	325	3.23	42.2	SF	S	557	1468	192	0.86	V	100	81.4	602	N/A	36	0.41	157.9	2.430	S
25	200	400	325	3.23	71.6	SF	S	557	1468	192	0.86	V	100	81.4	602	N/A	36	0.41	165.8	2.551	S

Table 2.10. Characteristics of beams tested by Tottori et al. (1993)

Beam No.	b_w mm	h mm	d mm	a/d	f'_c MPa	Reinforcement code	type	A_{fl} mm^2	f_{ful} Mpa	E_{fl} Gpa	ρ_{fl} %	type	S mm	A_{fvl} mm^2	f_{fuv} MPa	f_{bend} MPa	E_{fv} GPa	ρ_{fv} %	V_{test} kN	V_u MPa	Mode of failure
(1)	(2)	(3)	(4)	(5)	(6)	(7)	(8)	(9)	(10)	(11)	(12)	(13)	(14)	(15)	(16)	(17)	(18)	(19)	(20)	(21)	(22)
26	200	400	325	4.31	50.6	SF	S	557	1468	192	0.86	V	100	81.4	602	N/A	36	0.41	150.1	2.309	S
27	150	400	325	4.31	65.7	SF	S	557	1468	192	0.86	V	100	81.4	602	N/A	36	0.41	153.0	2.354	S
28	150	300	250	2.5	35.5	FF	C	206	1283	94	0.55	C	200	36.2	1283	N/A	94	0.12	57.9	1.543	S
29	150	300	250	2.5	37.6	FF	C	206	1283	94	0.55	C	100	36.2	1283	N/A	94	0.24	82.4	2.197	S
30	150	300	250	2.5	34.3	SF	C	395	1283	94	1.05	C	200	36.2	1283	N/A	94	0.12	71.4	1.903	S
31	150	300	250	2.5	34.2	SF	C	791	1283	94	2.11	C	200	36.2	1283	N/A	94	0.12	80.9	2.158	S
32	150	300	250	2.5	29.4	SF	S	774	397	206	2.06	C	200	36.2	1283	N/A	94	0.12	105.9	2.825	S
33	300	550	500	2.5	31.9	FF	C	791	1283	94	0.53	C	200	36.2	1283	N/A	94	0.06	160.4	1.069	S
34	150	300	260	3.08	38.8	SF	S	1161	369	206	2.98	A	300	56.6	1766	N/A	53	0.13	84.9	2.176	S
35	150	300	260	3.08	42.2	FF	A	1200	1278	63	3.08	A	300	56.6	1766	N/A	53	0.13	60.3	1.547	S
36	200	300	250	3.2	40.7	SF	S	2323	369	206	4.65	A	200	150	1278	N/A	64	0.38	191.8	3.836	S
37	200	300	250	2	77.5	FF	C	465	1766	137	0.93	A	100	56.5	1864	N/A	53	0.28	260.5	5.209	S

Table 2.10. Characteristics of beams tested by Tottori et al. (1993)

Beam No.	b_w mm	h mm	d mm	a/d	f'_c MPa	Reinforcement code	type	A_{fl} mm²	f_{ful} Mpa	E_{fl} Gpa	ρ_{fl} %	type	S mm	A_{fvl} mm²	f_{fuv} MPa	f_{bend} MPa	E_{fv} GPa	ρ_{fv} %	V_{test} kN	V_u MPa	Mode of failure
(1)	(2)	(3)	(4)	(5)	(6)	(7)	(8)	(9)	(10)	(11)	(12)	(13)	(14)	(15)	(16)	(17)	(18)	(19)	(20)	(21)	(22)
38	200	300	250	3	82.5	FF	C	465	1766	137	0.93	A	75	56.5	1864	N/A	53	0.38	172.2	3.443	S
39	200	300	250	3	82.5	FF	C	465	1766	137	0.93	C	1400	30.4	1766	N/A	137	0.15	194.2	3.885	S
40	200	300	250	3	82.5	FF	C	465	1766	137	0.93	A	125	56.5	1864	N/A	53	0.27	140.3	2.806	S
41	200	300	250	3	82.5	FF	C	465	1766	137	0.93	C	125	30.4	1766	N/A	137	0.12	182.9	3.659	S
42	200	400	325	2.15	44.6	FF	C	465	2070	137	0.70	-							98.1	1.509	S
43	200	400	325	3.23	44.5	F0	C	465	2070	137	0.70	-							122.6	1.887	S
44	200	400	325	4.31	45.0	F0	C	465	2070	137	0.70	-							117.7	1.811	S
45	200	400	325	2.77	46.9	F0	S	557	1468	192	0.86	-							147.1	2.264	S
46	200	400	325	3.23	46.9	F0	S	557	1468	192	0.86	-							93.2	1.434	S
47	200	400	325	4.31	46.9	F0	S	557	1468	192	0.86	-							78.5	1.207	S
48	200	400	325	2.15	46.9	F0	A	600	1297	58	0.92	-							152.0	2.339	S
49	200	400	325	3.23	46.9	F0	A	600	1297	58	0.92	-							61.8	0.951	S
50	200	400	325	4.30	46.9	F0	A	600	1297	58	0.92	-							47.14	0.724	S

2.6 Near Surface Mounted (NSM)

A recent and hopeful method for shear strengthening of reinforced concrete (RC) members is the use of near-surface mounted (NSM) fibre-reinforced polymer (FRP) reinforcement (Rizzo and Lorenzis, 2007).

Near surface mounted (NSM) is one of the most recent and promising strengthening techniques for reinforced concrete (RC) structures. NSM is based on the use of circular (Lorenzis and Nanni, 2002) or rectangular cross section bars (Blaschko and Zilch, 1999) of carbon or glass fibre reinforced polymer (CFRP or GFRP) materials installed into pre-cut slits opened on the concrete cover of the elements to strengthen. NSM requires no surface preparation work and, after cutting the slit, requires minimal installation time compared to the externally bonded reinforcing (EBR) technique. A further advantage associated with NSM is its ability to significantly reduce the probability of harm resulting from acts of vandalism, mechanical damages and aging effects. When NSM is used, the appearance of a structural element is practically unaffected by the strengthening intervention. Since both faces of the laminate are bonded to concrete when using CFRP laminates, high strengthening efficacy has been pointed to the NSM technique on the flexural (Barros and Fortes, 2005; El-Hacha and Rizkalla, 2004; Tan et al., 2002; Bonaldo et al., 2005) and shear strengthening (Barros and Dias, 2003; Nanni et al., 2004) of concrete structures.

The NSM technique was made up of the following steps:

(a) Using a diamond blade cutter, slits of 4–5 mm width and 12–15 mm depth were cut on the concrete surface of the elements to strengthen;

(b) Slits were cleaned by compressed air;

63

(c) CFRP laminates were cleaned by acetone;

(d) Epoxy adhesive was produced according to supplier recommendations;

(e) Slits were filled with the epoxy adhesive;

(f) Epoxy adhesive was applied on the faces of the laminates;

(g) Laminates were introduced into the slits and epoxy adhesive in excess was removed.

2.6.1   Using FRP as Shear Reinforcement in NSM Method

NSM-FRP reinforcement can be used externally to increasing the shear capacity for RC beams. As mentioned above, FRP bars or strips can be installed, whether vertical or inclined in slots or grooves cut on both sides of the RC beam. Very limited research was done on the shear strengthening using NSM FRP reinforcement and will be summarized below.

De Lorenzis and Nanni (2001) tested eight full-scale reinforced concrete beams with T-section having a span of 3 meters long. Six beams were without steel stirrups and two contained steel stirrups less than that required by the ACI 318-02. The examined variables were the spacing between the NSM-FRP bars, inclination of bars whether vertical or inclined at 45° with the beam axis. NSM-FRP bars were anchored in the flange in two beams. It was found that using NSM as shear reinforcement can increase the capacity of the beam up to 106% with respect to the control beam without shear reinforcement and can also be significant in increasing the beam carrying capacity in the presence of internal steel stirrups.

Nanni et al. 2004 reported the test results of a single full scale PC girder taken from a bridge and strengthened in flexural with CFRP laminate and in shear with NSM-CFRP rectangular strips at 60° inclination with the beam axis (The increase in the shear capacity was of at least 53%). The beam failed in flexure at a shear force close to the

shear resistance predicted by De Lorenzis and Nanni (2001c), which will be discussed later in sec. 2.6.1.1.
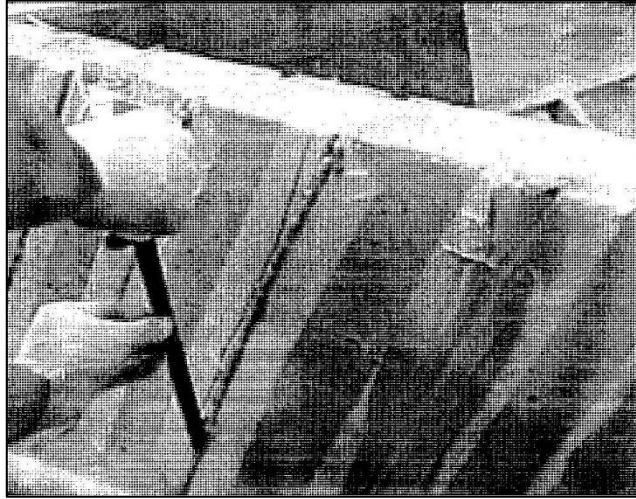
Figure 2.17. Installation of CFRP for shear strengthening, (Nanni et al. 2004)

Barros and Dias (2003) tested 20 RC beams with different dimension and without steel stirrups. The beams were divided to four groups with different stirrups spacing. Each group consists of five beams, one without any steel stirrups, one with steel stirrups, one with externally bonded laminates and the last two with NSM strips inclined and vertical. The reported increase in strength was about 54 and 83% for the externally-bonded reinforcement and the NSM techniques, respectively.

2.6.1.1 Modes of failure for shear strengthening

The observed mode of failure for shear strengthening was debonding of one or more of the FRP bars due to splitting of the epoxy cover. But this was overcome by increasing the bonded, length by inclination of the bar by 45° or by anchorage of the NSM bar in the beam flange, (De Lorenzis and Nanni 2001c). Once the debonding of the FRP bar is prevented the mode of failure changed to concrete cover splitting at the level of the

longitudinal reinforcement. This can be explained as the difference in configuration between the internal stirrups and NSM reinforcement. As the NSM bars were not able to restrain the dowel force subjected on the longitudinal reinforcement. These forces, in conjunction with the wedging action of the deformed reinforcement, give rise to tensile stresses in the surrounding concrete that may eventually lead to cover delamination and loss of anchorage.

a) Splitting of epoxy cover   b) Splitting of concrete cover at the
                                      longitudinal reinforcement
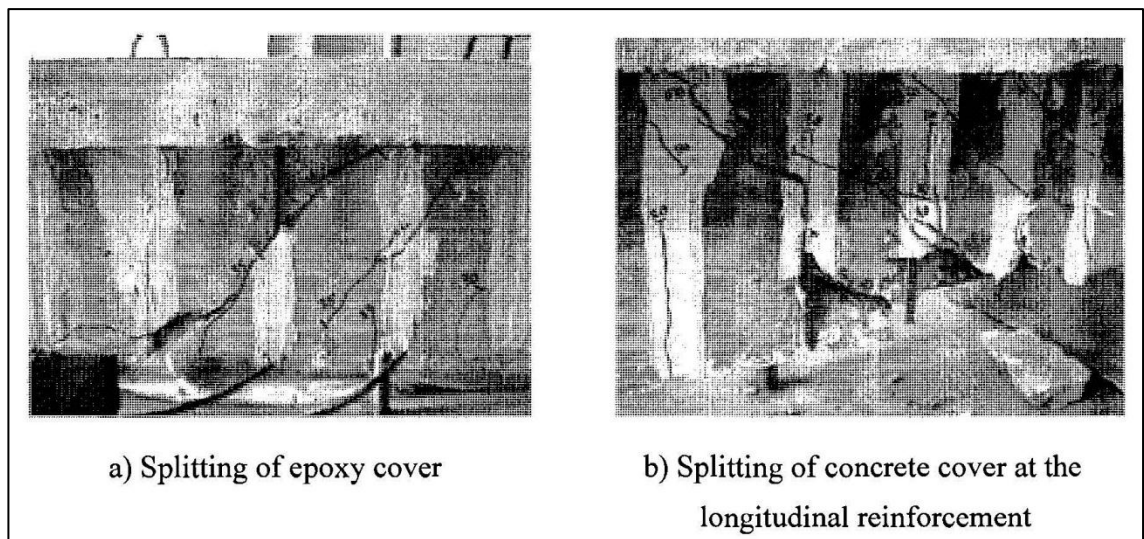
Figure 2.18. Modes of failure of shear strengthening, (De Lorenzis andNanni 2001)

2.6.1.2 Design equations for Shear strengthening

It is not yet possible to develop a comprehensive design approach for NSM shear strengthening including all the significant parameters. The nominal shear strength of a reinforced concrete beam may be computed by the basic design equation presented in ACI 318-99 (1999).

$$V_n = V_c + V_s \qquad\qquad\qquad (2.49)$$

V_n is the nominal shear strength which is given by the sum of the shear strength of the concrete, V_c, and the shear strength provided by the steel shear reinforcement, V_s. In the case of beams externally strengthened with FRP, the nominal shear strength can be computed by adding a third term to account for the contribution of the FRP reinforcement

$$V_n = V_c + V_s + V_{FRP}$$

(2.50)

The design shear strength is obtained by applying a strength reduction factor, $\emptyset$, to the nominal shear strength.

Several parameters influence the NSM FRP bars contribution VFRP to the shear capacity such as quality of bond, FRP bar type, groove dimensions and quality of substrate material.

Two design equations was given by Lorenzis and Nanni (2001) to obtain VFRP and suggests taking the lower of the two results as the contribution of NSM FRP bars to the shear capacity. The first equation VIFRP computes the FRP shear strength contribution related to bond-controlled shear failure, the second equation V2FRP calculates the shear resisted by NSM FRP bars when the maximum strain in the bars is equal to $4,000\mu\varepsilon$. VIFRP is computed using the following assumptions:

    (a) The inclination angle of the shear cracks equals $45°$.

    (b) The bond stresses are uniformly distributed along the effective lengths of the FRP bars at ultimate.

    (c) The ultimate bond stress is reached in all the bars intersected by the crack at ultimate.

(d) The shear force resisted by the FRP may be computed as the sum of the forces resisted by the FRP bars intersected by a shear crack. Each rod intersected by a crack may ideally be divided in two parts at the two sides of the crack. The force in each of these bars at the crack location can be calculated as the product of the average bond strength and the surface area of the effective length of the FRP rod.

$$V_{1\,FRP} = 2\,\pi\,d_b\tau_b L_{totmin} \tag{2.51}$$

Where

$$L_{totmin} = d_{net} - s \qquad if\ \frac{d_{net}}{3} < s\ < d_{net} \tag{2.52}$$

$$L_{totmin} = 2\,d_{net} - 4s \qquad if\ \frac{d_{net}}{4} < s\ < \frac{d_{net}}{3} \tag{2.53}$$

$$d_{net} = d_r - 2\,c \tag{2.54}$$

Where $d_r = length$ of the rods, c is concrete cover of the internal longitudinal reinforcement and s is the spacing of the NSM rods.

While in computing V_{2FRP} the same assumptions that are used in computing V_{1FRP} are considered. The effective length of an FRP rod crossed by the crack corresponding to a strain of $4,000\mu\varepsilon$ and the average bond strength τ_b is

$$\vec{L_\iota} = 0.001\,d_b\,\frac{E_b}{\tau_b} \tag{2.55}$$

$\frac{d_{net}}{2} < s\ < d_{net}$ and if $\ \vec{L_\iota} > d_{net} - s\ $ so bond failure occurs before $\vec{L_\iota}$ the maximum strain reaches $4,000\mu\varepsilon$, therefore, $V_{1\,FRP}$ controls but if $\ \vec{L_\iota} < d_{net} - s\ $ so $V_{2\,FRP}$ with the value

$$V_{2\,FRP} = 2\,\pi\,d_b\tau_b L_{totmin} \tag{2.56}$$

$\frac{d_{net}}{3} < s\ < \frac{d_{net}}{2} V_{1\,FRP}$ controls but if $\vec{L_\iota} > s\ $ but if $\ \vec{L_\iota} < s\ $ so $V_{2\,FRP}$ with the value

$$V_{2\,FRP} = 2\,\pi\,d_b\tau_b L_{totmin}\,(\overrightarrow{L_i} + d_{net} - 2s) \qquad if\; d_{net} - 2s < \overrightarrow{L_i} < s \qquad (2.57)$$

$$V_{2\,FRP} = 4\,\pi\,d_b\tau_b L_{totmin}\,\overrightarrow{L_i} \qquad\qquad if\; \overrightarrow{L_i} < d_{net} - 2s \qquad (2.58)$$

$\frac{d_{net}}{4} < s < \frac{d_{net}}{3}$ $V_{1\,FRP}$ controls but if $\overrightarrow{L_i} > d_{net} - 2s$ but if $\overrightarrow{L_i} < d_{net} - 2s$ so $V_{2\,FRP}$

with the value

$$V_{2\,FRP} = 2\,\pi\,d_b\tau_b L_{totmin}\left(\overrightarrow{L_i} + d_{net} - 2s\right) \qquad if\; d_{net} - 2s > \overrightarrow{L_i} > s \qquad (2.59)$$

$$V_{2\,FRP} = 2\,\pi\,d_b\tau_b L_{totmin}\left(2\overrightarrow{L_i} + d_{net} - 3s\right) \qquad if\; s > \overrightarrow{L_i} > d_{net} - 2s \qquad (2.60)$$

$$V_{2\,FRP} = 6\,\pi\,d_b\tau_b L_{totmin}\,\overrightarrow{L_i} \qquad\qquad if\; \overrightarrow{L_i} < d_{net} - 3s \qquad (2.61)$$

Lorenzis and Nanni (2001b) used the force resulting from the tensile stress in the FRP bars across the assumed crack to calculate the shear strength provided by the NSM reinforcement and it is expressed for rectangular bars by:

$$V_{FRP} = 4(a + b)\tau_b\,L_{tot} \qquad (2.62)$$

Where a and b represent the cross-sectional dimension of the rectangular FRP bars, τ_b represents the average bond stress of the bars crossed by the shear crack L_{tot} can be expressed as $\Sigma_i L_i$ where L_i represents the length of each single NSM bar intercepted by a shear crack and is expressed as:

$$L_i = \begin{cases} \dfrac{S}{\cos\alpha + \sin\alpha} \quad i \leq l_{0.004} \dots\dots\dots\dots i = 1 \dots\dots\dfrac{n}{2} \\ l_{net} - \dfrac{S}{\cos\alpha + \sin\alpha} \quad i \leq l_{0.004} \dots\dots i = \dfrac{n}{2} + 1 \dots n \end{cases} \qquad (2.63)$$

where a represents the slope of the FRP bar with respect to the longitudinal axis of the beam, s is the horizontal FRP bar spacing, and l_{net} is defined as follows:

$$l_{net} = l_b - \frac{2c}{\sin a} \tag{2.64}$$

Where l_b is the actual length of the FRP bar is, c is the clear concrete cover of the internal longitudinal reinforcement.

Where the first part of the equation takes into account bond as the controlling failure mechanics and represents the minimum effective length of a FRP bar intercepted by a shear crack as a function of the term n:

$$n = \frac{l_{eff}(1 + \cot a)}{s} \tag{2.65}$$

where n is rounded off to the lowest integer and /^represents the vertical length of l_{net} and the second part of equation (2.62) takes into account the shear integrity of the concrete by limiting at 0.004 the maximum strain in the FRP reinforcement and $l_{0.004}$ can be determined as follows

$$l_{0.004} = 0.002 \frac{E_f}{\tau_b} \frac{ab}{a+b} \tag{2.66}$$

The CHBDC (CAN/CSA-S6-06 2006) has also a provision for shear strengthening of timber bridges, which states that;

(a) The minimum volume fraction of GFRP bars is 60%.

(b) Horizontal splits in beams, if present, are closed by a mechanical device before the insertion of the GFRP bars.

As shown in Figure 2.18, there are at least three GFRP bars at each end of the beam. The diameter of the GFRP bar, db, is at least 15 mm, and the minimum diameter of hole containing a bar is db+3 mm.

The spacing of bars along the length of the beam is 25 mm ± h, the depth of the beam. The adhesive used for bonding the GFRP bars to the timber beam is compatible with the preservative treatment used on the timber and chosen such that it is compatible with the expected volumetric changes of the timber.

As shown in Figure 2.18, the GFRP bars are inclined to the beam axis at an angle of 45°±10° from the horizontal. The top ends of the inclined GFRP bars are within 10 to 25 mm from the top of the beam.

When there are daps present, the ingress of the drilled hole should be 100 mm ±10 mm from the edge of the dap.
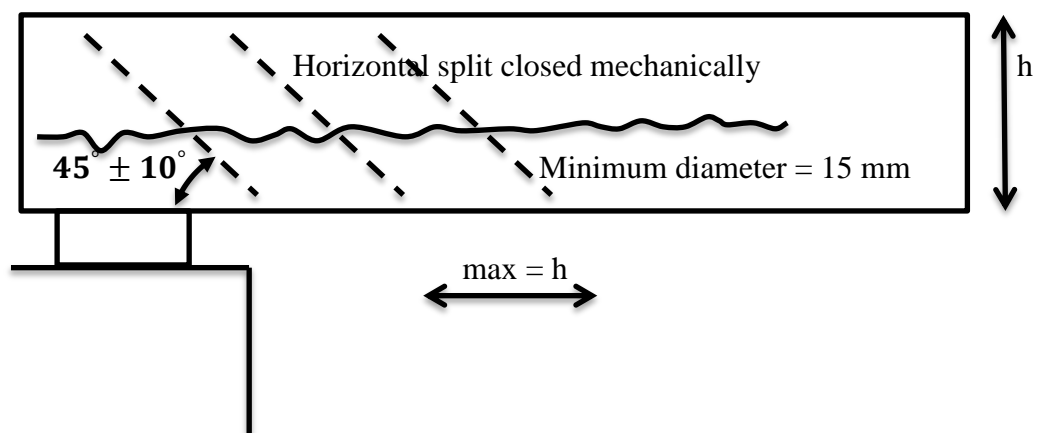
Figure 2.19 Elevation of timber beam with GFRP bars for shear strengthening, (CSA, 2006)

2.7 Self-Compacting Concrete (SCC)

Self-compacting concrete (SCC) is a new category of high performance concrete (HPC) characterized by its ability to spread to places under its own weight without the need of vibration, and is self-compact without any segregation and blocking (Sonebi, 2004). SCCs are extremely workable concretes that can be placed without requiring vibration. The high fluidity of these concretes is obtained by adding a super-plasticizer (SP) (Djelal et al., 2004).

For SCC, it is generally necessary to use super plasticizers in order to obtain high mobility. Adding a large volume of powdered material or viscosity modifying admixture can eliminate segregation. The powdered materials that can be added are fly ash, silica fume, lime stone powder, glass filler and quartzite filler.

SCC offers many advantages for the precast, pre-stressed concrete industry and forecast-in place construction:

    (a) Low noise-level in the plants and construction sites.

    (b) Eliminated problems associated with vibration.

    (c) Less labour involved.

    (d) Faster construction.

    (e) Improved quality and durability.

    (f) Higher strength.

SCC mixes must meet three key properties:

    (a) Ability to flow into and completely fill intricate and complex forms under its own weight.

    (b) Ability to pass through and bond to congested reinforcement under its own weight.

(c) High resistance to aggregate segregation.

Four tests are recommended for European standardization as reference methods:

(a) Slump flow test (total spread and T50 time): primarily to assess filling ability, suitable for laboratory and site use.

(b) L-box test: primarily to assess passing ability, suitable for laboratory use.

(c) J-ring test: primarily to assess passing ability, suitable for laboratory and site use.

(d) Sieve stability test: to assess segregation resistance, suitable for laboratory and site use.

Three other tests are recommended for standardization as alternative methods.

(a) V-funnel test: partially indicates filling ability and blocking, suitable for laboratory and site use.

(b) Orimet test: partially indicates filling ability and blocking, suitable for laboratory and site use.

(c) Penetration test: to assess segregation, possibly used in combination with the sieve stability test

2.8 Mix Design Properties

There is no standard method for SCC mix design and many academic institutions, admixture, ready-mixed, precast and contracting companies have developed their own mix proportioning methods (The European Guidelines for Self Compacting Concrete, 2005).

Mix designs often use volume as a key parameter because of the importance of the need to over fill the voids between the aggregate particles. Some methods try to fit available

constituents to an optimised grading envelope. Another method is to evaluate and optimise the flow and stability of first the paste and then the mortar fractions before the coarse aggregate is added and the whole SCC mix tested (The European Guidelines for Self Compacting Concrete, 2005).

Some mix design methods developed at academic and other institutions have been published:

Okamura H and Ozawa K (1994). Self-compactable high performance concrete. International Workshop on High Performance Concrete.American Concrete Institute; Detroit,31- 44.

Ouchi M, Hibino M, Ozawa K, and Okamura H (1998). A rational mix-design method for mortar in self-compacting concrete.Proceedings of Sixth South-East Asia Pacific Conference of Structural Engineering and Construction.Taipei, Taiwan, 1307-1312.

Nawa T, Izumi T, and Edamatsu Y (1998). State-of -the-art report on materials and design of self-compacting concrete. Proceedings of International Workshop on Self-compacting Concrete, Kochi University of Technology, Japan, 160-190.

Domone P, Chai H and Jin J (1999). Optimum mix proportioning of self-compacting concrete. Proceedings of International Conference on Innovation in Concrete Structures: Design and Construction, Dundee, Thomas Telford; London, 277-285.

Billberg, P (1999). Self-compacting concrete for civil engineering structures - the Swedish Experience. Report no 2:99. Swedish Cement and Concrete Research Institute. Stockholm.

Su N, Hsu K-C and Chai H-W (2001). A simple mix design method for self-compacting concrete Cement and Concrete Research, 31 :1799-1807.

Gomes P.C.C, Gettu R, Agullo L, Bernard C (2002). Mixture proportioning of high strength, Self-Compacting Concrete: Performance and Quality of concrete structures. Third CANMET/ACI Intnl Conf. (Recefi, Brazil) Supplementary CD, 12.

Bennenk, H. W., J.VanSchiindel (2002). The mix design of SCC, suitable for the precast concrete industry. Proceedings of the BIBM Congress, Istanbul, Turkey.

Billberg, P (2002). Mix design model for SCC (the blocking criteria). Proceedings of the first North American conference on the design and use of SCC, Chicago.

Table 2.3 gives an indication of the typical range of constituents in SCC by weight and by volume. These proportions are in no way restrictive and many SCC mixes will fall outside this range for one or more constituents.

Table 2.11 Typical Range of SCC Composition (The European Guidelines for Self Compacting Concrete, 2005)

Constituent	Typical range by mass Kg/m^3	Typical range by mass Liters/m^3
Powder	380-600	
Paste		300-380
Water	150-210	150-210
Coarse aggregate	750-1000	270-360
Fine aggregate	Content balance the volume of the other constituents, typically 48-55% of total aggregate weight.	
Water/Powder ratio by Vol		0.85-1.10

The mix design is generally based on the approach outlined below:

    (a) evaluate the water demand and optimise the flow and stability of the paste

    (b) determine the proportion of sand and the dose of admixture to give the required robustness

    (c) test the sensitivity for small variations in quantities (the robustness)

    (d) add an appropriate amount of coarse aggregate

(e) produce the fresh SCC in the laboratory mixer, perform the required tests

(f) test the properties of the SCC in the hardened state

(g) produce trial mixes in the plant mixer.

2.9 Summary

This chapter was presented the shear behaviour in reinforced concrete beams with/without shear reinforcement, after that was investigated on properties of FRP materials and whether this material is a good replacement for steel or not. And later, the new method of shear strengthening which named NSM was studied and whether how to use this method externally. Also idea of this research derived from NSM technique. And finally, details, characteristics and mix design of self-compacting concrete were presented.

3.0 COMPUTER PROGRAMMING

3.1 Introduction

This project involves the development of a computer application that analyses the structural concrete beams which are reinforced with FRP bars. The program also aims at emphasizing the importance of computers in the solution of everyday engineering problems.

3.2 Introduce the Program and Flowchart

The program developed analyses one span beam and includes a module for the design of reinforced concrete beams. This program was created using the FORTRAN language and it was written within seven months.

The application also discusses various theoretical analysis techniques that can be implemented in developing a computer program. The main theoretical methods used in this project are the Ultimate Moment, and the Reinforced concrete design which is based on the ACI-440 code.

This chapter includes the program source and shows how one can solve an example by applying this computer programme according to ACI-440 code.

The outline of this computer programme is shown in the following flowchart.

START

INPUT: $\beta_1, f_c, f_{FRP}, W_{LL}, W_{DL}, L_{span}, E_f$

Step 1: Estimate the cross sectional dimension of beam

Step 2: Compute the factored load

Step 3: Compute the design rupture stress of FRP bars

Step 4: Determine the area of FRP bar required for flexural strength

If $\emptyset M_n > M_u$

NO

YES

Step 5: Check the crack width

NG

OK

78
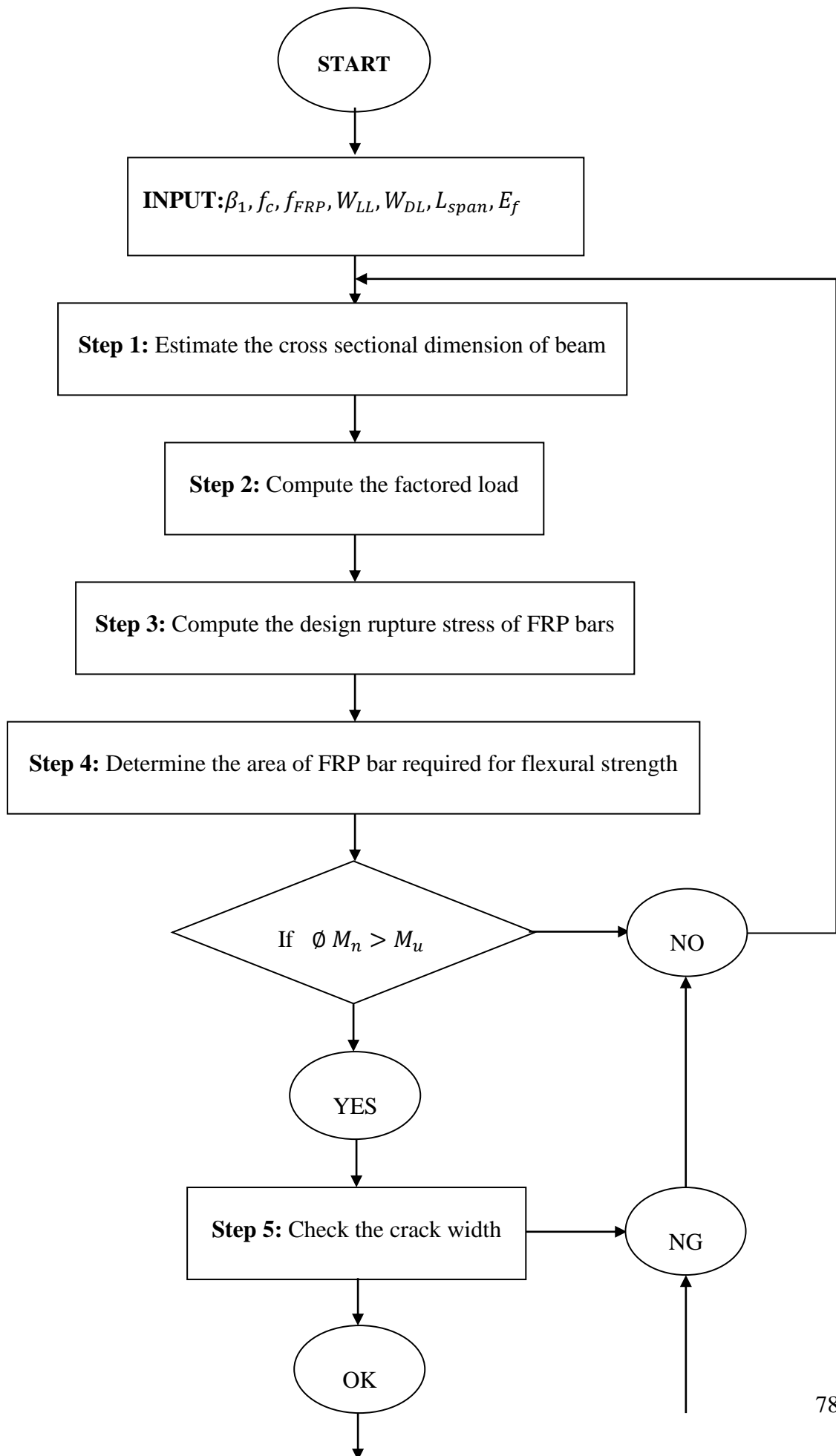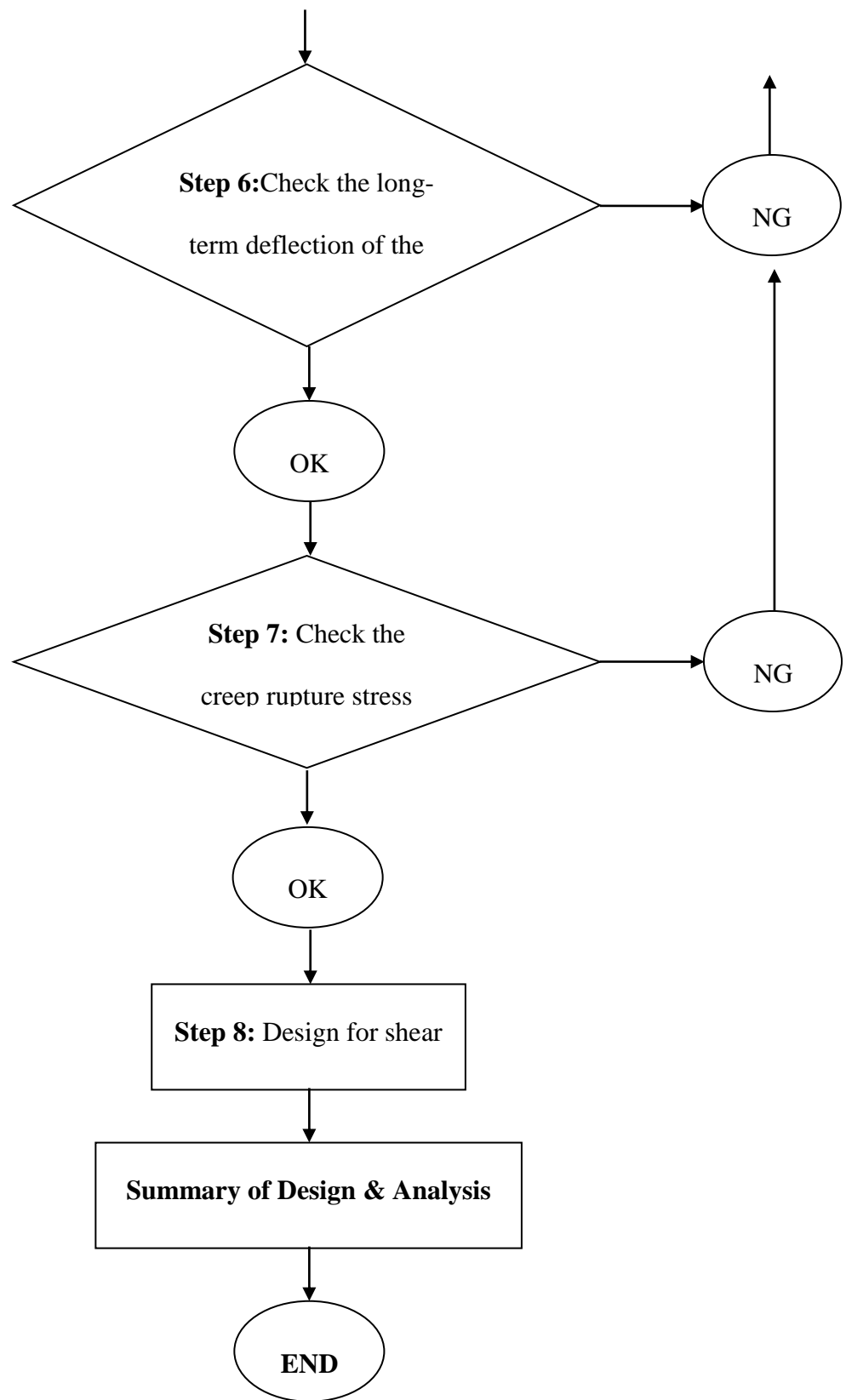
Figure3.1. Flowchart of programme

3.3 Solved Example

This example of beam design follows the ultimate strength approach described in this document and includes the load factors according to ACI 318-05. A simply supported, normal weight concrete beam with fc'= 27.6 MPa is needed in a medical facility to support an MRI unit. The beam is an interior beam. The beam is to be designed to carry a service live load of *W live load*= 5.8 kN/m (20% sustained) and a superimposed service dead load of *W service dead load* = 3.0 kN/m over a span of L = 3.35 m. The beam deflection should not exceed l/240, which is the limitation for long-term deflection. Due to construction restriction, the depth of the member should not exceed 356 mm.

Manufacturer's reported GFRP bar properties:

Table 3.1. Properties of used GFRP

Tensile strength *ffu*	620.6 MPa
Rupture strain ε*fu*	0.014
Modulus of elasticity	44,800 MPa

GFRP reinforcing bars are selected to reinforce the beam; material properties of the bars (as reported by the bar manufacturer) are shown in Table 13.1 (ACI – 440).

The design procedure presented hereafter is equally applicable to CFRP and AFRP bars, with use of appropriate manufacturer's reported material properties similar to Table 13.1 (ACI – 440).

(a) Solve the example manually:

Step 1: Estimate the appropriate cross-sectional dimensions of the beam.

An initial value for the depth of a simply supported reinforced concrete beam can be estimated from Table 8.2 (ACI 440).

$$h = \frac{3.35m}{10} = 0.335\ m$$

$Try\ h = 305\ mm < 335\ mm$

$Assuming\ \emptyset\ 19\ mm\ bars\ for\ main$

$Assuming\ \emptyset\ 9.5\ mm\ bars\ for\ shear$

$Cover = 38\ mm$

$Try\ b = 178\ mm$

$$Estimated\ d = 305\ mm - 38\ mm - 9.5 - \frac{19\ mm}{2} = 248\ mm$$

Step 2: Compute the factored load.

The uniformly distributed dead load can be computed including the self-weight of the beam.

$$w_{DL} = w_{SDL} + w_{SW}$$

$$w_{DL} = \left(3.0\frac{kN}{m}\right) + (0.178\ m)(0.305\ m)\left(24\frac{kN}{m^3}\right) = 4.3\frac{kN}{m}$$

$$w_u = 1.2\ w_{DL} + 1.7\ w_{LL}$$

$$w_u = 1.2\ \times 4.3 + 1.7\ \times 5.8 = 14.4\frac{kN}{m}$$

$$M_u = \frac{w_u l^2}{8} = \frac{14.4 \times 3.35^2}{8} = 20.2\ kN.m$$

Step 3: Compute the design rupture stress of the FRP bars.

The beam will be located in an interior conditioned space. Therefore, for glass FRP bars, an environmental reduction factor CE of 0.80 is as per Table 7.1 (ACI 440).

$$f_{fu} = C_E f_{fu}^* = 0.8 \times 620.6 \, MPa = 496 \, MPa$$

Step 4: Determine the area of GFRP bars required for flexural strength.

Find the reinforcement ratio required for flexural strength by trial and error using Eq. (8-1), (8-4d), and (8-5) regarding to ACI 440.

Assume an initial amount of FRP reinforcement:

$$\rho_{fb} = 0.85 \frac{f_c'}{f_{fu}} \beta_1 \frac{E_f \varepsilon_{cu}}{E_f \varepsilon_{cu} + f_{fu}} = 0.85 \frac{27.6}{496} \, 0.85 \frac{44800 \times 0.003}{(44800 \times 0.003) + 496} = 0.0086$$

$$\rho_f = \frac{A_f}{bd} = \frac{567}{178 \times 248} = 0.0128$$

$$f_f = \left[\sqrt{\frac{(E_f \varepsilon_{cu})^2}{4} + \frac{0.85 \, \beta_1 f_c'}{\rho_f} E_f \varepsilon_{cu}} - 0.5 \, E_f \varepsilon_{cu} \right] = 395.3 \, MPa$$

$$M_n = \rho_f f_f \left(1 - 0.59 \frac{\rho_f f_f}{f_c'} \right) b \, d^2 = 49.4 \, kN.m$$

$$\emptyset = 0.65$$

$$\emptyset \, M_n = 32.1 \, kN.m \geq M_u = 22.3 \, kN.m$$

$$k = \sqrt{2 \rho_f n_f + (\rho_f n_f)^2} - \rho_f n_f$$

$$k = \sqrt{2(0.0128)(1.8) + [(0.0128)(1.8)]^2}$$
$$- (0.0128)(1.8) = 0.193$$

$$f_f = \frac{M_{DL+LL}}{A_f d(1 - k/3)}$$

$$f_f = \frac{14.17 \times 10^{-6} \text{ N·mm}}{(567\,\text{mm}^2)(248\,\text{mm})(1 - 0.193/3)}$$
$$= 107.7 \text{ MPa}$$

$$\beta = \frac{h - kd}{d(1 - k)}$$

$$\beta = \frac{305 \text{ mm} - (0.193)(248 \text{ mm})}{(248 \text{ mm})(1 - 0.193)} = 1.285$$

$$dc = h - d = 57 \; mm$$

$$w = 2\frac{f_f}{E_f}\beta k_b \sqrt{d_c^2 + \left(\frac{s}{2}\right)^2}$$

$$w = 2\frac{(107.7 \text{ MPa})}{(44{,}800 \text{ MPa})}(1.285)(1.4)\sqrt{(57 \text{ mm})^2 + \left(\frac{64 \text{ mm}}{2}\right)^2} = 0.57 \text{ mm} < 0.7 \text{ mm}$$

Step 6: Check the long-term deflection of the beam

Compute the gross moment of inertia for the section.

$$I_g = \frac{bh^3}{12}$$

Calculate the cracked section properties and cracking moment.

$$f_r = 0.62\sqrt{f_c'}$$

$$f_r = 0.62\sqrt{27.6} \text{ MPa} = 3.26 \text{ MPa}$$

$$M_{cr} = \frac{2f_r I_g}{h}$$
$$M_{cr} = \frac{2(3.26)(4.209 \times 10^8)}{305} = 9.00 \text{ kN·m}$$

$$I_{cr} = \frac{bd^3}{3} k^3 + n_f A_f d^2 (1 - k)^2$$

$$I_{cr} = \frac{(178)(248)^3}{3} (0.193)^3 +$$

$$1.8(567)(248)^2(1 - 0.193)^2 = 4.74 \times 10^7 \text{ mm}^4$$

Compute the modification factor β_d.

$$\beta_d = \frac{1}{5}\left[\frac{\rho_f}{\rho_{fb}}\right]$$

$$\beta_d = \frac{1}{5}\left[\frac{0.0128}{0.0086}\right] = 0.30$$

Compute the deflection due to dead load plus live load.

$$(I_e)_{DL+LL} = \left(\frac{M_{cr}}{M_a}\right)^3 \beta_d I_g + \left[1 - \left(\frac{M_{cr}}{M_a}\right)^3\right] I_{cr}$$

$$(I_e)_{DL+LL} = \left(\frac{9.00}{14.17}\right)^3 (0.30)(4.209 \times 10^8) + \left[1 - \left(\frac{9.00}{14.17}\right)^3\right](4.74 \times 10^7) = 6.76 \times 10^7 \text{ mm}^4$$

Compute the deflection due to dead load alone and live load alone.

$$(\Delta_i)_{DL+LL} = \frac{5 M_{DL+LL}\ell^2}{48 E_c (I_e)_{DL+LL}}$$

$$(\Delta_i)_{DL} = \frac{5(14.17 \times 10^6 \text{ N·mm})(3350 \text{ mm})^2}{48(2.49 \times 10^4 \text{ mm})(6.67 \times 10^7 \text{ mm}^4)} = 10 \text{ mm}$$

$$(\Delta_i)_{DL} = \frac{w_{DL}}{w_{DL+LL}}(\Delta_i)_{DL+LL}$$

$$(\Delta_i)_{LL} = \frac{w_{LL}}{w_{DL+LL}}(\Delta_i)_{DL+LL}$$

$$(\Delta_i)_{DL} = \frac{4.3 \text{ kN/m}}{4.3 \text{ kN/m} + 5.8 \text{ kN/m}}(10 \text{ mm}) = 4.3 \text{ mm}$$

$$(\Delta_i)_{LL} = \frac{5.8 \text{ kN/m}}{4.3 \text{ kN/m} + 5.8 \text{ kN/m}}(10 \text{ mm}) = 5.7 \text{ mm}$$

Compute the long-term deflection (initial deflection due to live load plus the time-dependent deflection due to sustained loads).

$$\Delta_{LT} = (\Delta_i)_{LL} + \lambda[(\Delta_i)_{DL} + 0.20(\Delta_i)_{LL}]$$

$$\Delta_{LT} = (5.7 \text{ mm}) + 1.2[(4.3 \text{ mm}) + 0.2(5.7 \text{ mm})] = 12.2 \text{ mm}$$

Check computed deflection against deflection limitations.

$$\Delta_{LT} \le \frac{\ell}{240}$$

$$12.2 \text{ mm} < \frac{3350 \text{ mm}}{240} = 14 \text{ mm}$$

Step 7: Check the creep rupture stress limits.

Compute the moment due to all sustained loads (dead load plus 20% of the live load).

$$M_s = \frac{w_{DL} + 0.20 w_{LL}}{w_{DL} + w_{LL}} M_{DL+LL}$$

$$M_s = \frac{4.3 \text{ kN/m} + 0.20 \cdot 5.8 \text{ kN/m}}{4.3 \text{ kN/m} + 5.8 \text{ kN/m}} 14.17 \text{ kN·m} = 7.66 \text{ kN·m}$$

Compute the sustained stress level in the FRP bars.

$$f_{f,s} = \frac{M_s}{A_f d(1 - k/3)}$$

$$f_{f,s} = \frac{7.66 \times 10^6 \text{ N·mm}}{(567 \text{ mm}^2)(248 \text{ mm})(1 - 0.193/3)} = 58.2 \text{ MPa}$$

Check the stress limits given in Table 8.2 in ACI 440 for glass

FRP bars.

$$f_{f,s} \le 0.20 f_{fu}$$

$$58.2 \text{ MPa} \le 0.20(496) = 99.2 \text{ MPa}$$

Step 8: Design for shear.

Determine the factored shear demand at a distance d from the support.

$$V_u = \frac{w_u \ell}{2} - w_u d$$

$$V_u = \frac{(14.4 \text{ kN/m})(3.35 \text{ m})}{2} - (14.4 \text{ kN/m})(0.248 \text{ m}) = 20.6 \text{ kN}$$

Compute the shear contribution of the concrete for an FRP-reinforced member.

$$V_c = \frac{2}{5}\sqrt{f_c'}\, b_w c$$

$$V_c = \frac{2}{5}\sqrt{27.6 \text{ MPa}}\,(178 \text{ mm})(47.9 \text{ mm}) = 17.9 \text{ kN}$$

FRP shear reinforcement will be required. The FRP shear reinforcement will be assumed to be No. 3closed stirrups oriented vertically. To determine the amount of FRP shear reinforcement required, the effective stress level in the FRP shear reinforcement must be determined. This stress level may be governed by the allowable stress in the stirrup at the location of a bend, which is computed as follows:

$$f_{fb} = \left(0.05\frac{r_b}{d_b} + 0.3\right)f_{fu}$$

$$f_{fb} = \left(0.05\frac{3(9.5)}{9.5} + 0.3\right)(496 \text{ MPa}) = 223.2 \text{ MPa}$$

The design stress of FRP stirrup is limited to:

$$f_{fv} = 0.004E_f \le f_{fb}$$

$$f_{fv} = 0.004(44{,}800 \text{ MPa}) = 179.2 \text{ MPa} \le 223.2 \text{ MPa}$$

The required spacing of the FRP stirrups can be computed by rearranging Eq. (9-4) reported in ACI 440.

$$s = \frac{\phi A_{fv} f_{fv} d}{(V_u - \phi V_c)}$$

$$s = \frac{0.75(2 \times 71 \text{ mm}^2)(179.2 \text{ MPa})(248 \text{ mm})}{(20{,}600 \text{ N} - 0.75(17{,}900 \text{ N}))} = 660 \text{ mm}$$

Check maximum spacing limit = $d/2$ or 24 in.

$s \leq (248 \text{ mm}/2) = 124 \text{ mm}$ $s \leq 600 \text{ mm}$

$$s \leq \frac{(2)(71 \text{ mm}^2)(179.2 \text{ MPa})}{(0.3)(178 \text{ mm})} = 477 \text{ mm}$$

(b) Solve example using software
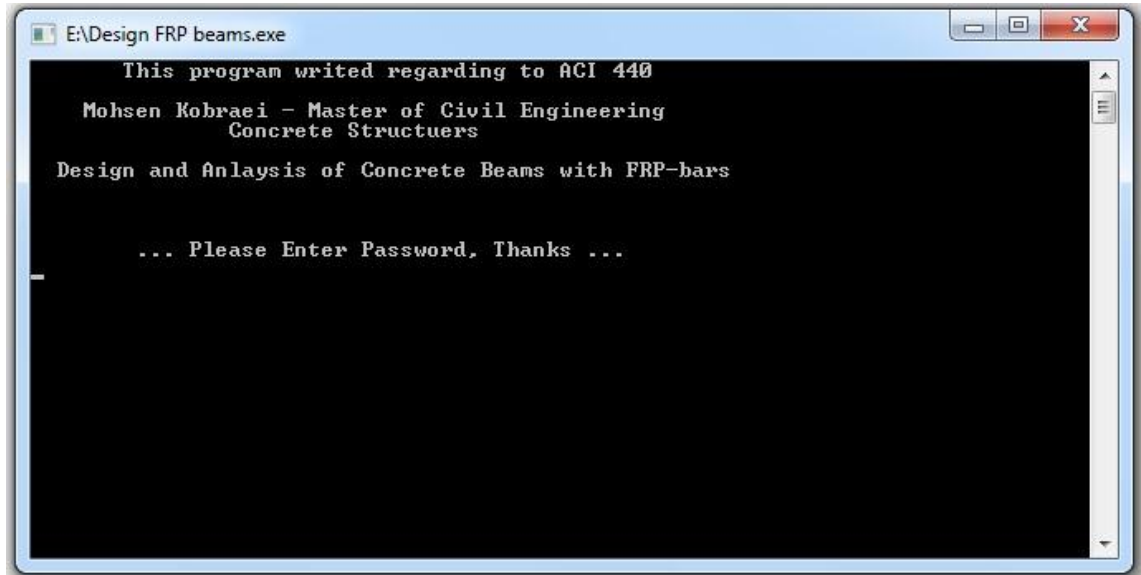
Figure3.2. Screen shot of solved example by running programme

```
■■ E:\Design FRP beams.exe                                    ─ □ ✗

          This program writed regarding to ACI 440

      Mohsen Kobraei - Master of Civil Engineering
                 Concrete Structuers

   Design and Anlaysis of Concrete Beams with FRP-bars



          ... Please Enter Password, Thanks ...
080084
 Enter your values =
 Beta 1
0.85
 f Concrete        MPa
27.6
 f FRP        MPa
620.6
 W Live Load        kN/m
5.8
 W Service Dead Load       kN/m
3
   Span of L        m
3.35
   Modulus of Elasticity FRP      Ef =      MPa
44800

**********************************************************
Step1-Estimate the appropriate dimensions of the BEAM.
**********************************************************

  h= Span/10  =     meter    .335
  Enter your h, it MUST be =< than above       mm
305
  Enter your b (width)       mm
178
  Cover= ?       mm
38
  Enter (fi) of bars for MAIN       mm
19
  Enter (fi) of bars for SHEAR       mm
9.5


 Estimated  d= h - cover - db shear - db/2    mm=  248.00


**********************************************************
          Step2 - Compute the factored load.
**********************************************************

  W DL= W SDL + W SW        kN/m  4.30



  Wu= 1.2W DL + 1.7W LL        kN/m 15.02



  Mu= (Wu L^2)/8       kN.m 21.08
**********************************************************
Step3-Compute the design rapture stress of the FRP bar
**********************************************************
 ACI 440 - Table 7.1
```

Cont. Figure3.2. Screen shot of solved example by running programme

89

```
E:\Design FRP beams.exe                              [ - ] [ □ ] [ X ]
***********************************************************
Step3-Compute the design rapture stress of the FRP bar
***********************************************************

 ACI 440 - Table 7.1
 ...................
 Enviromental Reduction Factor for
 Various Fiber And Exposure Condition


 _____
 Exposure Condition! Fiber Type ! CE

 Concrete NOT Ex.  !   Carbon    ! 1.0
      to Earth     !   Glass     ! 0.8
    And Weather    !   Aramid    ! 0.9
 _____
 Concrete Exposure !   Carbon    ! 0.9
      to Earth     !   Glass     ! 0.7
    And Weather    !   Aramid    ! 0.8
 _____

 Please Enter your CE from the Table 7.1
.8
Ffu= CE x F FRP      MPa        496.48
***********************************************************
   Step4 - Determine the area of FRP bars Required
               for flexural strength.
***********************************************************

 Assume an initial amount of FRP Reinforcement=
 19.0
How many FRP bars you want to use?
2

 Compute the balanced FRP Reinforcement ratio


Pfb= 0.85 (fc/fu) B1[(0.003 Ef)/(0.003 Ef + fu)] =   .00856


Pf= Af/bd =  .01284


Max P is 1.4 Pfb =        .01198


 A= (.003Ef)^2/4
 B= (0.85B1 fc 0.003EF/Pf)
 C= (0.5*.003Ef)
Ff=SQRT[ A + B ]- C  =       Mpa       394.60



Mn= Pf.Ff[1-0.59 Pf.Ff/fc] bd^2 =      kN.m     49.46


Compute the strength reduction factor ...
```

Cont. Figure3.2. Screen shot of solved example by running programme

```
 E:\Design FRP beams.exe                                    - □ x

Compute the strength reduction factor ...




Pfb < Pf < 1.4 Pfb      Q=0.3+0.25 Pf/Pfb =      .550

Q . Mn =         kN.m   27.202

Q.Mn > Mu               Checked ...... OK
*****************************************************
          Step5 - Check the Crack width
*****************************************************
Compute the stress level in the FRP bars
    under dead load plus live load.

M DL= (W DL x L^2)/8 =         kN.m     6.04

M DL= (W LL x L^2)/8 =         kN.m     8.14

M DL + LL =         kN.m    14.17


nf= Ef/Ec =          1.80

k= SQRT[2Pf nf + (PF nf)^2] - Pf nf =       .193

ff= M DL+LL / [Af.d (1-k/3)]=         Mpa    107.76

 Determine the strain gradient used to transform
 reinforcement level strains to the near surface
 of the beam where cracking is expected.

B= h-kd /d(1-k) =     1.28

 Calculate the distance form the extreme tension fiber
 of the concrete to the concrete to the centerline of
           the flexural reinforcement.

dc= h - d =         mm 57.00

 Claculate bars spacings.
s= b - 2dc =        mm 64.00


 Compare the crack width. using the reccomended value
        of kb=1.4 for deformed FRP bars.
```

Cont. Figure3.2. Screen shot of solved example by running programme

Cont. Figure3.2. Screen shot of solved example by running programme

```
E:\Design FRP beams.exe                                    ─ □  ✕

***********************************************************
        Step7 - Check the Creep Rupture Stress Limits
***********************************************************

Ms= Ma*[W DL+0.2W LL]/[W LL + W DL]=          kN.m   7.00

 Compute the sustained stress level in the FRP bars.
Ff,s= Ms/[Af d(1-k/3)]=              Mpa      53.24


 Check the stress limits given in Table 8.3

 Table 8.3: Creep rupture stress limits in FRP RC

  ---------------------------------------------------------
  |     Fiber Type     |  GFRP   |  AFRP   |   CFRP   |
  ---------------------------------------------------------
  |     Creep rupture  |         |         |          |
  |stress limits Ff,s  | 0.20Ffu | 0.30Ffu | 0.55ffu  |
  ---------------------------------------------------------


        Enter your ratio according to Table 8.3
.2
According to Table 8.3,Ffs is =         Mpa      99.30


      the calculated Ffs < Ffs Table 8.3 . . . . .  OK


***********************************************************
            Step8 - Design For Shear.
***********************************************************

 Detremine the factored shear deman at a distance d
                from the support

 Vu= [Wu L/2]-Wu d =                  kN    21.44

 Compute the shear contribution of the concrete for
            an FRP-Reinforced member.

 Vc= 0.4 Sqrt[Fc]* b * k * d=         kN    17.89

 FRP shera reinforcement will be required.
 The FRP shear reinforcement will be assumed to be NO3
 closed stirrups oriented vertically.
 To determine the amount of FRP shear reinforcement
 required,the effective stress level in the FRP shear
 reinforcement  must be determined.This stress level
 may be governed by the allowable stress in the
 stirrup at the location of a band,
 which is computed as follows:

ffb= [0.05 3rb/db + 0.3] Ffu =        Mpa     223.42

 Note that the minimum radius of the bend is 3 bar dia

 The design stress of FRP stirrup is limited to:

   ffv= 0.004 Ef -----> must be =< ffb       Mpa     179.20
       Checked ....... OK

 The reqired spacing of the FRP stirrups can be
```

Cont. Figure3.2. Screen shot of solved example by running programme

93

```
E:\Design FRP beams.exe                                    [_][□][X]

The reqiured spacing of the FRP stirrups can be
        computed by rerranging follow Eq.
 s= 0.75Afv ffv d / [Vu - 0.75Vc]=           mm        589.00

   Chech maximum spacing limit= d/2 or 600mm

    d/2=          mm   124.00

The minimum spacing amount can be computed as follow
 s min= Afv ffv / 0.35b =              mm        475.49


 *-*-*-*-*-*-*-*-*-*-*-*-*-*-*-*-*-*-*-*-*-*-*-*-*
              Summary of this Design
 *-*-*-*-*-*-*-*-*-*-*-*-*-*-*-*-*-*-*-*-*-*-*-*-*
  W DL= W SDL + W SW          kN/m  4.30


  Wu= 1.2W DL + 1.7W LL        kN/m 15.02

  Mu= (Wu L^2)/8              kN.m 21.08

Mn= Pf.Ff[1-0.59 Pf.Ff/fc] bd^2 =      kN.m    49.46

Pfb < Pf < 1.4 Pfb     Q=0.3+0.25 Pf/Pfb =     .550

Q . Mn=         kN.m   27.202
Q.Mn > Mu   OK

M DL= (W DL x L^2)/8 =         kN.m      6.04
M DL= (W LL x L^2)/8 =          kN.m      8.14
M DL + LL =                   kN.m     14.17

(Delta i) DL+LL = [5 Ma L^2]/[48Ec Ie]= mm   9.85
(Delta i) DL = W DL/[W DL+LL] * Delta DL+LL =  mm  4.19
(Delta i) LL = W LL/[W DL+LL] * Delta DL+LL =  mm  5.65

Delta LT= De LL + 1.2[De DL + 0.2 De LL]=   mm 12.04
          De LT < L/240 . . . . O K
  Vu= [Wu L/2]-Wu d =                  kN    21.44
Vc= 0.4 Sqrt[Fc]* b * k * d=       kN    17.89
  s= 0.75Afv ffv d / [Vu - 0.75Vc]=         mm        589.00
   Chech maximum spacing limit= d/2 or 600mm
```

Cont. Figure3.2. Screen shot of solved example by running programme

```
 E:\Design FRP beams.exe

 s min= Afv ffv / 0.35b =              mm        475.49


    *-*-*-*-*-*-*-*-*-*-*-*-*-*-*-*-*-*-*-*-*
              Summary of this Design
    *-*-*-*-*-*-*-*-*-*-*-*-*-*-*-*-*-*-*-*-*

  W DL= W SDL + W SW          kN/m  4.30


   Wu= 1.2W DL + 1.7W LL       kN/m 15.02


   Mu= (Wu L^2)/8              kN.m 21.08


Mn= Pf.Ff[1-0.59 Pf.Ff/fc] bd^2 =      kN.m     49.46


Pfb < Pf < 1.4 Pfb    Q=0.3+0.25 Pf/Pfb =      .550


Q . Mn=           kN.m    27.202

Q.Mn > Mu    OK


M DL= (W DL x L^2)/8 =         kN.m      6.04
M DL= (W LL x L^2)/8 =         kN.m      8.14
M DL + LL =                    kN.m     14.17


(Delta i) DL+LL = [5 Ma L^2]/[48Ec Ie]=  mm   9.85
(Delta i) DL = W DL/[W DL+LL] * Delta DL+LL =  mm   4.19
(Delta i) LL = W LL/[W DL+LL] * Delta DL+LL =  mm   5.65


Delta LT= De LL + 1.2[De DL + 0.2 De LL]=      mm 12.04
          De LT < L/240 . . . . O K

  Uu= [Wu L/2]-Wu d =                     kN    21.44

 Vc= 0.4 Sqrt[Fc]* b * k * d=        kN     17.89

  s= 0.75Afv ffv d / [Uu - 0.75Vc]=        mm        589.00

    Chech maximum spacing limit= d/2 or 600mm

    d/2=                      mm    124.00

 The minimum spacing amount can be computed as follow

 s min= Afv ffv / 0.35b =           mm        475.49
 ***************************************************
           Thank you for your attention
      Mohsen Kobraei - University of Malaya
     For more info. please Call +60-12-668-7348
            email: mkobraei@yahoo.com
 ***************************************************
```

Cont. Figure3.2. Screen shot of solved example by running programme

3.4 Summary

In this chapter at first introduced the written computer programme, and then the flowchart of the programme is presented. In the last part of this section, solutions to an example were provided both manually and by the software.

4.0 EXPERIMENTAL PROGRAMME

4.1   Introduction

The experimental programme consisted of seven RC beams. The RC beams were divided into two groups. The first group were strengthened using steel and CFRP longitudinal reinforcement of 12mm diameter while the second group were strengthened by steel bars of 14mm diameter. One of the beams in the group one was selected as the control beam with normal stirrups. Straight shear reinforcement was used in five beams consisting of CFRP-bars and steel bars.

4.2   Properties of Materials

Three types of materials were used in this study. These materials were CFRP, steel bars, and concrete. The following section presents the characteristics of the materials used in this study.

4.2.1 CFRP bars

The data sheet provided by the manufacturer shows that the modulus of elasticity is 200 GPa for CFRP bars. The CFRP exhibits a linear elastic behaviour up to failure. Therefore, the ultimate strength of the CFRP rod based on the failure strain would be about 2400 MPa. Thus it has a high strength and a high modulus. Pre-fabricated carbon FRP (12mm diameter) was used as shear and longitudinal reinforcement for the beam specimens. The CFRP bars had a sand-coated surface as shown in Figure 4.1 to enhance the bond performance between the FRP bars and the surrounding concrete. In addition, Figure 4.2 shows the tested CFRP-bars to illustrate the material's failure. Table 4.1 shows the details of the CFRP. All the FRP reinforcement used in this study was manufactured by LAMACO Inc.
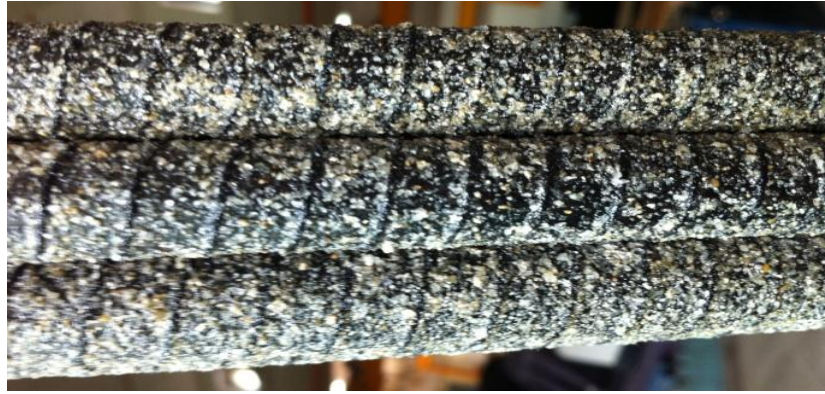
Figure 4.1 Sand-coated CFRP bars

Figure 4.2 Failure of used CFRP-bars in different views

Table 4.1 Details of used CFRP

Nominal diameter ,,,,,	Tensile strength MPa	Modulus of elasticity GPa	Carbon fibre linear weight g/mm^2	Density g/cm^2	Normal area mm^2
12	2400	200	195	1.65	113

4.2.2 Steel Reinforcement

Deformed steel bars of 14 mm in diameter and 12 mm in diameter were used in longitudinal and shear reinforcement, respectively. Based on the test results, the yielded stress and the modulus of elasticity were 450 MPa and 200 GPa, respectively. Additionally, 12 mm-diameter steel bars were used to fabricate the stirrups for the control beam. The yielded stress and its modulus of elasticity were 550 MPa and 200 GPa, respectively.

4.2.3 Concrete

The beam specimens were fabricated using self-compacting concrete (SCC) provided by a tested mix design and cast in place in the concrete laboratory. The concrete used was high strength concrete (HSC) with a target compressive strength of 95 MPa when cured for 28 days. The mix design properties and SCC tests results are shown in Tables 4.2, 4.3 and Figures 4.3.1, 4.3.2, 4.3.3 and 3.3.4. Thirty-six cube specimens of 100 mm size were cast and cured under the same conditions as the test beams.

Eight cubic samples were tested in compression after 28 days; four cubic samples were tested in compression on the day of beam testing and the stress-strain relationship was measured. Four cylinders also were tested in tension by performing the splitting tensile strength test on the day of beam testing. The average compression strength ranged from

93.5 to 98.5 MPa and the average tensile strength ranged from 4.602 to 4.631 MPa. The average modulus of elasticity measured to be 34.838 GPa.

Table 4.2 Mix design proportion $\left(kg / m^{3} \right)$

Cement	Silica Fume	Super Plasticiser	Limestone	Coarse aggregate	Fine aggregate	Water
490	40	9.5	74.5	755	755	191

Table 4.3 SCC tests results

Slump Flue		V Funnel	L Box	Segregation Ratio
T50 = 5.5 sec	Dmax = 65 cm	4 sec	H2/H1 = 0.83	14%

Figure 4.3.1 SCC tests - T50 &Dmax

Figure 4.3.2 SCC tests - L Box

Figure 4.3.3 SCC tests - V Funnel

Figure 4.3.4 SCC tests - Segregation

4.3   SPECIMENS

In this study, seven beams were made and tested; the test specimens had a total length of 3005 mm with a clear span of 2850 mm. The overall cross section measured 250 mm deep and 200 mm wide. The shear span of the test specimens was kept constant at 925 mm. In addition, all beams were provided with different longitudinal reinforcement. All details of fabricated SCC reinforced beams are shown in Table 4.4.

Group-I: The control beam was reinforced with a longitudinal steel bar (12mm) and a normal steel stirrup (12mm), its name was $B_3S_{12}NS_{12@10}$. Two beams were reinforced with No. 12 steel longitudinal reinforcement with different shear reinforcement bars. The beam called $B_1S_{12}S_{12@10}$ used No. 12 steel shear bars which are equally spaced at 100 mm, that represents $d/2$. The beam named $B_5S_{12}C_{12@10}$used No. 12 CFRP shear bars with the spacing of the replacement equal to 100mm, which represents $d/2$.

One of the beams used No.12 CFRP longitudinal reinforcement with No.12 CFRP shear reinforcement. The shear bars were spaced at 100mm. The beam was named $B_2C_{12}C_{12@10}$. The group-I beams are shown in Figure 3.4 and Figures 4.5.1, 4.5.2, 4.5.3 and 4.5.4

Table 4.4 Details of SCC reinforced beams.

Group name	Beams symbol	Main reinforcement bar	Shear reinforcement bar	Shear reinforcement spacing
One (I)	$B_1S_{12}S_{12@10}$	Steel Ø 12	Steel Ø 12	10 cm
	$B_2C_{12}C_{12@10}$	CFRP Ø 12	CFRPØ 12	10 cm
	$B_3S_{12}NS_{12@10}$	Steel Ø 12	Steel Ø 12	10 cm
	$B_5S_{12}C_{12@10}$	Steel Ø 12	CFRP l Ø 12	10 cm
Two (II)	$B_4S_{14}C_{12@10}$	Steel Ø 14	CFRP Ø 12	10 cm
	B_6S_{14}	Steel Ø 14	-	-
	$B_7S_{14}C_{12@7}$	Steel Ø 14	CFRP Ø 12	7 cm

$B_1S_{12}S_{12@10}$ $B_2C_{12}C_{12@10}$

$B_3S_{12}NS_{12@10}$ $B_5S_{12}C_{12@10}$
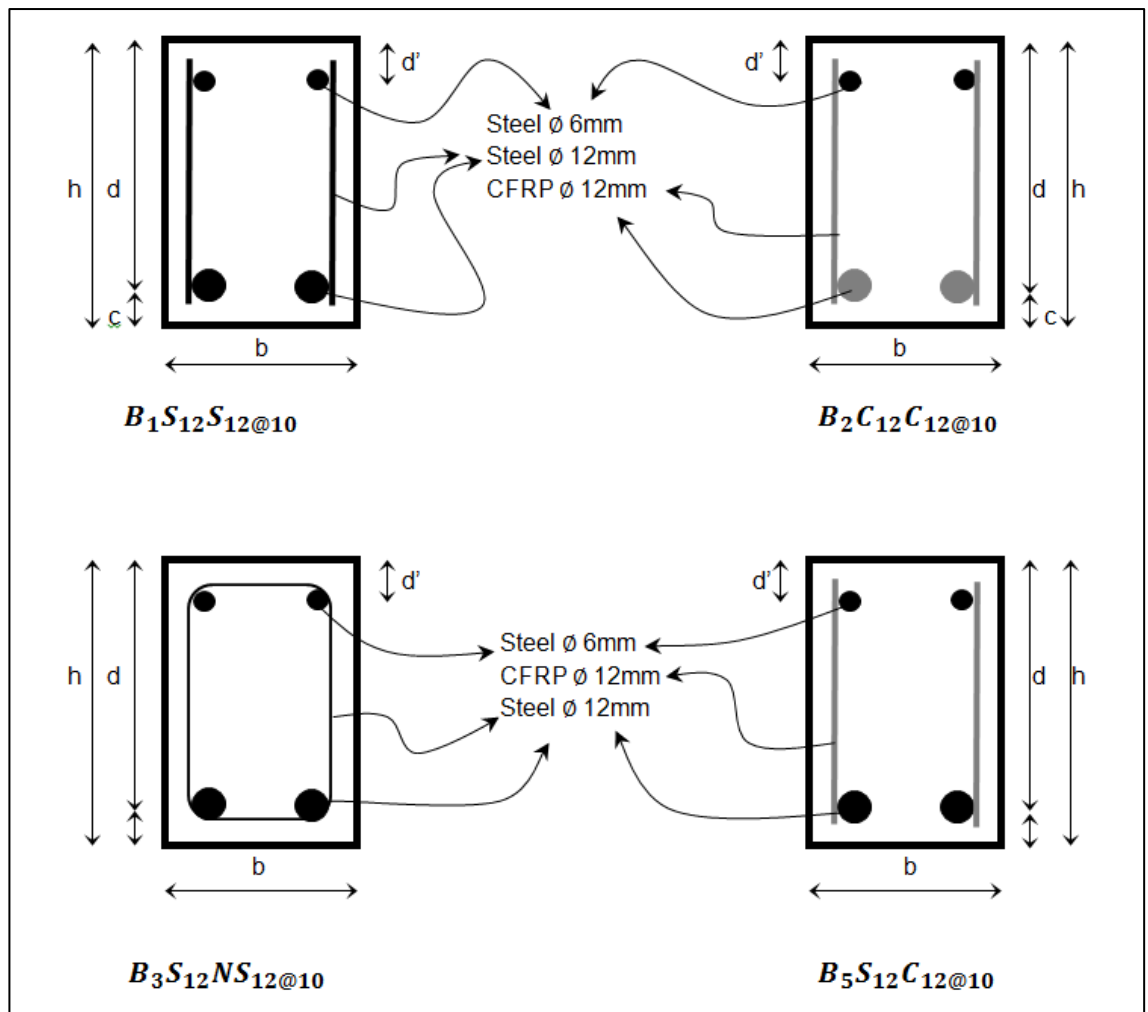
* h = 250mm , d = 220mm , cover = 30mm , d' = 35 mm , length of shear

reinforcement = 230mm

Figure 4.4 Group-I beams

Figure 4.5.1 Group-I beams in moulds to cast - $B_1 S_{12} S_{12@10}$

Figure 4.5.2 Group-I beams in moulds to cast - $B_2 C_{12} C_{12@10}$

Figure 4.5.3 Group-I beams in moulds to cast $-B_3S_{12}NS_{12@10}$

Figure 4.5.4 Group-I beams in moulds to cast $-B_5S_{12}C_{12@10}$

Group-II: Three beams were reinforced with No.14 steel longitudinal reinforcement. Two beams in this group used CFRP bars as shear reinforcement $-B_4S_{14}S_{12@10}$ with an equal spacing of 100mm and $B_7S_{12}C_{12@7}$ with an equal spacing of 70 mm, which represents $d/3$. The third beam was B_6S_{14} without shear reinforcement or stirrups. The results for group-II beams are shown in Figure 4.6 and Figures 4.7.1, 4.7.2 and 4.7.3. In addition, Figures 4.8.1, 4.8.2 and 4.8.3 shows how to tie and install the shear reinforcement bars to the main reinforcement bars.
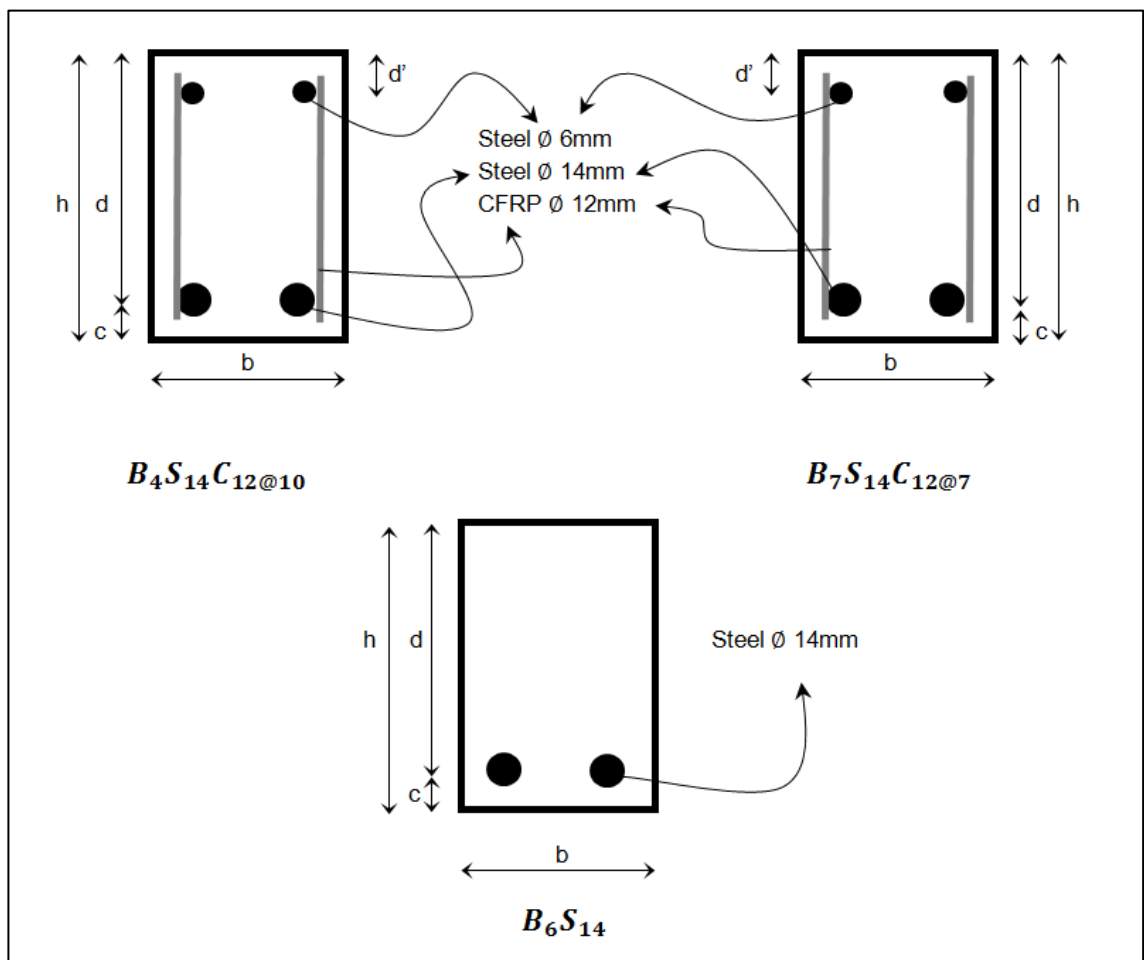
* h = 250mm , d = 220mm , cover = 30mm , d' = 35 mm , length of shear reinforcement = 230mm

Figure 4.6 Group-II beams

Figure 4.7.1 Group-II beams in moulds to cast - $B_4 S_{14} C_{12@10}$

Figure 4.7.2 Group-II beams in moulds to cast - $B_6 S_{14}$

Figure 4.7.3 Group-II beams in moulds to cast - $B_7 S_{14} C_{12@7}$

Figure 4.8.1 Installation and setup of shear reinforcement bars

Figure 4.8.2 Installation and setup of shear reinforcement bars

Figure 4.8.3 Installation and setup of shear reinforcement bars

As depicted in Figure 4.9, in order to determine the compressive strength of the concrete beams, four samples for each beam were taken during casting of the prepared concrete. The beams were removed from the moulds after three days, and were kept in the laboratory under wet sacks and large plastic bags for 28 days. After this period, the samples were stored in the laboratory for another166 days before beams were tested.

Figure 4.9 Samples for compressive strength, modulus of elasticity, tensile strength and flexural strength tests

4.4 Test Setup and Procedure

Different instruments to monitor the behaviour of the sample beams have been used. The deflection at the mid-span, strains in the shear and flexural reinforcement, strains in concrete, and the crack widths has been measured. Some of the equipments and techniques used include Linear Variable Displacement Transducers (LVDTs) is used for measurement of vertical deflection, while strain gauges are used for strain measurement in the steel or concrete. In addition, a demec gauge of 200 mm length for measuring the neutral axis was used. Moreover, the locations of the strain gauges attached to the longitudinal flexural reinforcement and shear reinforcements are detailed in Figure 4.10 for all tested beams.

.
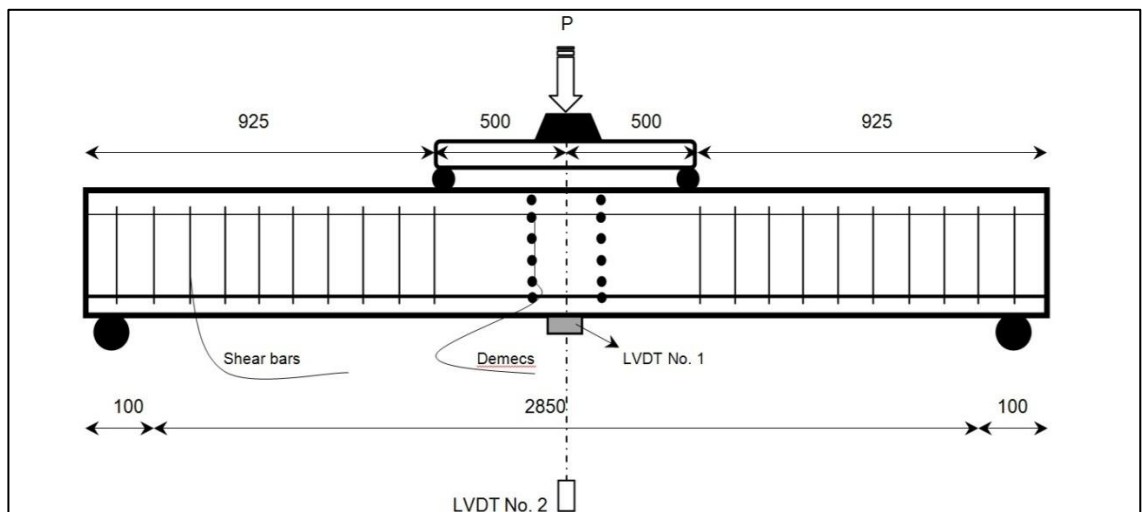
Figure 4.10 Schematic shape

As shown in Figure 3.10, the beams were located over a simply supported clear span of 2850mm. For all specimens, the load was automatically applied using one actuator of

600 kN capacity with a load controlled rate of 6 kN/min. The load was applied at a displacement controlled rate of 0.2 mm/min to avoid any sudden accidental movements and brittle shear failure. While testing, the load was stopped at 10 kN intervals until 80% of the calculated design is reached. At each stop the crack widths and demecs were measured. The first initial crack widths were measured using a hand-held microscope with a magnifying power of 50X. The applied loads, deflection, and strains in reinforcement were recorded using a data acquisition system connected to a computer.

4.5   Summary

In this section detailed some of the properties of used materials have been detailed. Then the procedures of manufacturing the created laboratory specimens, SCC concrete were explained. Lastly conducting tests and the set-up procedures were described.

5.0 RESULTS AND DISCUSIONS

5.1   Introduction

This section will present the summary of results in Table 5.1. Then, topics such as: calculation of nominal moments and capacity of beams, comparison of ultimate load and moment of beams, and comparison of load-deflection and investigation on mode of failure will be discussed. Later in this section, the investigation of flexural and shear cracks and investigation of neutral axis of beams will be considered.

5.2   Summary of Results

Table 5.1 Summary of Result

Beams	*Designed moment M_n kN.m	*Designed vertical load V_n kN	* Computed						Ultimate moment M_u kN.m	Ultimate vertical load V_u kN
			ρ	ρ_f	$\rho_{\min}$	$\rho_{f,\min}$	ρ_b	ρ_{fb}		
$B_1 S_{12} S_{12@10}$	22.45 kN.m		0.0026		0.0025		0.041		32.14 kN.m	
$B_2 C_{12} C_{12@10}$	74 kN.m			0.0025		0.0014		0.002	61.32 kN.m	
$B_3 S_{12} NS_{12@1}$	22.45 kN.m		0.0026		0.0025		0.041		32.82 kN.m	
$B_4 S_{14} S_{12@10}$	30.36 kN.m		0.0035		0.0025		0.041		46.60 kN.m	
$B_5 S_{12} C_{12@10}$	22.45 kN.m		0.0026		0.0025		0.041		31.26 kN.m	
$B_6 S_{14}$		95.8 kN	0.0035		0.0025		0.041			98.76 kN
$B_7 S_{14} C_{12@7}$	30.36 kN.m		0.0035		0.0025		0.041		54.42 kN.m	

* To design and compute the $M_n, V_n, \rho, \rho_f, \rho_{min}, \rho_{f,min}, \rho_b$ and ρ_{fb} author has used his written computer programme which presented on CHAPTER 3.

5.3   Calculation of Nominal Moments and Capacity of Beams

According to produced beams, CFRP and steel bars were used as main and shear reinforcement bars. Therefore, to predict and determine the shear and flexural capacity of those beams and compare them with experimental results, ACI 440 (Guide for the Design and Construction of Structural Concrete Reinforced with FRP Bars) and ACI 318 (Building Code Requirements for Structural Concrete and Commentary) are used.

5.3.1   Calculation of Nominal Moment of $B_2 C_{12} C_{12@10}$

$B_2 C_{12} C_{12@10}$ has been reinforced by CFRP bars as main and shear reinforcement bars. To calculate the nominal moment of this beam, ACI 440 suggest following equation (5.2). In equation (5.2), the f_f comes from equation (5.1).

$$f_f = \left(\sqrt{\frac{(0.003E_f)^2}{4} + \frac{0.85\beta_1 f_c{}'}{\rho_f}} - 0.0015E_f \right) \qquad (5.1)$$

$$M_n = \rho_f f_f \left(1 - 0.59 \frac{\rho_f f_f}{f_c{}'} \right) bd^2 \qquad (5.2)$$

5.3.2   Calculation of Nominal Moment for $B_1 S_{12} S_{12@10}$ - $B_3 S_{12} NS_{12@10}$ - $B_4 S_{14} C_{12@10} - B_5 S_{12} C_{12@10}$ - $B_7 S_{14} C_{12@7}$

These previously mentioned beams above all have been reinforced by steel bars as main and shear reinforcement bars. To calculate the nominal moment of these beams, ACI 318 suggest following equation (5.4). In equation (5.4), the a comes from equation (5.3).

$$a = \frac{A_s f_y}{0.85 f_c' b} \tag{5.3}$$

$$M_n = A_s f_y \left(d - \frac{a}{2} \right) \tag{5.4}$$

5.3.3 Calculation of Nominal shear strength for $B_6 S_{14}$

This beam has been reinforced by steel bars as main bars. According to ACI 318 to determine the nominal moment of the beam without shear reinforcement bar, following equation (5.5) is suggested.

$$V_c = \frac{\sqrt{f_c'}}{8} bd \tag{5.5}$$

5.3.4 Calculate ρ_b and ρ_{min}

Based on ACI 318 and ACI 440 to compute ρ_{min} in concrete beams using steel and FRP as main bars, equations (5.6) and (5.7) are suggested respectively. Furthermore, to determine ρ_b equations (5.8) and (5.9) are recommended respectively.

$$\rho_{min} = \frac{1.4}{f_y} \tag{5.6}$$

$$\rho_{f,min} = \frac{0.4 \sqrt{f_c'}}{f_{fu}} \tag{5.7}$$

$$\rho_b = \left(\frac{0.85\beta_1 f_c^{'}}{f_{fu}}\right)\left(\frac{600}{600+f_y}\right) \tag{5.8}$$

$$f_{fu} = C_E f_{fu}^{*} \qquad \rho_{fb} = \left(\frac{0.85\beta_1 f_c^{'}}{f_{fu}}\right)\left(\frac{E_f \varepsilon_{cu}}{E_f \varepsilon_{cu} + f_{fu}}\right) \tag{5.9}$$

All details of nominal moments are given in Table 5.2.

Table 5.2 Design* parameters properties

Beams	Designed moment M_n kN.m	Designed vertical load V_u kN	Computed ρ	Computed ρ_f	Computed ρ_{min}	Computed $\rho_{f,min}$	Computed ρ_b	Computed ρ_{fb}
$B_1S_{12}S_{12@10}$	22.45 kN.m		0.0026		0.0025		0.041	
$B_2C_{12}C_{12@10}$	74 kN.m			0.0025		0.0014		0.002
$B_3S_{12}NS_{12@10}$	22.45 kN.m		0.0026		0.0025		0.041	
$B_4S_{14}S_{12@10}$	30.36 kN.m		0.0035		0.0025		0.041	
$B_5S_{12}C_{12@10}$	22.45 kN.m		0.0026		0.0025		0.041	
B_6S_{14}		95.8 kN	0.0035		0.0025		0.041	
$B_7S_{14}C_{12@7}$	30.36 kN.m		0.0035		0.0025		0.041	

* To design and compute the $M_n, V_n, \rho, \rho_f, \rho_{min}, \rho_{f,min}, \rho_b$ and ρ_{fb} author has used his written computer programme

which presented on CHAPTER 3.

5.4   Comparison of Ultimate Load and Moment of Beams

Compatible results has been found for the ultimate moment of $B_1 S_{12} S_{12@10}$, $B_3 S_{12} NS_{12@10}$ and $B_5 S_{12} C_{12@10}$. It also has been found that the ratio of UM/DM is bigger than 1.0 for all of them, having values from 1.39 to 1.46. Only the beam called $B_2 C_{12} C_{12@10}$, where CFRP-bars were used as the main and shear reinforcement bars, had the ratio of $\dfrac{M_u}{M_n}$ lower than 1. The reason for this can be attributed to the high tensile strength of CFRP (ACI Committee 440, 2006). The flexural zone had a good resistance and the cracks shifted to the shear zone. The shear zone could not accommodate more cracks and the beams suddenly broke in the shear area for any additional loading. Furthermore, the failure is a brittle type in the shear area of the beams that used CFRP bars as the main reinforcement, (ACI Committee 440, 2006). During loading of $B_2 C_{12} C_{12@10}$, the cracks have gone to be shear crack and, finally, in the shear area the main bars showed brittle failure. This problem could be prevented by reducing the spacing of the CFRP shear reinforcement bars. Instead of d/2 for example, d/3 or d/4 may be selected. The details are shown in Table 5.3.

Table 5.3 Details of ultimate-nominal moment in group-I

Beams	M_n (kN.m)	M_u (kN.m)	$\dfrac{M_u}{M_n}$
$B_1 S_{12} S_{12@10}$	22.45	32.14	1.43
$B_2 C_{12} C_{12@10}$	74	61.32	0.83
$B_3 S_{12} NS_{12@10}$	22.45	32.82	1.46
$B_5 S_{12} C_{12@10}$	22.45	31.26	1.39

In the group-II beams, the ratio of $\frac{M_u}{M_n}$ was bigger than 1.5 in which the largest was 1.77

for $B_7S_{14}C_{12@7}$. However, it is necessary to explain that shear failure seen in B_6S_{14}, did

not have shear reinforcement bars. Although the final rupture was a kind of shear failure

and brittle, but was horizontal. The graph in Figure 5.1, for 90 kN loading, shows that

the concrete has shown good shear resistance and partly succeeded to control the shear

cracks. Furthermore, the main bars reached plastic behaviour; shear failure occurred

after continued loading (Faisal F. W. et al., 1994). This shear crack could be observed

within 10 minutes before the collapse. Details are given in Table 5.4.

Table 5.4 Details of ultimate- nominal load and moments in group-II

Beams	$M_{n\ (kN.m)}$	M_u $(kN.m)$	$\frac{M_u}{M_n}$	V_c (kN)	V_u (kN)	$\frac{V_u}{V_c}$
$B_4S_{14}C_{12@10}$	30.36	46.60	1.53			
B_6S_{14}				95.8	98.76	1.03
$B_7S_{14}C_{12@7}$	30.36	54.42	1.77			

According to Table 5.3 and 5.4, it can be concluded for beams in which their ρ is 50%

to 85% ρ_b , the usage of CFRP bars as shear reinforcement represent a good alternative

for the traditional stirrups.

5.5 Comparison of Load-Deflection and Investigation of Modes of Failure

In group-I and in the control beam, $B_3S_{12}NS_{12@10}$, from 0 to 20kN the beam behaviour was linear and un-cracked. From this point the main bars showed elastic behaviour. The yield point was 61kN. From 0 to 61kN, a small deflection (20mm) was observed. With increase loading from 61kN to 70kN, a large deflection was seen (60mm) and the beam started to show plastic behaviour. It can be said that the behaviour of $B_1S_{12}S_{12@10}$ beam is 90% similar to $B_3S_{12}NS_{12@10}$. The yield point is 59kN with a recorded deflection of 17mm. With a loading of 70kN the deflection increased to 80mm. Performance of $B_5S_{12}C_{12@10}$ is also the same as $B_1S_{12}S_{12@10}$, with the only difference being the initial deflection. In $B_1S_{12}S_{12@10}$ less initial deflection compared with $B_5S_{12}C_{12@10}$ was observed. However, the difference was minimal.

The performance of the beams with FRP as reinforcement bars is totally different from the RC beams with steel bars. In $B_2C_{12}C_{12@10}$ CFRP-bars for the main reinforcement bars has been used and the behaviour of the beams was linear. As predicted, there was not have a yield point and after reaching the failure point, the bars will rupture. In this beam the failure point was at 132.6 kN with 60mm deflection. It can be said that the higher ultimate load with less deflection in reinforced FRP beams in comparison with the similar RC beams reinforced with steel is noteworthy. In addition, it is clear that the disadvantage of FRP RC beams is the brittle failure (ACI Committee 440, 2006).

In group-II and in $B_4 S_{14} C_{12@10}$, the yield point started at 84kN and continued to 105 kN with 55mm deflection. Regarding the use of CFRP shear reinforcement, it can be said that $B_4 S_{14} C_{12@10}$ has shown a good behaviour that is comparable to that of a normal beam. Figure 5.2 indicates that the behaviour of the shear reinforcement bars is similar to normal stirrups; this beam failed in the flexural zone.

In $B_6 S_{14}$, which had two main bars without shear reinforcement bars, the failure happened in the shear zone as predicted. As can be seen in Figure 5.1, until 90 kN the Load-Deflection curves was linear and only after 90 kN to 95 kN it can be seen that the main bar partly yielded due to the good shear strength of concrete. In high strength concrete beams without shear reinforcement bars, the ratio of $\frac{\alpha}{d}$ is very critical. If this ratio is $4 < \frac{\alpha}{d} < 6$, then the mode of failure is shear-flexural (Faisal F. W. et al., 1994). The ultimate capacity, $B_6 S_{14}$ and $B_4 S_{14} C_{12@10}$ are very similar while many differences in their deflection has been observed. It can be comprehended that both have same deflections of 20 mm up to 90 kN, however from this point to the ultimate load, the deflection increased to 27 mm and 80 mm for $B_6 S_{14}$ and $B_4 S_{14} C_{12@10}$ respectively. Comparison of $B_4 S_{14} C_{12@10}$ and $B_6 S_{14}$ yielded no significant difference in their ultimate capacity, however the usage of shear reinforcement in $B_4 S_{14} C_{12@10}$ in absence of brittle rupture in the shear zone.
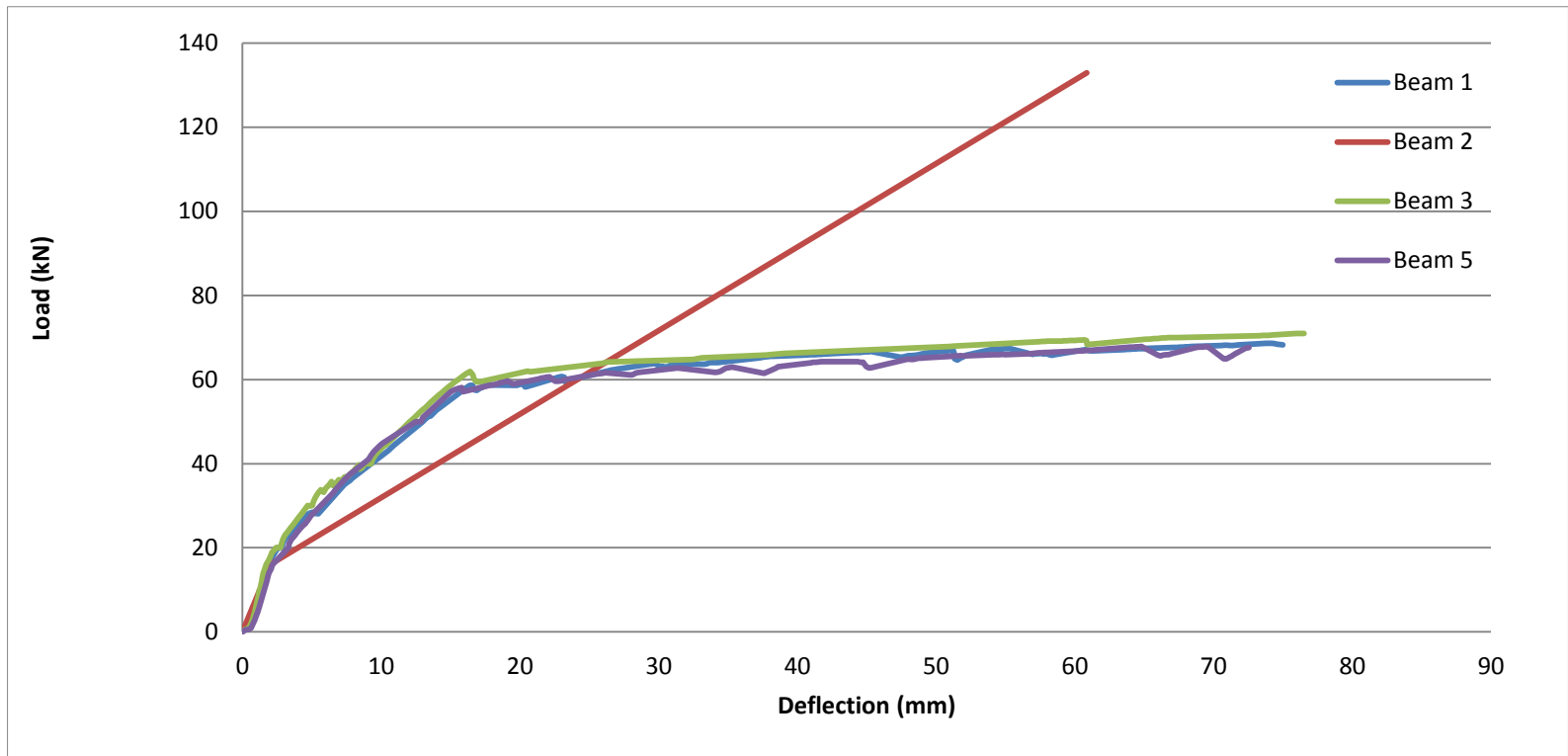
Figure 5.1 Group-I load and deflection curve.

Similar manufacturing procedure was used for both $B_7S_{14}C_{12@7}$ and $B_4S_{14}C_{12@10}$. But the spacing distance of CFRP shear reinforcement

for $B_4S_{14}C_{12@10}$ was $\dfrac{d}{2}$ whereas this interval in $B_7S_{14}C_{12@7}$ was $\dfrac{d}{3}$. The yield point in $B_7S_{14}C_{12@7}$ was at 98 kN with 18mm deflection.

From additional loading up to 116.5 kN, the deflection increased to 85mm. Such a good performance by the beams indicates that usage of

shear reinforcement bars can prevent shear failure.
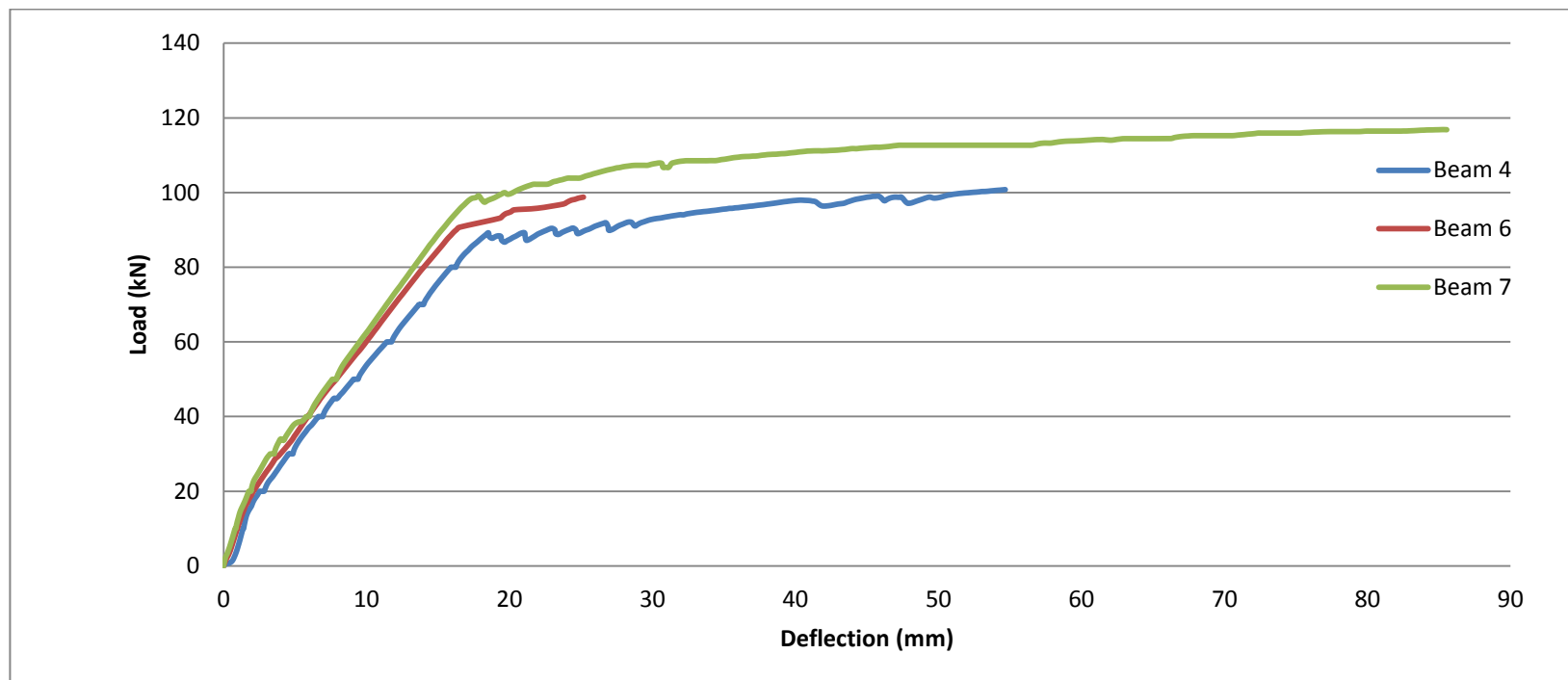
Figure 5.2 Group-II load and deflection curve.

5.6   Investigation of Flexural and Shear Cracks

The analysis and comparison of our results reveal that for all beams the first crack appeared in the flexural zone with the load ranging from 16.3 kN to 20 kN. Additional increase in loading has led to observation of more flexural cracks. At 40 to 60 % of the ultimate load, these cracks emerged in the shear zone.

Group-I: According to Table 4.4, the analysis of the crack modes shown in Figure 5.3.1, and comparison of $B_3 S_{12} N S_{12@10}$, $B_1 S_{12} S_{12@10}$ and $B_5 S_{12} C_{12@10}$, lead us to believe that shear reinforcement bars can be an alternative to stirrups. And the mode of cracks in these beams are very similar to each other. A good crack extension was observed in $B_2 C_{12} C_{12@10}$ beam, however the crack width was larger (Chitsazan I. et al., 2010). Although the cracks lengths were satisfactory before rupture, for reasons that were investigated previously the failure was brittle in nature and happened in the shear area.

Group-II: Regarding the lack of shear reinforcement bars in $B_6 S_{14}$, less number of cracks was recorded. The type of cracking developed in $B_4 S_{14} C_{12@10}$ and $B_7 S_{14} C_{12@7}$ was similar. However, more cracking was seen for $B_7 S_{14} C_{12@7}$, in which the distance of the replaced shear reinforcement bars were closer than in $B_4 S_{14} C_{12@10}$. Table 5.5 and Figure 5.3.2 show the mode of cracks, details of crack width, and load of first cracks.

Table 5.5 Details of crack widths and load of first cracks

Beams	Load of first crack (kN)	Width at first crack (mm)	FCL* / UL*	Average load of first crack (kN)	Average of FCL / UL
$B_1S_{12}S_{12@10}$	20	0.08	0.28	18.66	0.21
$B_2C_{12}C_{12@10}$	17.35	0.12	0.13		
$B_3S_{12}NS_{12@10}$	19.2	0.08	0.27		
$B_4S_{14}C_{12@10}$	16.3	0.04	0.16		
$B_5S_{12}C_{12@10}$	17.8	0.08	0.26		
B_6S_{14}	20	0.06	0.20		
$B_7S_{14}C_{12@7}$	20	0.02	0.17		

*FCL is first crack loading, UL is ultimate load

5.6.1 Cracks simulation: Group-I:

Figure 5.3.1 and Figure 5.3.2 show the group-I and group-II beams under loading and crack simulation.

Figure 5.3.1 Details of mode of cracks (group-I)

Group-II:

Figure 5.3.2 Details of mode of cracks (group-II)

5.7 Investigation of Neutral Axis of Beams

Group-I: The neutral axis in $B_3S_{12}NS_{12@10}$ was observed at 70% of the ultimate load, 30 kN. The neutral axis of $B_3S_{12}NS_{12@10}$ was located at 170 mm from the bottom. In $B_1S_{12}S_{12@10}$the neutral axis was 179 mm from the bottom. Similar results have been found for both $B_5S_{12}C_{12@10}$ and $B_1S_{12}S_{12@10}$showing their neutral axes located above the neutral axis in $B_3S_{12}NS_{12@10}$. The position of the neutral axis in $B_5S_{12}C_{12@10}$ was 173 mm. In $B_2C_{12}C_{12@10}$, which used CFRP bars as the main reinforcement, the neutral axis moved significantly higher, and is located at 191mm. This behaviour has been reported in previous studies (Chitsazan I. et al., 2010).
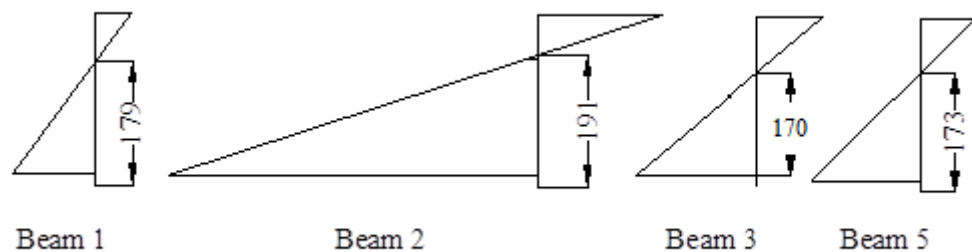
Figure 5.4 Group-I neutral axis (mm)

Group-II: The highest position for neutral axis in this category was recorded to be 185 mm forB_6S_{14}at 40 kN. When CFRP shear reinforcement was used, the position of the neutral axis would be located lower to use more of the compressive capacity of the concrete. From a comparison of $B_4S_{14}C_{12@10}$ and $B_7S_{14}C_{12@7}$ in Figure 5.5, it can be said that if the distance of placing CFRP shear reinforcement is closer, the position of the neutral axis can be lower. At 40 kN loading, the position of the neutral axes in

$B_4S_{14}C_{12@10}$ and $B_7S_{14}C_{12@7}$ were161mm and 148mm, respectively. The position of the neutral axis in $B_7S_{14}C_{12@7}$ was lower than $B_3S_{12}NS_{12@10}$ at 40 kN loading.

Beam 4　　　　　　Beam 6　　　　　　Beam 7
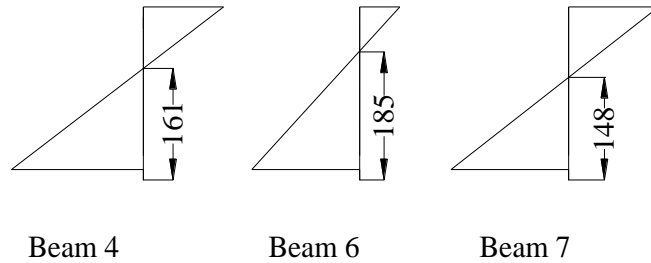
Figure 5.5 Group-II neutral axis (mm)

5.8　Brief Comparison of Beams Behaviour

The following six tables and figures have shown very brief comparison between beams which have been discussed previously.

5.8.1　Comparison of $B_1S_{12}S_{12@10}$　and　$B_3S_{12}NS_{12@10}$

$B_1S_{12}S_{12@10}$ has been reinforced with steel bar (12 mm) as longitudinal bar and straight shear reinforcement bar. The straight shear reinforcements spacing were 10 cm. The tested moment capacity of this beam is 32.14 kN.m. First crack appeared at 20 kN.m of loading with 0.08 mm width.

$B_3S_{12}NS_{12@10}$ has been reinforced with steel bar (12 mm) as longitudinal bar and conventional steel stirrups. The steel stirrups spacing were 10 cm.

The tested moment capacity of this beam is 32.82 kN.m. First crack of this beam appeared at 19.2 kN.m of loading with 0.08 mm width. This beam reinforced with steel as longitudinal and stirrups bars were tested as control specimens. The variable of this comparison was difference of straight shear reinforcement and conventional stirrup.

Details and test results of these beams are summarized in Table 5.6 and Figure 5.6. Regarding to Table 5.6 and Figure 5.6 it can be said that these beams have shown similar behaviour in ultimate moment, load of first crack, width at first crack and deflections. As mentioned above the $B_3S_{12}NS_{12@10}$ has been reinforced with normal steel stirrups and the $B_1S_{12}S_{12@10}$ has been reinforced with straight steel bar as shear reinforcement.

Table 5.6 Comparison of $B_1S_{12}S_{12@10}$ with $B_3S_{12}NS_{12@10}$

Beams	M_n (kN.m)	Computed ρ	Computed ρ_{min}	Computed ρ_b	M_u (kN.m)	$\dfrac{M_u}{M_n}$	Load of first crack (kN)	Width at first crack (mm)
$B_1S_{12}S_{12@10}$	22.45 kN.m	0.0026	0.0025	0.041	32.14	1.43	20	0.08
$B_3S_{12}NS_{12@10}$	22.45 kN.m	0.0026	0.0025	0.041	32.82	1.46	19.2	0.08
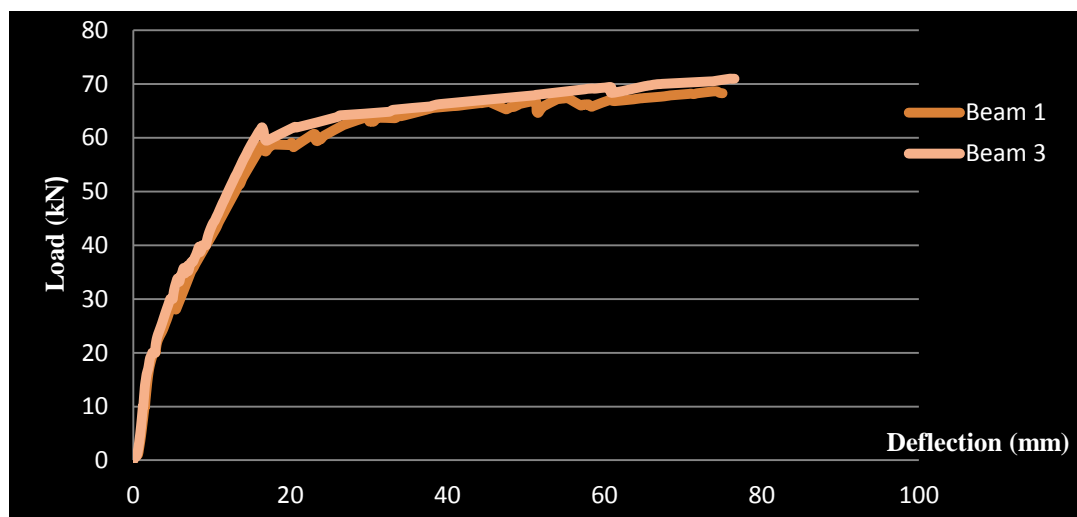
Figure 5.6. Load-deflection curve of $B_1S_{12}S_{12@10}$ and $B_3S_{12}NS_{12@10}$

5.8.2 Comparison of $B_1S_{12}S_{12@10}$ and $B_2C_{12}C_{12@10}$

$B_2C_{12}C_{12@10}$ has been reinforced with CFRP bar (12 mm) as longitudinal and straight shear reinforcement bar . The straight shear reinforcement bars spacing were 10 cm. The tested moment capacity of this beam is 61.32 kN.m. First crack of this beam looked at 17.35 kN.m of loading with 0.12 mm width. This comparison provides a contrast between different materials used to manufacture of these beams. Details and test results of these beams are summarized in Table 5.7 and Figure 5.7. According to Table 5.7 and Figure 5.7 it can be observed that behaviours of these beams are totally different due to used longitudinal reinforcement. $B_2C_{12}C_{12@10}$ has been reinforced with CFRP bar and $B_1S_{12}S_{12@10}$ has been fabricated by steel bar.

Table 5.7 Comparison of $B_1S_{12}S_{12@10}$ with $B_2C_{12}C_{12@10}$

Beams	M_n (kN.m)	Computed ρ	Computed ρ_{min}	Computed ρ_b	M_u (kN.m)	$\dfrac{M_u}{M_n}$	Load of first crack (kN)	Width at first crack (mm)
$B_1S_{12}S_{12@10}$	22.45 kN.m	0.0026	0.0025	0.041	32.14	1.43	20	0.08
$B_2C_{12}C_{12@10}$	74 kN.m	0.0025	0.0014	0.02	61.32	0.83	17.35	0.12
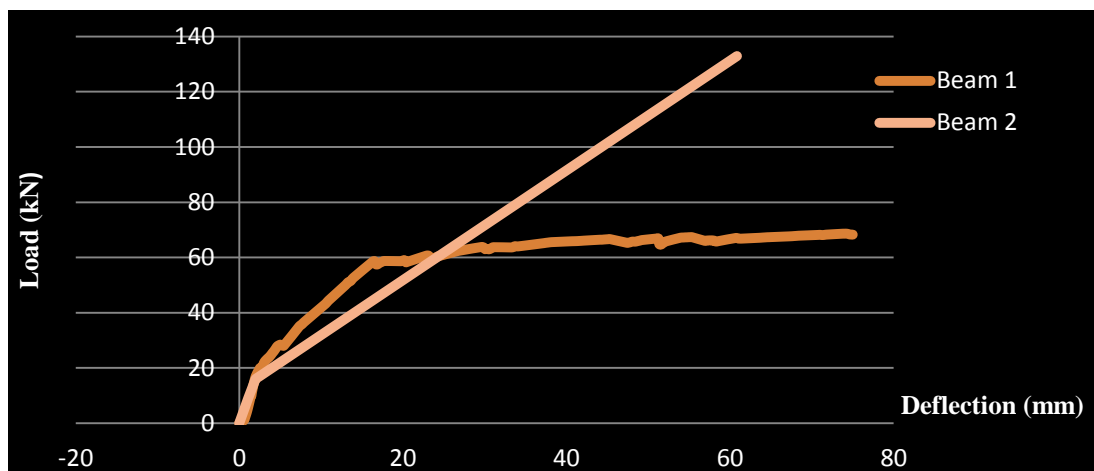
Figure 5.7. Load-deflection curve of $B_1S_{12}S_{12@10}$ and $B_2C_{12}C_{12@10}$

131

5.8.3 Comparison of $B_1 S_{12} S_{12@10}$ and $B_5 S_{12} C_{12@10}$

$B_5 S_{12} C_{12@10}$ has been reinforced with steel bar (12 mm) as longitudinal bar and CFRP (12 mm) as straight shear reinforcement bar. The straight shear reinforcements spacing were 10 cm. The tested moment capacity of this beam is 31.26 kN.m. First crack appeared at 17.8 kN.m of loading with 0.08 mm width. This comparison of a beam which has been reinforced with straight CFRP shear reinforcement bars, reveals the effect of different type of materials used in reinforcing shear zone. Details and test results of these beams are summarized in Table 5.8 and Figure 5.8.

Table 5.8 Comparison of $B_1 S_{12} S_{12@10}$ with $B_5 S_{12} C_{12@10}$

Beams	M_n (kN.m)	Computed ρ	Computed ρ_{min}	Computed ρ_b	M_u (kN.m)	$\dfrac{M_u}{M_n}$	Load of first crack (kN)	Width at first crack (mm)
$B_1 S_{12} S_{12@10}$	22.45 kN.m	0.0026	0.0025	0.041	32.14	1.43	20	0.08
$B_5 S_{12} C_{12@10}$	22.45 kN.m	0.0026	0.0025	0.041	31.26	1.39	17.8	0.08
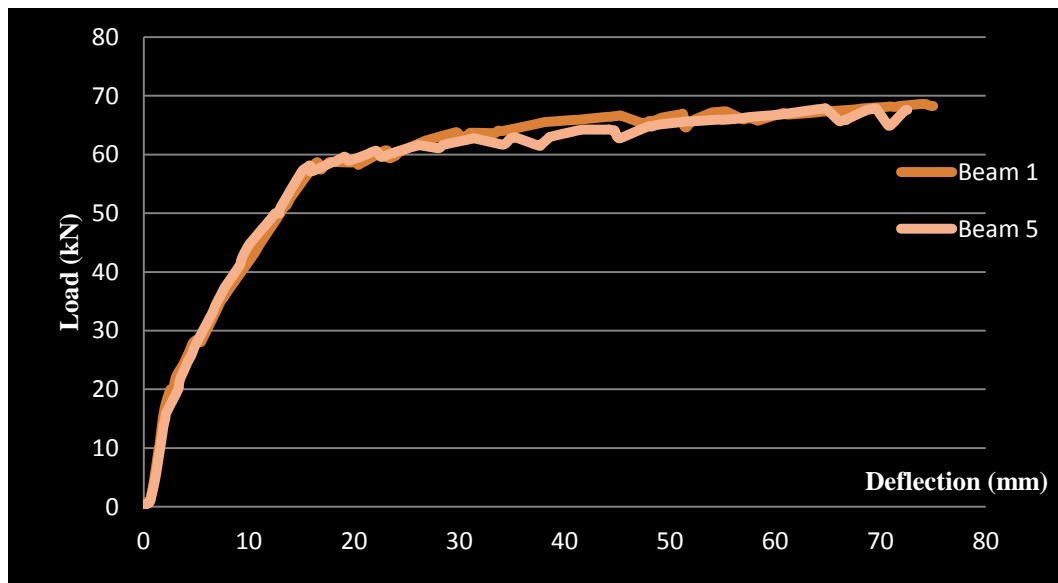
Figure 5.8. Load-deflection curve of $B_1 S_{12} S_{12@10}$ and $B_5 S_{12} C_{12@10}$

5.8.4 Comparison of $B_4S_{14}C_{12@10}$ and $B_5S_{12}C_{12@10}$

$B_4S_{14}C_{12@10}$ has been reinforced with steel bar (14 mm) as longitudinal bar and CFRP shear reinforcement bar (12 mm). The shear reinforcements spacing were 100 mm. The tested moment capacity of this beam is 46.60 kN.m. First crack appeared at 16.3 kN.m of loading with 0.04 mm width. This comparison was made to demonstrate the difference in diameter size of main bars along with the difference in used material to reinforcing shear area. Details and test results of these beams are summarized in Table 5.9 and Figure 5.9. It can be observed that with using greater longitudinal bars, behaviour of beam will be improved.

Table 5.9 Comparison of $B_4S_{14}C_{12@10}$ with $B_5S_{12}C_{12@10}$

Beams	M_n (kN.m)	Computed ρ	Computed ρ_{min}	Computed ρ_b	M_u (kN.m)	$\dfrac{M_u}{M_n}$	Load of first crack (kN)	Width at first crack (mm)
$B_4S_{14}C_{12@10}$	30.36 kN.m	0.0035	0.0025	0.041	46.60	1.53	16.3	0.04
$B_5S_{12}C_{12@10}$	22.45 kN.m	0.0026	0.0025	0.041	31.26	1.39	17.8	0.08
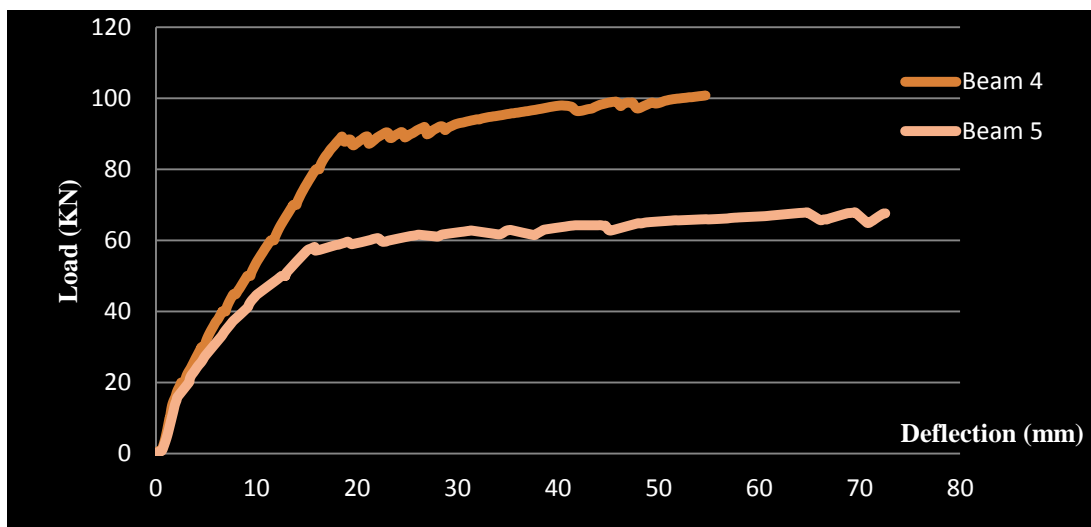
Figure 5.9. Load-deflection curve of $B_4S_{14}C_{12@10}$ with $B_5S_{12}C_{12@10}$

5.8.5 Comparison of $B_5 S_{12} C_{12@10}$ and $B_7 S_{14} C_{12@7}$

$B_7 S_{14} C_{12@7}$ has been reinforced with steel bar (14 mm) as longitudinal bar and CFRP shear reinforcement bar (12 mm). The shear reinforcements spacing were 70 mm. The tested moment capacity of this beam is 54.42 kN.m. First crack appeared at 20 kN.m of loading with 0.02 mm width. The variables of this comparison were difference in (i) shear reinforcement spacing and (ii) ratio of longitudinal bars . Details and test results of these beams are summarized in Table 5.10 and Figure 5.10. the results shows that with increase ratio of longitudinal bars and decrease shear reinforcement spacing ultimate moment, deflection, load of first crack and width at first crack will be improved and beam shows better behaviour.

Table 5.10 Comparison of $B_5 S_{12} C_{12@10}$ with $B_7 S_{14} C_{12@7}$

Beams	M_n (kN .m)	Computed ρ	Computed ρ_{min}	Computed ρ_b	M_u (kN .m)	$\dfrac{M_u}{M_n}$	Load of first crack (kN)	Width at first crack (mm)
$B_5 S_{12} C_{12@10}$	22.45 kN.m	0.0026	0.0025	0.041	31.26	1.39	17.8	0.08
$B_7 S_{14} C_{12@7}$	30.36 kN.m	0.0035	0.0025	0.041	54.42	1.77	20	0.02
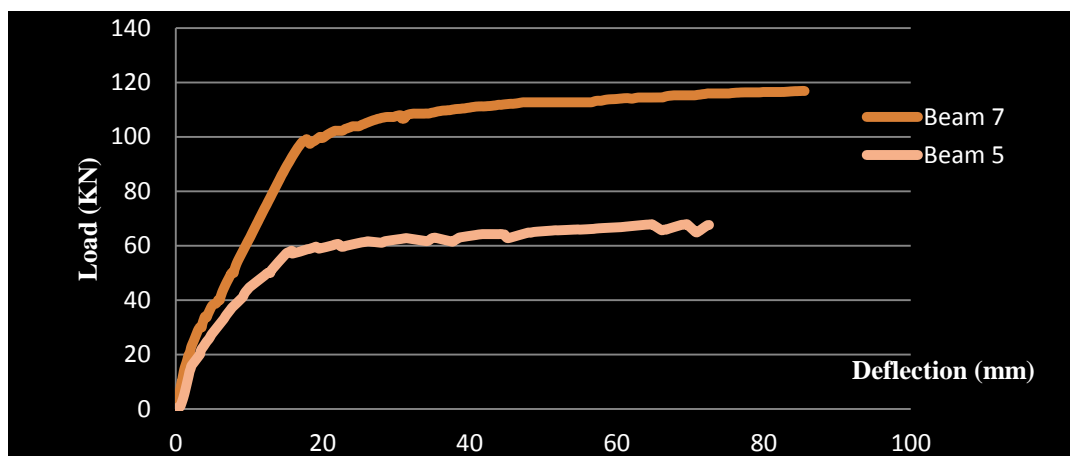
Figure 5.10. Load-deflection curve of $B_5 S_{12} C_{12@10}$ and $B_7 S_{14} C_{12@7}$

5.8.6 Comparison of $B_4S_{14}C_{12@10}$ and B_6S_{14}

B_6S_{14} has been reinforced with steel bar (14 mm) as longitudinal bar. The tested shear capacity of this beam is 98.76 kN. First crack appeared at 20 kN.m of loading with 0.06 mm width. This beam has not been reinforced in shear area. The variables of this comparison was difference in using shear reinforcement bar in $B_4S_{14}C_{12@10}$. Details and test results of these beams are summarized in Table 5.11 and Figure 5.11. These tow beams has been fabricated with steel bar (14 mm) but it is obvious that B_6S_{14} which does not have shear reinforcement bar shows same behaviour until to reach at yielded point. After yielding shear reinforcement shows its role to avoid brittle rupture. Figure 5.11 shows the shear reinforcement of $B_4S_{14}C_{12@10}$ displays good behaviour and B_6S_{14} had brittle rupture.

Table 5.11 Comparison of $B_4S_{14}C_{12@10}$ with B_6S_{14}

Beams	M_n (kN.m)	Computed ρ	Computed ρ_{min}	Computed ρ_b	M_u (kN.m)	V_c (kN)	V_u (kN)	$\frac{V_u}{V_c}$	$\frac{M_u}{M_n}$	Load of first crack (kN)	Width at first crack (mm)
$B_4S_{14}C_{12@10}$	30.36	0.0035	0.0025	0.041	46.60				1.53	16.3	0.04
B_6S_{14}		0.0035	0.0025	0.041		95.8	98.76	1.03		20	0.06
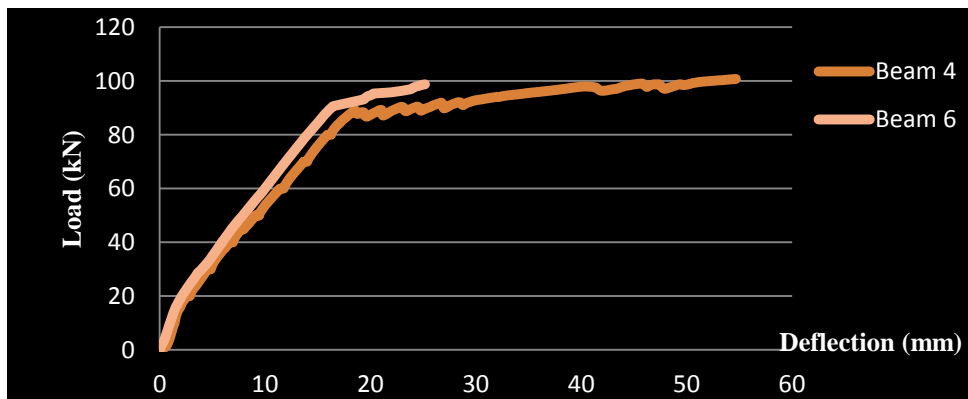
Figure 5.11. Load-deflection curve of $B_4S_{14}C_{12@10}$ and B_6S_{14}

5.8.7   Comparison of $B_4 S_{14} C_{12@10}$ and $B_7 S_{14} C_{12@7}$

$B_4 S_{14} C_{12@10}$ has been reinforced with steel bar (14 mm) as longitudinal bar and CFRP shear reinforcement bar (12 mm). The shear reinforcements spacing were 100 mm. $B_7 S_{14} C_{12@7}$ has been reinforced with steel bar (14 mm) as longitudinal bar and CFRP straight shear reinforcement bar (12 mm). The shear reinforcements spacing were 70 mm. The variable of this comparison was the difference in shear reinforcement bar spacing. Details and test results of these beams are summarized in Table 5.12 and Figure 5.12. As Table 5.12 and Figure 5.12 show, decreasing the spacing of the shear reinforcement, will reduce the width at first crack, decrease the load of first crack and increase the ultimate load of the beam.

Table 5.12 Comparison of $B_4 S_{14} C_{12@10}$ with $B_7 S_{14} C_{12@7}$

Beams	M_n (kN.m)	Computed ρ	Computed $\rho_{\min}$	Computed ρ_b	M_u (kN.m)	$\dfrac{M_u}{M_n}$	Load of first crack (kN)	Width at first crack (mm)
$B_4 S_{14} C_{12@10}$	30.36	0.0035	0.0025	0.041	46.60	1.53	16.3	0.04
$B_7 S_{14} C_{12@7}$	30.36 kN.m	0.0035	0.0025	0.041	54.42	1.77	20	0.02
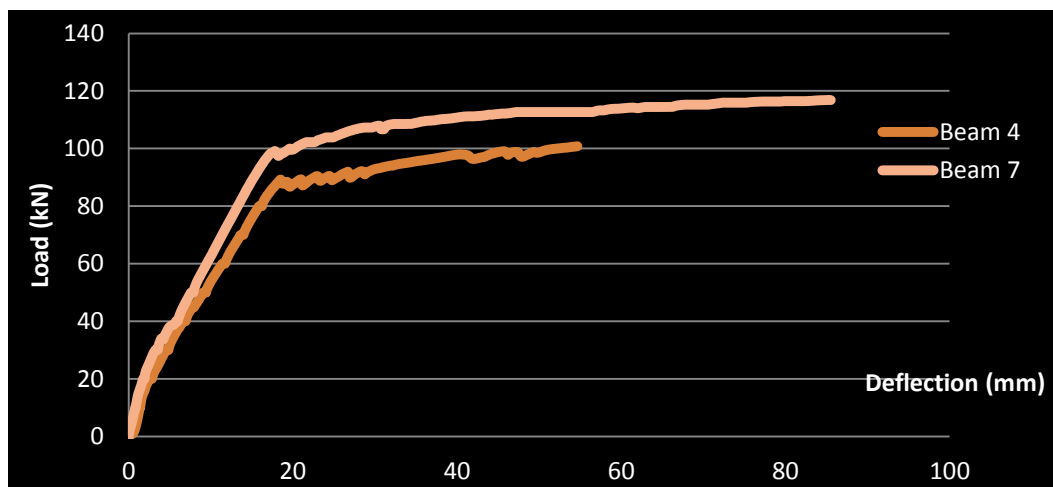
Figure 5.12 Load-deflection curve of $B_4 S_{14} C_{12@10}$ and $B_7 S_{14} C_{12@7}$

136

5.9   Summary

This chapter introduced the summary of results firstly and later presented discussions about results in five following sections:

Calculate nominal moments and capacity of beams, comparison of ultimate load and moment of beams, comparison of load-deflection and investigation on mode of failure, investigation of flexural and shear cracks and investigation of neutral axis of beams..

6.0 CONCLUSIONS AND RECOMMENDATIONS

6.1 Conclusions

This research has conducted on seven full scale RC beams which were made of self-compacting concrete with 95 MPa average compressive strength. The main parameters of this research were steel shear reinforcement bar, CFRP shear reinforcement bar, the longitudinal reinforcement ratio and decrease distance of CFRP shear reinforcement spacing. The analysis of experimental results and comparative study in this research reveal the following conclusions:

(a) When using straight CFRP shear reinforcement bars, the ultimate capacity of self-compacting reinforced concrete beam result in 95% similarity with concrete beams using normal steel stirrups. Therefore, using CFRP shear reinforcement will help to avoid brittle rupture and beams exhibit more deflection. It can be said that straight CFRP shear reinforcement bars in RC beams are an excellent alternative replacement of normal steel stirrups in RC beams.

(b) The RC beam with CFRP as shear reinforcement bar in comparison with the RC beams with normal stirrups and straight steel bar as shear reinforcement shown to have similar behaviour. Results are compatible within 97% for deflections, 97% for ultimate shear, and 95% for flexural capacity. However, CFRP shear reinforcement bar have a better cracks pattern which make them to avoid expansion of shear cracks.

(c) With decrease CFRP shear reinforcement bars spacing, more cracking with less width was observed. In addition with increase in the bar ratio and decrease CFRP shear reinforcement spacing, bend capacity will be increased significantly.

(d) The CFRP RC beam had more capacity with less deflection in comparing with steel RC beam.

(e) A computer programme to analysis of reinforced concrete beams by FRP materials was developed in FORTRAN programming language.

6.2   Recommendations for Future Work

Based on the conducted experimental investigations and their findings, the following recommendations for future work are proposed:

(a) The behaviour of normal concrete beams reinforced with FRP-bars as shear reinforcement.

(b) To use different FRP shear reinforcement bars ratio should be investigated to evaluate the shear compression failure.

(c) The shear behaviour of pre-stressed concrete beams reinforced with FRP stirrups needs to be investigated.

(d) More experimental work is needed to refine the shear crack width predictions and develop a rational model.

(e) Investigations on normal concrete beams reinforced with kind of FRP-bars as main and shear reinforcement bars and compare them with finite element modeling.

REFRENCES

ACI 440.3R-04 (2004). Guide test methods for fiber-reinforced polymers (FRPs) for reinforcing or strengthening concrete structures. American Concrete Institute, Farmington Hills, MI, USA.

ACI Committee 318 (1999). Building code requirements for structural concrete (ACI 318-99) and commentary (318R-99). American Concrete Institute, Farmington Hills, Mich.

ACI Committee 440 (2006). Guide for the design and construction of concrete reinforced with FRP bars (ACI 440.1R-06). American Concrete Institute, Farmington Hills, Mich.

AIJ (1987). Data for Ultimate Design of Reinforced Concrete Structures, Architectural Institute of Japan. 52-55.

AlMusallam TH, Al-Salloum YA, Alsayed SH, Amjad MA (1997). Behavior of concrete beams doubly reinforced by FRP bars. Proceedings of the third international symposium on non-metallic (FRP) reinforcement for concrete structures (FRPRCS-3), Japan, 2: 471–478.

Alsayed SH, Al-Salloum Y. AlMusalaam T. & Amjad M., (1996). Evaluation of Shear Stresses in Concrete Beams Reinforced by FRP Bars. Proceeding of the Second International Conference on Advanced Composite Materials for Bridge and Structures (ACMBS-II), Montreal, Quebec, August. 173-179.

Alsayed SH, Al-Salloum Y. AlMusalaam T. & Amjad M., (1997). Shear Design of GFRP Bars. Proceeding of the Third International Symposium on Non-Metaliv (FRP) Reinforced for Concrete Structures, Sapporo, Japan, 2(10): 285-292.

Alsayed SH (1998). Flexural behaviour of concrete beams reinforced with GFRP bars. Cem. Concr. Compos. 20(1): 1–11.

ASCE-ACI Committee 426 on Shear and Diagonal Tension, (1973), The Shear Strength of Reinforced Concrete Members, ASCE Journal of the Structural Division. 99(5): 1091-1185.

ASCE-ACI Committee 445 on Shear and Torsion, (1999), Recent Approaches to Shear Design of Structural Concrete, ASCE Journal of Structural Engineering. 124(12) : 1375-1417.

ASTM D618-61 (1995). Standard practice for conditioning plastics and electrical insulating materials for testing. Annual Book of ASTM Standards, vol. 8.01. Philadelphia, PA: American Society for Testing and Materials.

Badawi M and soudki K (2009). Flexural strengthening of RC beams with prestressed NSM CFRP rods – Experimental and analytical investigation. Cons. Buil. Mate. 23(10): 3292–3300.

Barros JAO, Dias SJE (2003). Shear strengthening of reinforced concrete beams with laminate strips of CFRP. International conference composites in constructions – CCC2003, Cosenza, Italy, 16–19 September. 289-94.

Barros JAO, Fortes AS (2005). Flexural strengthening of concrete beams with CFRP laminates bonded into slits, Cem. Conc. Compo. 27(4): 471-480.

Blaschko M, Zilch K (1999). Rehabilitation of concrete structures with strips glued into slits. Proceedings of the 12th Int. Conference on Composite Materials, Paris.

Bonaldo E, Barros JAO. Lourenço PB (2005). Steel fibre reinforced and laminate strips for high effective flexural strengthening of RC slabs. Report 05-DEC/E-14, Civil Engineering Department, University of Minho, Portugal.

Canadian Standard Association (CSA) (1994). Design of Concrete Structures for Buildings (CAN-A23.3-94), Rexdale, Ontario, 220.

Canadian Standard Association (CSA) (2006). Canadian High-Way Bridges Design Code.CAN/CSA-S6-06, Canadian Standard Association, Rexdale, Ontario, Canada.

Chitsazan I, Kobraei M, Zamin Jumaat M, Shafigh P (2010). An experimental study on the flexural behavior of FRP RC beams and a comparison of the ultimate moment capacity with ACI, J. Civ. Eng. Cons. Tech. 1(2): 27-42.

Collins M., Mitchell D., Adebar P., Vecchhio F., (1996). A General Shear Design Method, ACI Structural Journal, 93(1): 36-45.

Djelal C., Vanhove Y. and Magnin A. (2004), Tribologicalbehavior of self compacting concrete, Cement and Concrete Research, 34 : 821–828.

Duranovic N., Pilakoutas K. & Waldron P. (1997). Tests on Concrete Beams Reinforced with GFRP Bars. Proceeding of the Third International Symposium on Non-Metaliv (FRP) Reinforced for Concrete Structures, Sapporo, Japan, 2(10): 479-486.

El-Hacha R, Rizkalla SH (2004). Near-surface-mounted fibre-reinforced polymer reinforcements for flexural strengthening of concrete structures. Stru. J. 101 (5): 717-726.

Eik M.A., Bakht B. (1996). None-Metalic Shear Reinforcement for RC Beams. Proceeding of the 24th Annual Conference, Canadian Society of Civil Engineering, CSCE, Edmonton, Albertra. 1(5): 159-165.

Eurocode No. 2, (1992). Design of Concrete Structures – Part 1: General rules and rules for buildings, European Committee for Standardization, Lausanne, 253.

Eurocrete Project (1996), Modification of Design Rules to Incorporate Non-ferrous Reinfprcement, perepared by Clarke J.L., O'Regan D.P. & Thirugnanedran C, January. 34.

Faisal FW, Samir AA, Ghazi SH (1994). Shear behaviour of reinforced high-strength concrete beams without shear reinforcement. Eng. J. Qatar University, 7: 91-113.

Ginley T.J and Choo B.S (1990), Reinforced Concrete Design Theory and Examples Second edition, 85-87.

Islam AKM (2009). Effective methods of using CFRP bars in shear strengthening of concrete girders. Eng. Stru. 31(3): 709-714.

Lorenzis De L., & Nanni, A. (2001). Characterization of FRP Rods as Near-Surface Mounted Reinforcement, Journal of Composites for Construction, 5(2): 114-121.

Lorenzis De L. & Nanni A.,(2001b). Shear Strengthening of Reinforced Concrete Beams with Near-Surface Mounted Fiber-Reinforced Polymer Rods. ACI Structural Journal, American Concrete Institute, (98(1): 60-68.

Lorenzis De L., Nanni A. (2002). Bond between near-surface mounted FRP rods and concrete in structural strengthening, ACI Stru. J. 99 (2): 123-133.

MacGregor, J. (1997), Reinforced Concrete: Mechanics and Design, 3rd Edition, Prentice Hall, Englewood Cliffs, N.J., 939.

Maruyama K. & Zhao W., (1996). Size Effect in Shear Behaviour of FRP Reinforced Concrete Beams. Proceedings of the Second International Conference on Advanced Composite Materials for Bridges and Structures (ACMBS-II), Montreal, Quebec, August. 227-234.

Michaluck C. R., Rizkalla S. H., Tadros G., Benmokrane B. (1998), Flexural Behavior of One-Way Slabs Reinforced by Fiber Reinforced Plastic Reinforcements, ACI Structural Journal, 95(5) : 353-365.

Mohamed Ali M.S., Oehlers D.J., Griffith M.C., Seracinob R. (2008), Interfacial stress transfer of near surface-mounted FRP-to-concrete joints, Engineering Structures , 1861–1868.

Nagasaka T., Fukuyama H. & Tanigaki M., (1997). Shear Behaviour of Concrete Beams Prestressed with CFRP Tendons: Perliminary Tests Evaluation, Proceeding of the Third International Symposium on Non-Metallic FRP Reinforcement for Structures, Sapporo, Japan, 2(10): 679-686.

Nakano K., Matsuzaki Y., Fukuyama H. & Teshigawara M. (1993), Flexural performance of concrete beams reinforced with continuous fibre bars. In ACI Int. Symposium 1993, Fibre Reinforcement for Concrete Structures, Ed. A. Nanni, Detroit, MI, 743–751.

Nanni A (1999). Composites: Coming on Strong, Con. Constr. 44(1): 120-124.

Nanni A., Ludovico M. Di and Parretti R. (2004), Shear strengthening of a PC bridge girder with NSM CFRP rectangular bars, 7(4) : 97–109.

Nawy E. G., Neuwerth G. E. and Philips C. J. (1971), Behavior of Fiber Reinforced Concrete Beams, Journal of the Structural Engineering, ASCE Proceedings, 97(9) : 2203-2215.

Nielsen M., (1984). Limit Analysis and Concrete Plasticity, Prentice-Hall, Inc., Englewood Cliffs, New Jersey, 421.

Niwa J., Hirai Y. & Tanabe T. (1997). Size Effect in Shear Sterength of Concrete Beams Reinfoprced with FRP Rods, Proceeding of the Third International Symposium on Non-Metaliv (FRP) Reinforced for Concrete Structures, Sapporo, Japan, 2(10): 293-300.

Novidis D, Pantazopoulou SJ, Tentolouris E (2007). Experimental study of bond of NSM-FRP reinforcement. Cons. Buil. Mate. 21(8): 1760–1770.

Okumura K., Saito H, Akiyama H. & Nakamura H. (1993). Mechanical Properties of Concrete Structures Reinfprced by CFRP Rods as Shear Reinforcement. FIP Symposium. 93, Kyoto, Japan, 2(10): 819-826.

Rizzo A, De Lorenzis L (2009). Behavior and capacity of RC beams strengthened in shear with NSM FRP reinforcement. Cons. BuiL. Mate. 23 (4): 1555-1567.

Sonbe Y., Kanakube T., Fujisawa M., Tanigaki M. & Okamoto T. (1995). Structural Performance of Concrete Beams Reinforced with Diagonal FRP Bars, Non-Metalic (FRP) Reinforcement for Concrete Structures, Proceeding of the Second International RILEM Symposium (FRPRCS-2), edited by Taerwe L. & FN E. SPON, Great Britain. 344-351.

Sonebi M (2004). Medium strength self-compacting concrete containing fly ash: modeling using factorial experimental plans, Cement Concrete Res. 34: 1199-1208.

Tan K, Tumialan G, Nanni A. (2002). Evaluation of CFRP systems for the strengthening of RC slabs, CIES 02 38, Final Report, University of Missouri Rolla, 120.

The European Guidelines for Self Compacting Concrete (2005).

Thériault M, Benmokrane B (1998). Effects of FRP reinforcement ratio and concrete strength on flexural behavior of concrete beams. J. Compo. Const. 2(1): 7–16.

Tottori S., & Wakui H. (1993). Shear Capacity of RC and PC Beams Using FRP Reinforcement, American Concrete Institute, ACI SP-138, edited by Nanni A. and Dolan C.W. 615-631.

Tureyen AK, Frosch RJ (2002). Shear tests of FRP-reinforced concrete beams without stirrups. ACI Struc. J. 99(4): 427–434.

Vijay P., Kumar S. & GanaRao H., (1996). Shear and Ductility Behaviour of Concrete Beams Reinforced with GFRP Bars, Proceeding of the Second International Conference on Advanced Composite Materials for Bridge and Structures (ACMBS-II), Montreal, Quebec, August, 217-252.

Wang B, Teng JG, Lorenzis LD, Zhou LM, Ou J, Jin W, Lau KT (2009). Strain monitoring of RC members strengthened with smart NSM FRP bars. Cons. Buil. Mate. 23(4): 1698–1711.

Winter, G., and Nilson, A. H. (1979). Design of Concrete Structure, 9th Edition, McGraw Hill Book Company, New York, USA. 647.

Yang J, Wu YF (2007). Interfacial stresses of FRP strengthened concrete beams: Effect of shear deformation, Compo. Struc., 80(3): 343–351.

Yonekura A., Tazawa E. & Nalayama H. (1993). Flexural and Shear Behaviour of Prestressed Concrete Beams Using FRP Rods as Prestressing Tendons, American Concrete Institute, ACI SP-138, edited by Nanni A. and Dolan C.W. 525-548.

Yost JR, Goodspeed CH, Schmeckpeper ER (2001). Flexural performance of concrete beams reinforced with FRP grids. J. Compo. Constr. 5(1): 18–25.

Zhao W., Maruyama K. & Suzuki H. (1995). Shear Behaviour of Concrete Beams Reinforced by FRP Rods as Longitudinal and Shear Reinforcement. Non-Metaliv (FRP) Reinforcement for Concrete Structures, Proceedings of the Second International RILEM Symposium (FRPRCS-2), Edited by L. Taerwe, E & FN SPON, Great Britain. 352-359

APPENDIX

Source of Program

```
C    PROGRAM MAIN


C        ************************************************************

C                "Mohsen  Kobraei  Master  of  CIVIL  Engineeringn  -  CONCRETE
STRAUCTUERS."


C        ************************************************************
        implicit real*8(a-h,o-z)
write(*,*)'      This program writed regarding to ACI 440    '
        write(*,*)'                                              '
        write(*,*)'   Mohsen Kobraei - Master of Civil Engineering'
        write(*,*)'              Concrete Structuers              '
        WRITE(*,*)'                                              '
        write(*,*)'  Design and Anlaysis of Concrete Beams with FRP-bars'
        write(*,*)'                                             '
        write(*,*)'                                             '
        write(*,*)'                                             '
        write(*,*)'        ... Please Enter Password, Thanks ...   '
        read(*,*)pass
        if(pass==080084)then
```

```fortran
      continue

      elseif(pass/=080084)then

      stop

      endif


      WRITE(*,*)'              Enter your values in SI Units            '


write(*,*)' f Concrete      MPa'

read(*,*)b


      WRITE(*,*)' f FRP      MPa'

read(*,*)c


write(*,*)' W Live Load      kN/m'

read(*,*)d


      write(*,*)' W Service Dead Load      kN/m'

read(*,*)e


      WRITE(*,*)'  Span of L      m'

read(*,*)f


      write(*,*)'  Modulus of Elasticity FRP      Ef=      MPa'

read(*,*)h
```

```fortran
        write(*,*)'                                          ,

        write(*,*)'*********************************************'

        write(*,*)'Step1-Estimate the appropriate dimensions of the BEAM.'

        write(*,*)'*********************************************'

        write(*,*)'                                          ,

write(*,1)f/10

1       format(' Recommended h =  Span/10 =    meter ',f6.3)


    200 write(*,2)

2       format('   Enter your h      mm',f6.2)

read(*,*)ai


        write(*,3)

3       format('   Enter your b (width)      mm',f6.2)

read(*,*)am


write(*,4)

4       format('   Cover= ?       mm',f6.2)

read(*,*)aj


        write(*,5)

5       format('   Enter (fi) of bars for MAIN      mm',f6.2)

read(*,*)ak
```

```
                    write(*,6)

6       format('   Enter (fi) of bars for SHEAR      mm',f6.2)

read(*,*)al

        write(*,*)'                                                    ,

        write(*,*)'                                                      ,

        r=ai-aj-al-ak/2

        write(*,7)r

7       format('   Estimated  d= h - cover - db shear - db/2    mm=',f8.2)


write(*,*)'                                              ,

        write(*,*)'                                                ,


        write(*,*)'****************************************************'

        write(*,*)'          Step2 - Compute the factored load.'

        write(*,*)'****************************************************'


        if(b<30)then

        a=.85

        endif

        if(b>56)then

        a=0.65

        endif

        if(30<b.and.b<56)then

        a=.65-.005*(b-30)/7
```

151

```fortran
      endif

write(*,*)'                                                    ,

      o=e+(am/1000)*(ai/1000)*24

      write(*,8)o
8     format('   W DL= W SDL + W SW       kN/m',f6.2)
write(*,*)'                                                  ,


      write(*,*)'                                             ,
      write(*,*)'                                               ,


      write(*,*)'                                             ,

      p=1.2*o+1.7*d

write(*,9)p
9     format('   Wu= 1.2W DL + 1.7W LL       kN/m',f6.2)
write(*,*)'                                             ,

      write(*,*)'                                           ,
      write(*,*)'                                           ,
      write(*,*)'                                             ,


      q=p*f*f/8

      write(*,10)q

10    format('   Mu= (Wu L^2)/8        kN.m',f6.2)
write(*,*)'                                           ,
```

152

```
      write(*,*)'*********************************************'


      write(*,*)'Step3-Compute the design rapture stress of the FRP bar'

      write(*,*)'*********************************************'
write(*,*)'                                      '


      write(*,*)' ACI 440 - Table 7.1'
write(*,*)' .................'


      write(*,*)' Enviromental Reduction Factor for '




write(*,*)' Various Fibre And Exposure Condition'
      write(*,*)'                                      '

      write(*,*)'                                      '

      write(*,*)'                                      '

      write(*,*)'------------------------------------'
write(*,*)' Exposure Condition| Fibre Type | CE '

      write(*,*)'                                      '
write(*,*)' Concrete NOT Ex.  |   Carbon   | 1.0'

      write(*,*)'      to Earth     |   Glass  | 0.8'

      write(*,*)'     And Weather   |  Aramid| 0.9'



      write(*,*)'------------------------------------'
```

```fortran
      write(*,*)' Concrete Exposure |  Carbon  | 0.9'
      write(*,*)'     to Earth  |   Glass| 0.7'
      write(*,*)'   And Weather  |   Aramid | 0.8'
      write(*,*)'------------------------------------'
      write(*,*)'                                    '
      write(*,*)' Please Enter your CE from the Table 7.1'
      read(*,*)bb


      bc=bb*c
      write(*,11)bc


11    format(' Ffu= CE x F FRP     MPa   ', f10.2)


      write(*,*)'*********************************************************'


      write(*,*)'  Step4 - Determine the area of FRP bars Required '
      write(*,*)'            for flexural strength.'
      write(*,*)'*********************************************************'
write(*,*)'                                                      '


write(*,*)' Assume an initial amount of FRP Reinforcement='
      write(*,15)ak
15    format(f6.1)
      write(*,14)
```

154

```
14    format(' How many FRP bars you want to use?',f6.2)

read(*,*)bb


      write(*,*)'                                                    '

      write(*,*)' Compute the balanced FRP Reinforcement ratio'

      write(*,*)'                                                   '

      write(*,*)'                                                   '

      write(*,*)'                                                   '


bd=.85*(b/bc)*a*((0.003*h)/(0.003*h+bc))

write(*,12)bd

12    format(' Pfb= 0.85 (fc/fu) B1[(0.003 Ef)/(0.003 Ef + fu)] =',f9.5)



write(*,*)'                                                        '

      write(*,*)'                                                   '

      write(*,*)'                                                   '



      be=(bb*3.14*ak*ak/4)/(r*am)

write(*,13)be

13    format(' Pf= Af/bd =',f8.5)


write(*,*)'                                                        '

      write(*,*)'                                                   '
```

```fortran
      bi=1.4*bd

      write(*,18)bi

 18   format(' Max P is 1.4 Pfb =     ',f8.5)

write(*,*)'                                                      '

      write(*,*)'                                                  '

      write(*,*)'                                                  '


      WRITE(*,*)' A= (.003Ef)^2/4'

      WRITE(*,*)' B= (0.85B1 fc 0.003EF/Pf)'

      WRITE(*,*)' C= (0.5*.003Ef)'

      bf=(sqrt(((0.003*h)*(0.003*h)/4)+(0.85*a*b*.003*h/be))-(.0015*h))

      write(*,16)bf

 16   format(' Ff=SQRT[ A + B ]- C  =       Mpa   ',f10.2)

      write(*,*)'                                              '

      write(*,*)'                                              '

      write(*,*)'                                              '

      write(*,*)'                                              '


      bg=bf*be*am*r*r*(1-(.59*be*bf/b))

write(*,17)bg/1000000

 17   format(' Mn= Pf.Ff[1-0.59 Pf.Ff/fc] bd^2 =       kN.m    'f6.2)

write(*,*)'                                              '

      write(*,*)'                                              '

      write(*,*)'                                              '
```

```fortran
      write(*,*)'Compute the strength reduction factor ... '

      write(*,*)'                                              '

      write(*,*)'                                              '

      write(*,*)'                                              '

      write(*,*)'                                              '


if(be<bd)then

      bh=0.55

      write(*,19)bh

 19   format(' Pf <Pfb    Q=0.55',f6.3)

endif

      write(*,*)'                                              '


      if(be>1.4*bd)then

      bh=0.7

      write(*,20)bh

 20   format(' Pf > 1.4 Pfb    Q=0.70',f6.3)

endif

      write(*,*)'                                              '


      if(be<1.4*bd.and.be>bd)then

      bh=0.3+.25*be/bd

      write(*,21)bh

 21   format(' Pfb< Pf < 1.4 Pfb    Q=0.3+0.25 Pf/Pfb =    ',f6.3)
```

```fortran
          endif


    write(*,*)'                                            ,

        write(*,*)'                                              ,


        bi=bh*bg/1000000

        write(*,23)bi

   23   format(' Q . Mn=          kN.m',f9.3)

        write(*,*)'                                      ,

        write(*,*)'                                        ,


        if(bi>q)then

        write(*,24)

   24   format(' Q.Mn> Mu            Checked ...... OK')
          endif


        if(bi==q)then

        write(*,25)

   25   format('  Q.Mn> Mu              Checked ...... OK')
          endif

        if(bi<q)then

        write(*,26)

   26   format(' Checked--Not Accept-- Q.Mn< Mu --Change your Section')
```

```
        read(*,*)

        stop


        endif



        write(*,*)'                                                '
write(*,*)'*********************************************'
        write(*,*)'            Step5 - Check the Crack width'
        write(*,*)'*********************************************'
write(*,*)'                                            '



        write(*,*)'Compute the stress level in the FRP bars '
        write(*,*)'    under dead load plus live load. '
        write(*,*)'                                            '
        write(*,*)'                                            '



bk=o*f*f/8

        write(*,27)bk

27      format(' M DL= (W DL x L^2)/8 =           kN.m    ',f6.2)



        write(*,*)'                                            '
        write(*,*)'                                            '



bl=d*f*f/8
```

159

```fortran
        write(*,28)bl

28      format(' M LL= (W LL x L^2)/8 =            kN.m     ',f6.2)


write(*,*)'                                                       ,

        write(*,*)'                                                ,


bm=bl+bk

        write(*,29)bm

29      format(' M DL + LL =            kN.m    ',f6.2)


        write(*,*)'                                                ,

        write(*,*)'                                                ,

        write(*,*)'                                                ,



        bn=h/(4750*sqrt(b))

        write(*,30)bn

30      format(' nf= Ef/Ec =    ',f10.2)


        write(*,*)'                                                 ,

        write(*,*)'                                                ,



        bo=sqrt((2*be*bn)+(be*bn)**2)-(be*bn)

        write(*,31)bo

 31     format(' k= SQRT[2Pf nf + (PF nf)^2] - Pf nf=           ',f6.3)
```

160

```
      write(*,*)'                                             '

         write(*,*)'                                              '



         bp=bm/((bb*3.14*ak*ak/4)*r*(1-bo/3))*1000000

         write(*,32)bp

  32     format(' ff= M DL+LL / [Af.d (1-k/3)]=              Mpa    ',f6.2)

      write(*,*)'                                        '

         write(*,*)'                                             '



         write(*,*)' Determine the strain gradient used to transform '

         write(*,*)' reinforcement level strains to the near surface'

         write(*,*)' of the beam where cracking is expected.'

         write(*,*)'                                          '

         write(*,*)'                                           '



         bz=(ai-bo*r)/(r*(1-bo))

         write(*,33)bz

  33      format(' B= h-kd /d(1-k) =    ',f6.2)

      write(*,*)'                                          '

         write(*,*)'                                           '



         write(*,*)' Calculate the distance form the extreme tension fibre'

         write(*,*)' of the concrete to the concrete to the centerline of'

         write(*,*)'             the flexural reinforcement.          '
```

```fortran
      write(*,*)'                                              ,

      write(*,*)'                                                ,



      bx=ai-r

      write(*,34)bx

 34    format(' dc= h - d =              mm',f6.2)

write(*,*)'                                          ,

      write(*,*)'                                            ,



      write(*,*)' Claculate bars spacings. '

      write(*,*)'                                          ,

      bv=am-2*bx

      write(*,35)bv

 35    format(' s= b - 2dc =        mm',f6.2)

write(*,*)'                                        ,

      write(*,*)'                                          ,



      write(*,*)' Compare the crack width. using the reccomended value '

      write(*,*)'        of kb=1.4 for deformed FRP bars.        '

      write(*,*)'                                          ,

      cq=2*(bp*bz*1.4/h)*sqrt(bx*bx+(bv/2))

      write(*,36)cq

 36    format(' w= [2ff B kb / Ef] x SQRT[dc^2 + (s/2)]=      mm',f6.3)

write(*,*)'                                        ,
```

162

```fortran
      write(*,*)'                                        ,

      if(cq<.7)then

      write(*,37)

37    format(' w < 0.7           Checked ..... OK ..... Continue')

      endif

      write(*,*)'                                            ,


      if(cq==.7)then

      write(*,38)

38    format(' w =< 0.7           Checked ..... OK .....Continue' )

      endif

      write(*,*)'                                            ,


      if(cq>.7)then

      write(*,39)

39    format(' w > 0.7 NOT GOOD.....Try bigger bars(fi) for the Main')
write(*,40)

40        format('  w > 0.7  N.G...RUN  Again...Change  BIGER  (fi)  bars')
,

read(*,*)

      stop


      endif
```

```fortran
      write(*,*)'                                                    '

write(*,*)'*************************************************'

      write(*,*)'  Step6 - Check the Long Term Deflection of the Beam'

      write(*,*)'*************************************************'

write(*,*)'                                                  '



write(*,*)' Compute the gross moment of interia for the section'

      write(*,*)'                                                  '



      cw=(am*ai**3)/1200000000

      write(*,41)cw

 41   format(' Ig= bh^/12 =          mm^4         10^8    x ',f6.3)



      write(*,*)' Compute the cracked section properties '

      write(*,*)'          and cracking moment.         '

      write(*,*)'                                                  '



      ce=0.62*sqrt(b)

      write(*,42)ce

 42   format(' fr= 0.65 SQRT[fc]=               Mpa',f6.2)

write(*,*)'                                                  '



      cr=200*ce*cw/ai
```

164

```
        write(*,43)cr

 43     format(' Mcr= 2fr Ig/h =                      kN.m',f6.2)

write(*,*)'                                                           ,



        db=(am*(bo*bo*bo)*r*r*r)/3

        dn=bn*(bb*3.14*ak*ak/4)*r*r

        dm=(1-bo)*(1-bo)


        ct=db+dn*dm

        write(*,*)' Icr= [bd^3 k^3]/3 + [nfaf d^2 (1-k)^2]= '

write(*,44)ct/10000000

 44     format('          mm^4                  10^7   x ',f6.2)

write(*,*)'                                                     ,



        write(*,*)' Compute the modification factor Bd'

cy=(be/bd)*.2

        write(*,45)cy

 45     format(' Bd= 1/5 [Pf/Pfb] =          ',f6.2)

        write(*,*)'                                              ,



        write(*,*)' Compute the deflection due to Dead Load + Live Load'

        write(*,*)'                                              ,

        da=(cr/bm)*(cr/bm)*(cr/bm)
```

```
        ds=(cy*cw*100000000)

        dd=(1-da)*ct

        cu=da*ds+dd


        write(*,*)' [Ie] DL+LL = [Mcr/Ma]^3 BdIg + [1-(Mcr/Ma)^3]Icr'

        write(*,46)cu/10000000

46      format('   mm^4 =      10^7   x   ',f6.2)

        write(*,*)'                                                    ,


        ci=(5*bm*1000000*f*1000*f*1000)/(48*4750*sqrt(b)*cu*10000000)

        write(*,47)ci*10000000

47      format(' (Delta i) DL+LL = [5 Ma L^2]/[48Ec Ie]=  mm ',f6.2)

        write(*,*)'                                                    ,


        write(*,*)' Compute the Deflection due to DL alone and LL alone'

        write(*,*)'                                                    ,


        co=(ci*o)/(o+d)

        write(*,48)co*10000000

48      format(' (Delta i) DL = W DL/[W DL+LL] * Delta DL+LL =  mm',f6.2)

        write(*,*)'                                                    ,


        cp=(ci*d)/(o+d)

        write(*,49)cp*10000000
```

166

```
49    format(' (Delta i) LL = W LL/[W DL+LL] * Delta DL+LL =  mm',f6.2)
```

```
      write(*,*)'                                                    ,
```

```
      write(*,*)'                                                      ,
```

```
write(*,*)'                                                  ,
```

```
      write(*,*)' Compute the multiplier for time dependent deflection'
```

```
      write(*,*)' using a E=2.0 (recommended by ACI 318 for a duration'
```

```
      write(*,*)'                of more than 5 years).              '
```

```
      write(*,*)'                                                      ,
```

```
      write(*,*)' Landa= 0.60 x E= 1.2'
```

```
      write(*,*)'                                                      ,
```

```
write(*,*)'                                                  ,
```

```
      write(*,*)' Compute the long term deflection (initial deflection'
```

```
      write(*,*)' due to live load plus the time dependent deflection'
```

```
      write(*,*)'                due to sustained loads).       '
```

```
      write(*,*)'                                                      ,
```

```
      write(*,*)'                                                      ,
```

```
      ca=cp+1.2*(co+.2*cp)
```

```
      write(*,50)ca*10000000
```

```
50    format(' Delta LT= De LL + 1.2[De DL + 0.2 De LL]=      mm',f6.2)
```

```
write(*,*)'                                                  ,
```

```fortran
      write(*,*)'                                                  '

      write(*,*)'        Check computed deflection against   '

      write(*,*)'          against deflection limitations '

      write(*,*)'                                                  '


      cb=1000*f/240

      write(*,55)cb

55    format(f6.2)

      write(*,*)'                                                  '


if(ca<cb)then

      write(*,51)

51    format('            De LT < L/240 . . . .  O K')
endif


      if(ca==cb)then

      write(*,52)

52    format('            Den LT =<   L/240 . . . . O K')
endif


if(ca>cb)then

      write(*,53)

53    format('            De LT > L/240  . . . .N G . . . Check again')
```

168

```
        endif

        write(*,*)'                                                  '


        write(*,*)'                                                  '

write(*,*)'********************************************'

        write(*,*)'    Step7 - Check the Creep Rupture Stress Limits'

        write(*,*)'*************************************************'

write(*,*)'                                                    '


        eq=(o*0.2*d)

        ew=o+d

        cv=bm*eq/ew


write(*,54)cv

  54    format(' Ms= Ma*[W DL+0.2W LL]/[W LL + W DL]=        kN.m',f6.2)

write(*,*)'                                                  '


        write(*,*)' Compute the sustained stress level in the FRP bars. '

        er=(bb*3.14*ak*ak/4)*r

        et=1-bo/3

        ey=cv*1000000/(er*et)

        write(*,56)ey

  56    format(' Ff,s= Ms/[Af d(1-k/3)]=            Mpa      ',f6.2)

        write(*,*)'                                                  '
```
                                                                    169

```
      write(*,*)'                                                    ,


      write(*,*)' Check the stress limits given in Table 8.3'

      write(*,*)'                                                    ,

      write(*,*)'                                                    ,



write(*,*)' Table 8.3: Creep rupture stress limits in FRP RC '

      write(*,*)'                                                    ,

      write(*,*)' ---------------------------------------------------'

      write(*,*)' |    Fibre Type    |  GFRP  |  AFRP  |  CFRP  |'

      write(*,*)' ---------------------------------------------------'

      write(*,*)' |   Creep rupture  |        |        |        |'

      write(*,*)' |stress limits Ff,s | 0.20Ffu | 0.30Ffu | 0.55ffu |'

      write(*,*)' ---------------------------------------------------'

      write(*,*)'                                                    ,

      write(*,*)'                                                    ,



      write(*,*)'          Enter your ratio according to Table 8.3      ,

      read(*,*)eu

      write(*,*)'                                                    ,



      ei=eu*bc

      write(*,57)ei

57    format(' According to Table 8.3,Ffs is =          Mpa',f12.2)
```

170

```fortran
      write(*,*)'                                              ,

        write(*,*)'                                                   ,


        if(ey<ei)then

        write(*,58)

 58     format('         the calculated Ffs<Ffs Table 8.3 . . . .  OK')
endif


        if(ey>ei)then

        write(*,59)

 59     format('         the calculated Ffs>Ffs Table 8.3  . . . . N G ')

        endif

        write(*,*)'                                                   ,

        write(*,*)'                                                   ,


        write(*,*)'*******************************************'
           write(*,*)'            Step8 - Design For Shear.'
        write(*,*)'*******************************************'
write(*,*)'                                              ,


        write(*,*)' Detremine the factored shear deman at a distance d'

        write(*,*)'                    from the support            ,

        write(*,*)'                                                   ,

        eo=(f*p/2)-r*p/1000
```

171

```
        write(*,60)eo
 60     format('   Vu= [Wu L/2]-Wu d =                        kN    ',f6.2)
write(*,*)'                                                    '


        write(*,*)' Compute the shear contribution of the concrete for  '

        write(*,*)'              an FRP-Reinforced member.              '

        write(*,*)'                                                     '


        ep=(.4*sqrt(b)*bo*r*am)/1000

        write(*,61)ep
 61     format('   Vc= 0.4 Sqrt[Fc]* b * k * d=          kN     ',f6.2)
write(*,*)'                                                     '


        write(*,*)' FRP shera reinforcement will be required.     '

        write(*,*)' The FRP shear reinforcement will be assumed to be NO3'

        write(*,*)' closed stirrups oriented vertically.              '

        write(*,*)' To determine the amount of FRP shear reinforcement '

        write(*,*)' required,the effective stress level in the FRP shear'

        write(*,*)' reinforcement  must be determined.This stress level'

        write(*,*)' may be governed by the allowable stress in the   '

        write(*,*)' stirrup at the location of a band,                '

        write(*,*)' which is computed as follows:                    '

        write(*,*)'                                                   '

        ea=(0.45)*bc
```

```fortran
      write(*,62)ea

 62   format(' ffb= [0.05 3rb/db + 0.3] Ffu =        Mpa    ',f12.2)

write(*,*)'                                              '

write(*,*)' Note that the minimum radius of the bend is 3 bar dia'

      write(*,*)'                                              '


write(*,*)' The design stress of FRP stirrup is limited to:        '

      write(*,*)'                                              '


      es=0.004*h

      write(*,63)es

 63   format('     ffv= 0.004 Ef -----> must be =<ffbMpa  ',f12.2)

if(es<ea)then

      write(*,64)

 64   format('      Checked ....... OK    ')

endif

      if(es>ea)then

      write(*,65)

 65   format('      Checked ........NG   ')

endif

write(*,*)'                                              '

      write(*,*)'                                              '


write(*,*)' The reqiured spacing of the FRP stirrups can be '
```

173

```
      write(*,*)'          computed by rerranging follow Eq.     '

      write(*,*)'                                                 '



ed=.75*2*.785*al*al*es*r/(eo*1000-.75*ep*1000)

      write(*,66)ed
66    format('   s= 0.75Afv ffv d / [Vu - 0.75Vc]=          mm   ',f12.2)
write(*,*)'                                                '

      write(*,*)'                                                  '



write(*,*)'    Chech maximum spacing limit= d/2 or 600mm      '

      write(*,*)'                                                 '

      write(*,*)'                                                  '



ef=r/2

      write(*,67)ef
67    format('       d/2=           mm   ',f6.2)
write(*,*)'                                                '

      write(*,*)'                                                  '



write(*,*)' The minimum spacing amount can be computed as follow'

      write(*,*)'                                                 '



eg=2*.785*al*al*es/(.3*am)

      write(*,68)eg
```

174

```
68      format(' s min= Afvffv / 0.35b =            mm   ',f12.2)


        write(*,*)'                                            '

        write(*,*)'                                             '


        write(*,*)' *-*-*-*-*-*-*-*-*-*-*-*-*-*-*-*-*-*-*-*-*-*-*-*'

        write(*,*)'              Summary of this Design

        write(*,*)' *-*-*-*-*-*-*-*-*-*-*-*-*-*-*-*-*-*-*-*-*-*-*-*'

        write(*,*)'                                          '


        write(*,70)o

70      format('   W DL= W SDL + W SW          kN/m',f6.2)

write(*,*)'                                            '


        write(*,*)'                                           '

        write(*,*)'                                             '


write(*,71)p

71      format('   Wu= 1.2W DL + 1.7W LL       kN/m',f6.2)

write(*,*)'                                          '


        write(*,72)q

72      format('   Mu= (Wu L^2)/8              kN.m',f6.2)

write(*,*)'                                         '
```

175

```fortran
      write(*,*)'                                          ,

      write(*,73)bg/1000000
73    format(' Mn= Pf.Ff[1-0.59 Pf.Ff/fc] bd^2 =      kN.m    'f6.2)
      write(*,*)'                                          ,
      write(*,*)'                                          ,


      if(be<bd)then
      bh=0.55
      write(*,74)bh
74    format(' Pf <Pfb      Q=0.55',f6.3)
endif
      write(*,*)'                                          ,


      if(be>1.4*bd)then
      bh=0.7
      write(*,75)bh
75    format(' Pf > 1.4 Pfb      Q=0.70',f6.3)
endif
      write(*,*)'                                          ,


      if(be<1.4*bd.and.be>bd)then
      bh=0.3+.25*be/bd
      write(*,76)bh
```

176

```fortran
76      format(' Pfb< Pf < 1.4 Pfb      Q=0.3+0.25 Pf/Pfb =    ',f6.3)
endif


write(*,*)'                                                '
        write(*,*)'                                                  '


        bi=bh*bg/1000000

        write(*,77)bi

77      format(' Q . Mn=           kN.m',f9.3)

        write(*,*)'                                                '
        write(*,*)'                                                  '


        if(bi>q)then

        write(*,78)

78      format(' Q.Mn> Mu                Checked ...... OK')
endif


        if(bi==q)then

        write(*,79)

79      format('  Q.Mn> Mu                Checked ...... OK')
endif

        if(bi<q)then

        write(*,80)
```

```fortran
80      format(' Q.Mn< Mu                    Checked .......NG')

        read(*,*)

        stop


        endif


        write(*,*)'                                               '
        write(*,*)'                                               '


        write(*,81)bk

81      format(' M DL= (W DL x L^2)/8 =          kN.m    ',f6.2)


        write(*,*)'                                               '


bl=d*f*f/8

        write(*,82)bl

82      format('  M LL= (W LL x L^2)/8 =         kN.m    ',f6.2)


write(*,*)'                                               '


bm=bl+bk

        write(*,83)bm

83      format(' M DL + LL =                     kN.m    ',f6.2)

        write(*,*)'                                               '
```

178

```fortran
      write(*,*)'                                          ,

      write(*,85)ci*10000000
85    format(' (Delta i) DL+LL = [5 Ma L^2]/[48Ec Ie]=  mm ',f6.2)
      write(*,*)'                                          ,

      write(*,86)co*10000000
86    format(' (Delta i) DL = W DL/[W DL+LL] * Delta DL+LL =  mm',f6.2)
      write(*,*)'                                          ,

      write(*,87)cp*10000000
87    format(' (Delta i) LL = W LL/[W DL+LL] * Delta DL+LL =  mm',f6.2)
      write(*,*)'                                          ,
      write(*,*)'                                          ,

      write(*,88)ca*10000000
88    format(' Delta LT= De LL + 1.2[De DL + 0.2 De LL]=      mm',f6.2)
write(*,*)'                                          ,

if(ca<cb)then
      write(*,89)
89    format('              De LT < L/240 . . . .  O K')
endif
      if(ca==cb)then
```

```fortran
          write(*,90)
90    format('              Den LT =<    L/240 . . . . O K')
endif


if(ca>cb)then

      write(*,91)
91    format('              De LT > L/240  . . . . N G ')
      endif
      write(*,*)'                                                   ,


      write(*,92)eo
92    format('   Vu= [Wu L/2]-Wu d =                     kN    ',f6.2)
write(*,*)'                                                ,


      ep=(.4*sqrt(b)*bo*r*am)/1000
      write(*,93)ep
93    format('   Vc= 0.4 Sqrt[Fc]* b * k * d=            kN    ',f6.2)
write(*,*)'                                                ,


      write(*,94)ed
94    format('   s= 0.75Afv ffv d / [Vu - 0.75Vc]=        mm   ',f12.2)
write(*,*)'                                                ,


write(*,*)'    Chech maximum spacing limit= d/2 or 600mm      '
```

```fortran
      write(*,*)'                                              ,

write(*,95)ef

95    format('   d/2=                           mm   ',f6.2)

write(*,*)'                                         ,


write(*,*)' The minimum spacing amount can be computed as follow'

      write(*,*)'                                         ,


write(*,96)eg

96    format('   s min= Afvffv / 0.35b =              mm   ',f12.2)


      write(*,*)'*************************************************'

      write(*,*)'          Thank you for your attention           ,

write(*,*)'        Mohsen Kobraei - University of Malaya      ,

write(*,*)'     For more info. please Call +60-12-668-7348     ,

write(*,*)'              email: mkobraei@yahoo.com             ,

write(*,*)'*************************************************'

write(*,*)'                                           ,

read(*,*)xxx



end
```